INCREMENTAL COLLAPSE OF REINFORCED CONCRETE CONTINUOUS BEAMS

INCREMENTAL COLLAPSE OF REINFORCED CONCRETE CONTINUOUS BEAMS

by

KAROL HERKEL, DIPL.ING.

A THESIS

SUBMITTED TO THE FACULTY OF GRADUATE STUDIES

IN PARTIAL FULFILLMENT OF THE REQUIREMENTS

FOR THE DEGREE

MASTER OF ENGINEERING

McMASTER UNIVERSITY

HAMILTON, ONTARIO

1971

MASTER OF ENGINEERING (1971)

McMASTER UNIVERSITY

HAMILTON, ONTARIO

TITLE: INCREMENTAL COLLAPSE OF REINFORCED CONCRETE CONTINUOUS BEAMS

AUTHOR: KAROL HERKEL, DIPL.ING. (BRATISLAVA)

SUPERVISOR: Dr. R.M. Korol, Dr. R.G. Drysdale

NUMBER OF PAGES: (xi), 194

SCOPE AND CONTENTS:

A research program is presented for assessing the plastic collapse load and shake-down load of reinforced concrete continuous beams. This investigation attempts to establish a range of validity of simple plastic theory when applied to the under-reinforced concrete beams and to determine the sensitivity of such structures to variable repeated loading. In attempt for more accurate prediction of the behaviour of reinforced concrete beams when subjected to variable repeated loading, the numerical beam analysis was developed.

An experimental program was conducted on 10 reinforced concrete continuous beams. Deflections and strains of these specimens of nearly prototype size were measured and compared with predicted values at critical cross-sections. Resulting conclusions and recommendations for further research are made.

ACKNOWLEDGEMENTS

The author would like to express his appreciation to Dr. R.G. Drysdale and Dr. R.M. Korol for their guidance and advice during the course of this investigation. The valuable suggestions from members of the faculty and from friends are gratefully acknowledged. The author also takes this opportunity to thank the following:

1) McMaster University for financial support during this research.
2) The staff of the Applied Dynamics Laboratory for their help in the experimental program.
3) The Steel Company of Canada for providing the reinforcing steel.

and finally, the author wishes to express his gratitude to his friends at McMaster University for their encouragement and help during the course.

TABLE OF CONTENTS

TABLE OF CONTENTS CONT'D

TABLE OF CONTENTS CONT'D PAGE

TABLE OF CONTENTS CONT'D PAGE

LIST OF FIGURES

LIST OF FIGURES CONT'D PAGE

LIST OF FIGURES CONT'D PAGE

LIST OF TABLES

CHAPTER 1

INTRODUCTION

1.1 FORWARD

The plastic methods of analysis are very well developed for steel structures, especelly for a structure of a mild steel. The behaviour of steel structures is very close to the predicted actual behaviour when using the plastic theory. On the other hand development of a plastic theory of a reinforced concrete structure, particularly when subjected to variable repeated loading was rather neglected. Therefore it was decided that in this research program, number of tests with variable repeated loading will be done on the continuous reinforced concrete beams. Number of tests, as well as number of variables included in the testing program was limited by time requirements. This was the reason why the numerical beam analysis, which will be able to predict the behaviour of beams, was developed. The numerical beam analysis employes all the basic hypothesis used in the plastic methods of structural analysis. Only necessary changes caused by the different behaviour of reinforced concrete under repeated loading have been added. It was hoped that the results of this analysis, which is including the stress-strain history of concrete and steel in each investigated cross-section, should serve as a more accurate comparison of an overall

behaviour of the beam subjected to variable repeated loading. It was also hoped that the analysis, when some necessary adjustments are made, will be capable to predict the behaviour of the beams with a wider range of parameters.

Some of the effects associated with variations of the parameters involved in the prediction of the behaviour of the beam have been partly eliminated in this testing program by choosing a standard cross-section throughout most of the tests. However the nature of concrete combined with the curing conditions caused some changes in the concrete strength even though a standard mix was used. The accuracy of the corresponding theoretical analysis has been limited by the necessity of incorporating approximate assumptions which are discussed later.

1.2 PURPOSE AND SCOPE

The primary objective of this investigation was to contribute to the knowledge of the behaviour of beams. In a more restrictive sense the major area of investigation was concerned with the behaviour of continuous reinforced concrete beams and particularly their behaviour under variable repeated loading.

The purpose was to establish the actual value of shakedown load and the collapse load from the tests as well as to determine their theoretical values. In order to obtain these theoretical values it was used the plastic analysis and the

numerical analysis, which was adjusted as much as possible to the real behaviour of reinforced concrete structures. The validity of the method of numerical analysis will be checked by comparison with the test values using the corresponding known test properties.

1.3. SCOPE OF THE EXPERIMENTAL PROGRAM

The test specimen and the method of testing were chosen for many reasons. However, the main criteria were that the tests would be as simple as possible while providing useful information for understanding the behaviour of continuous beams.

It was observed that variable repeated loading of continuous beams was an important area of research which had been neglected. It was decided that in addition to the tests for incremental collapse will be done also the tests for proportional collapse. These tests would also be the same beam type, thereby providing a comparison basis for test and analysis.

It was preferred that the specimen dimensions be as large as was practical in order to reduce any doubts concerning size effects when relating test values to actual structural sizes. In addition, fabrication errors would be less significant for larger overall dimensions. A standard test beam was designed for use throughout the testing program.

The beam design called for a constant percentage, a

uniform type and an unchanging position of the reinforcement steel having a flat yield region in the stress-strain diagram was preferred. A uniform concrete was desired. To accomplish this, standard mixing procedures and curing conditions were planned.

1.4 BASIC HYPOTHESIS IN THE PLASTIC THEORY

The basic hypothesis of the plastic theory are concerned with the relation between bending moment and curvature for the structural members. The basic hypothesis underlying the plastic methods are summarised in Fig. 1.1. This figure shows the type of relation between bending moment M and curvature K which is assumed to hold at any cross-section of a typical structural number. The moment-curvature diagram shown in Fig. 1.1a is related to the behaviour of mild steel. A reinforced concrete member behaves differently and its behaviour depends on the reinforcement ratio. Generally a reinforced concrete member can be identified as an under-reinforced or an overreinforced cross-section. The typical moment-curvature diagrams for the underreinforced and over-reinforced cross-section are shown in Figure 1.1b and 1.1c respectively. If a bending moment is applied to a previously unloaded and unstrained structural member made of mild steel, the curvature at first increases linearly with increasing bending moment- This continues through the ordinary elastic range and is terminated when a bending moment MY is obtained.

This bending moment is such as to cause the yield stress in the most highly stressed outer fibres of the member. When a bending moment above the MY value is applied, the curvature begins to increase more rapidly per unit increase of bending moment and finally bends to infinity as a limiting value of the bending moment is approached. This limiting value is termed as the fully plastic moment, MP.

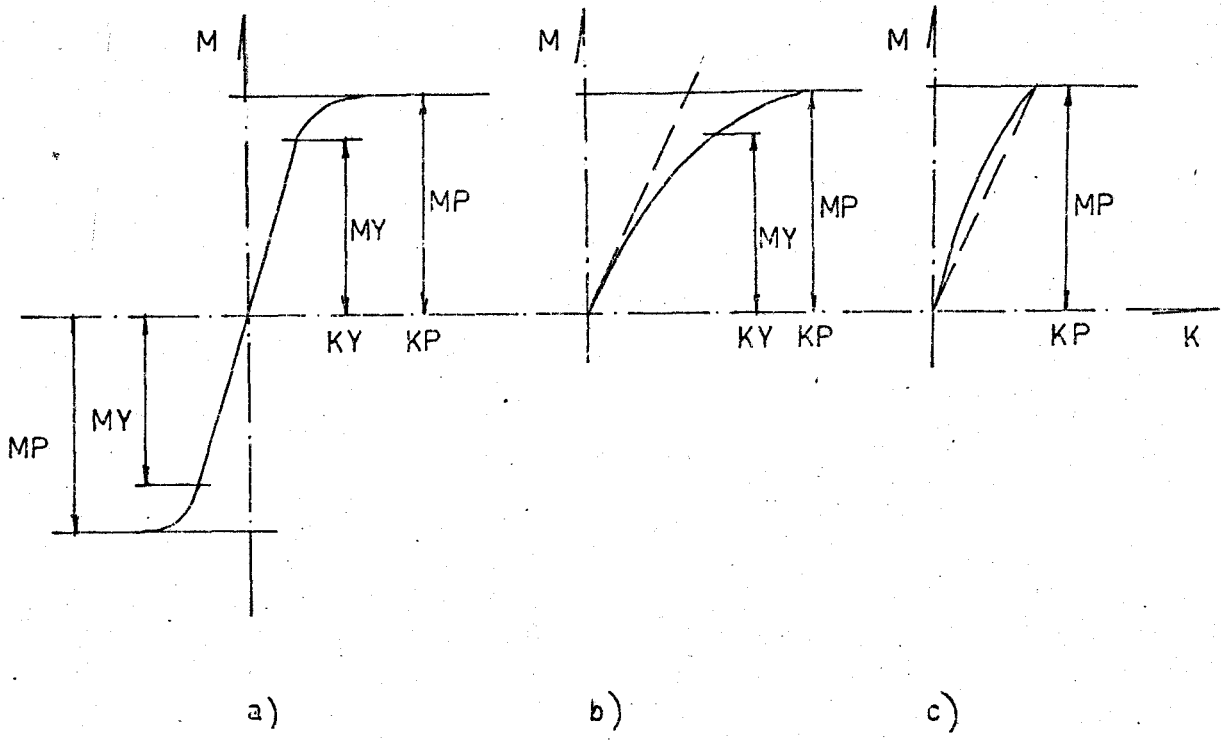

FIG. 1.1 MOMENT-CURVATURE RELATION

The attainment of the fully plastic moment may be thought of as corresponding physically to the development of the full yield stress down to the neutral axis of the beam in both tension and compression.

If at some section in a member the bending moment obtains the positive fully plastic moment, MP, it is assumed that as the bending moment reaches the value MP, the curvature tends to become infinitely large, so that a finite change of slope can occur over a small length of the member at this cross-section. Thus the behaviour at a section where MP is obtained can be described by imagining a hinge to be inserted in the member at this section. The hinge is described as being capable of resisting rotation until the fully plastic moment MP is obtained, and then permitting positive rotation of certain magnitude while the bending moment remains constant at the value MP.

As was mentioned before, reinforced concrete structures behave very differently. In the region subjected to sufficiently great bending moments, the concrete has a plastic component in compression and the reinforcement yields in tension. At fracture, the compressive strain of the concrete in the fibres of a bent member varies from 0.3 to 0.5%. Because this value is small, the limited rotation capacity of the plastic hinges frequently determines the failure load. The limited rotation capacity of a plastic hinge was the reason why the plastic hinge length was introduced in the numerical analysis.

The behaviour of statically indeterminable reinforced concrete structures further depends on the reinforcement ratio of the members.

a) Underreinforced structural members: The moment-curvature diagram for an underreinforced cross-section is shown in Fig. 1.1b. In general MY differs only slightly from MP. For small reinforcement ratios, the curvature K_p is much larger than K_y. Therefore a statically indeterminate structure consisting of reinforced beams with small reinforcement ratios behaves like a structure made of mild steel beams.

b) Overreinforced structural members: The behaviour of reinforced concrete beams changes drastically when the critical reinforcement ratio is exceeded. The critical reinforcement ratio can be described as the ratio, when at the same time the steel yields in tension and the stress in top compression fibres of concrete reaches its maximum value.

The moment versus curvature diagram (Fig. 1.1c) does not differ significantly from a straight line. The plastic rotation vanishes. Since the beneficial redistributions of bending moments stems from the great rotation capacity of the plastic hinges, it is practically nonexistent in a structure of this kind. For intermediate reinforcement ratios, fracture occurs at some cross-section before all the plastic hinges of the collapse mechanism have developed.

1.4 PLASTIC COLLAPSE OF SIMPLY SUPPORTED BEAM

The following illustration of plastic collapse is explained. A simply supported beam has a uniform underreinforced cross-section and is subjected to a central concen-

trated load, P, as shown in Fig. 1.2a. The bending moment diagram for this beam is shown in Fig. 1.2b. If the load P is increased steadily from zero the beam at first behaves elastically. At a certain value of the load the maximum central bending moment reaches the value MY and a plastic hinge starts forming. Further increase of the load causes rapid increase in curvature and finally at a magnitude of load, P_C, the bending moment reaches the value of fully plastic moment, MP. At this stage the plastic hinge had spread over a certain hinge length, which can be characterised as a segment of the beam length in which the degree of plastisation of the cross-sections is varying from partially plastic cross-sections (tension steel in yield) to fully plastic cross-sections (internal moment of the cross-section reaches the value of a fully plastic moment). However the plastic hinge can by the hypothesis undergo limited rotation through a certain angle while the bending moment, and therefore the load remains constant. The beam can thus continue to deflect at constant load due to this hinge action until the limiting strain in the concrete is reached.

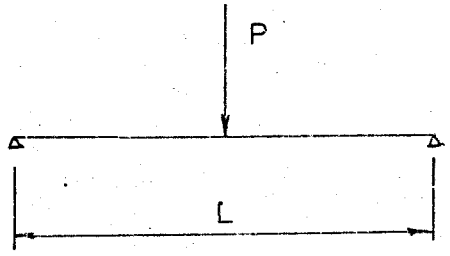

a) LOADING

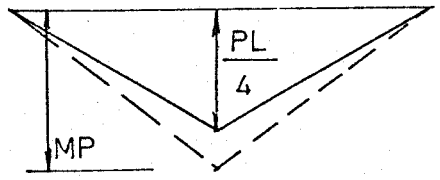

b) BENDING MOMENT DIAGRAM

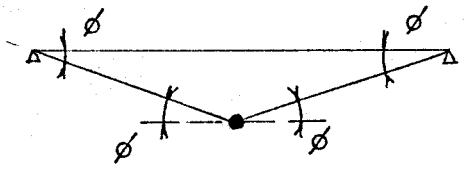

c) CHANGES OF DEFLECTION DURING COLLAPSE

FIG. 1.2 SIMPLY SUPPORTED BEAM WITH CENTRAL CONCENTRATED LOAD

The load at which this occurs is termed the plastic collapse load, and is denoted by P_c, its value is determined by equaling the magnitude of the central bending moment to the fully plastic moment, giving

$$\frac{1}{4} P_c L = MP$$

$$P_c = \frac{4MP}{L}$$

Since the bending moment at every cross-section except the hinged section is less than MY, the beam remains elastic everywhere except over the plastic hinge length and the

constant load and therefore constant bending moments during collapse implies constancy of the curvatures over the non-yielding region. The increases of deflection during collapse are therefore due solely to the rotation at the plastic hinge.

1.5 VARIABLE REPEATED LOADING

The structure under variable repeated loading may fail due to eventual development of excessive plastic flow in parts of the structure even though none of the loadings applied is ever sufficiently severe to cause failure by plastic collapse. There are two possible types of failure which can occur.

a) Alternating Plasticity

If the loads are essentially alternating in character then one or more of the members might be bent back and forth repeatedly so that yield occurred in the fibres alternately in tension and compression. Such behaviour is termed alternating plasticity. A condition of alternating plasticity in a structure would be expected to lead eventually to the fracture of a member. While a failure by alternating plasticity is due to the continuance of plastic flow in some part of the structure, the difference between this type of failure and a fatigue failure is one of degree rather than kind. Whereas fatigue failures are usually associated with a number of load reversals of the order of millions, alternating

plasticity failures would occur with a number of load reversals of the order of hundreds or perhaps thousands, but the eventual fracture is probably of a similar nature in both cases.

b) Shake-down

If a number of critical combinations of loads follow one another in fairly definite cycles and if the loads are all multiples of one of the loads P, it can be shown that if P exceeds a certain intensity P_s^1, increments of rotation at plastic hinges can take place at various cross-sections in the structure during each cylce of loading, these increments being in the same sense during each cycle of loading. If P, while exceeding P_s^1, is less than a higher critical value P_s, the increments which occur in the rotations at the plastic hinges during each cycle of loading become progressively smaller as the number of cycles of loading increases. When this happens, the structure is said to have shaken down.

After a number of loading cycles is applied it is possible that a sufficient number of plastic hinges are created at various cross-sections such if these hinges occurred simultaneously at all these cross-sections the structure would be transformed into a mechanism. For example if a sufficient number of plastic hinges to form a mechanism is 3, then if in part of each cycle of loading the plastic hinge rotations are taking place in hinges 1 and 3 so that these rotations change the residual bending moment in cross-section 2, the residual moment may act in such a way as to cause the

further formation and rotation of a plastic hinge in section 2. Generally, the rotation in a number of plastic hinges, which is insufficient for forming a mechanism, causes a build-up of the residual stresses (or strains) and therefore residual bending moments, which increase in such a way that after a sufficient number of loading cycles the structure creates a sufficient number of plastic hinges to form a mechanism.

When a load of a certain magnitude P_s is applied in a loading cycle and when only after an infinite number of loading cycles the mechanism is formed, this load is called shake-down load. It can also be called a lower limit of incremental collapse load, because all the loads of a magnitude higher than P_s and less than P_c cause incremental collapse. And all the loads of a magnitude lower than P_s finally result in an elastic change condition.

c) Incremental Collapse

If the magnitude of P exceeds the critical value P_s, the structure never shakes down, and definite rotations take place at the plastic hinges during each cycle of loading. If the peak load intensities do not vary from cycle to cycle, a steady regine is established in which the increment in the rotation at any given hinge is the same in each cycle so that in each cycle the deflections of the structure increase by a given amount. Incremental collapse in general only takes place when during each cycle of loading increments of plastic hinge rotation occur at a sufficient number of cross-sections

such that if hinges occurred simultaneously at all these cross-sections the structure would be transformed into mechanism.

The number of applied load cycles causes such an increase in residual stresses that if a sufficient number of cycles takes place, unacceptably large deflections will be built up, rendering the structure useless. The structure would then be said to have failed by incremental collapse.

1.6 SUMMARY

This chapter had generally described the purpose and scope of this research program. Also some basic hypothesis in the plastic theory and their application to the reinforced concrete and general behaviour of a continuous beam subjected to variable repeated loading has been introduced. In the following chapters there will be a more detailed analysis of the material properties and description of the numerical analysis. Chapter 4 will introduce the test results and analytical results, the errors of the results are in Chapter 5 and discussion and conclusion are in Chapters 6 and 7.

CHAPTER 2

MATERIAL PROPERTIES, TEST SPECIMEN AND EQUIPMENT AND INSTRUMENTATION

2.1 INTRODUCTION

This chapter provides information about the materials used for the experimental beam test program, about the test specimen and equipment used for testing. Properties of the concrete and the steel, such as the stress-strain relationships are introduced in both actual and theoretical forms. The real properties of materials were obtained from back-up tests, which were done for each beam testing program. The theoretical stress-strain relationships introduced in this chapter contain some simplified assumption and the results are compared with the real one.

The test specimen and the test equipment are detailed described at the end of the chapter. An analysis of the errors either in the test results or in the numerical analysis due to deviation from assumed or specified material properties, test specimen properties or the test equipment and testing techniques are described in Chapter 5.

2.2 CONCRETE PROPERTIES

Only one set of concrete mix properties were used in

this testing program.

2.2.1 CONCRETE MIX AND BATCHING PROCEDURE

Table 2.1 lists the properties by weight of the concrete mix as well as the weights required for each batch.

TABLE 2.1

CONCRETE MIX DATA

COMPONENT	PERCENTAGE BY WEIGHT	WEIGHT (lb)
PORTLAND CEMENT TYPE I	14.0	106
WATER	9.1	69
FINE AGGREGATE (WASHED PIT RUN SAND, FINENESS MODULUS = 2.51)	46.6	352
COARSE AGGREGATE (3/8" MAXIMUM SIZE CRUSHED LIMESTONE)	30.3	236
	100.0	763
VOLUME PER BATCH = 5 cubic feet		

The weight of the aggregate was for the air-dried condition. The concrete mix was designed to have a slump of 2 1/2 inches for standard 12 inch high slump cone. The fine aggregate and coarse aggregate were stored outside. The failure to properly account for the excess moisture and some variations in curing resulted in variations in concrete strength between different test specimens. Two batches of concrete were

required to complete the pouring of a test specimen and six cylinders. The cylinders were the standard 6 inch diameter by 12 inch long type. The test specimen was a beam which was 20 feet long with an eight inch square cross-section. Each batch was allowed to mix for five minutes after the last of the water had been added. The complete mixing and pouring operation took about half an hour. Steel forms were used for casting the beams. The horizontaly cast beams were poured in two equal layers corresponding to the two concrete batches. Each layer was placed and vibrated as soon as it was removed from the mixer. The concrete was internally vibrated by a 1 1/4 inch diameter poker type vibrator.

Standard cylinders were poured using a mixture of the concrete from the two batches. The cylinders were filled and vibrated in three layers as specified in ASTM C192.

2.2.2 CURING OF THE CONCRETE

About five hours after pouring, when the concrete had begun to harden, wet burlap was placed over the specimen and kept moist until the day of the test. The specimen and cylinders were removed from their forms at the age of one day. All the beams and cylinders were poured and cured in the laboratory, where the temperature was maintained between 68°F and 72°F and the relative humidity varied from about 20% to about 80%, depending upon the season. Three weeks after pouring the beam was removed from the curing place and was

placed on the supports. Usually on the day before the test was planned, the demec points and dial gauges were set up.

2.2.3 CONCRETE STRESS-STRAIN RELATIONSHIP

Age of testing: One or two cylinders were tested after 14 days to give an indication of the increase in concrete strength. The rest of the cylinders were tested at the day of the test, usually 28 days after pouring.

Concrete cylinder tests: Most of the cylinders were instrumented with two sets of gauge points placed on opposite sides of the cylinder. These gauge points were centered on the 12 inch length with an 8 inch gauge length. A demec mechanical strain indicator, was used to measure the strains. This instrument was calibrated into divisions of 0.00001 inches per inch and could be read accurately to one half of a division.

The cylinders were capped with a molten sulphur compound called VITROBOND, and were tested in a 300 kip capacity hydraulic cylinder testing machine. The test procedure adhered to ASTM specifications except for the taking of strain readings. Readings were taken at 10 kip intervals up to about 80% of the cylinder strength. After exceeding 80% of the cylinder strength the cylinder was loaded until material failure occurred. The averages of the strains from the cylinders were used for plotting the stress-strain curve.

Two of the cylinders were tested with repeated loading. The readings were taken each 10 kips up to 90% of the cylinder

strength, then the cylinders were unloaded and the readings were taken again each 10 kip. This cycle was repeated 2 to 3 times. The reason for taking the readings only up to 80% of the cylinder strength was that the readings above this range were difficult to obtain. The shape of the stress-strain curve as plotted from the average strain readings was quite similar to that of SINHA[3]. Fig. 2.1 contains a typical example plot of cylinder stress-strain data.

TABLE 2.2

AVERAGE CONCRETE STRENGTH

BEAM #	NUMBER OF CYLINDERS	AGE (days)	AVERAGE STRENGTH (PSI)	MEAN DEVIATION (PSI)	STANDARD DEVIATION (PSI)
1	6	28	3100	70	68
2	5	34	3340	39	40
3	5	30	3720	182	196
4	6	38	3880	52	59
5	4	28	3440	67	72
6	6	29	2950	240	308
7	5	34	3100	72	78
8	4	28	3130	143	216
9	6	32	3650	98	124
10	6	36	3820	40	48

$$\text{Average Strength} = \bar{f}'_c = \frac{\Sigma f'_c}{n}$$

$$\text{Mean Deviation} = \frac{\Sigma |f'_c - \bar{f}'_c|}{n}$$

$$\text{Standard Deviation} = \frac{\sqrt{\Sigma (f'_c - \bar{f}'_c)^2}}{n}$$

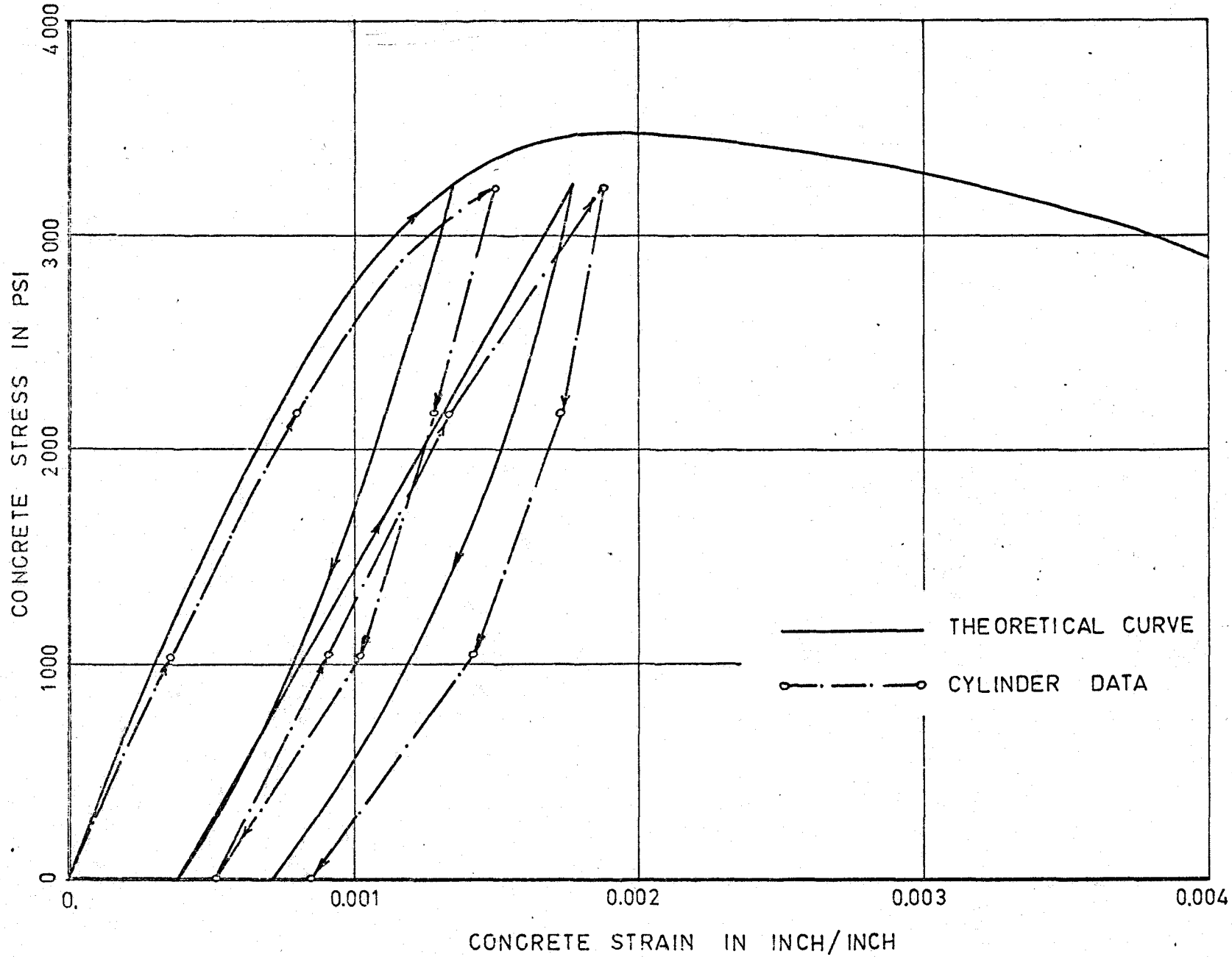

FIG. 2.1. CONCRETE STRESS-STRAIN RELATIONSHIP

Mathematical Expression of Concrete Stress-Strain Relationship

From the results of the extensive experiments Hansen, Hognestad and McHenry[1], Kriz and Lee[2] have established polynomial expressions for the usual stress-strain curve of concrete, of the form:

$$\sigma^2 + A\varepsilon^2 + B\sigma\varepsilon + C\sigma + D\varepsilon = 0 \qquad \text{(EQU. 1)}$$

in which the values of the coefficients for three strengths of concrete are given in Table 2.3 (where σ is in kips per sq. inch and ε in. x 10^{-3} inch per inch) The initial tangent modulus of the stress-strain curve is given by:

$$\left[\frac{d\sigma}{d\varepsilon} \right]_{\substack{\sigma = 0 \\ \varepsilon = 0}} = - \frac{D}{C}$$

TABLE 2.3

CONCRETE PROPERTIES

CONCRETE STRENGTH /psi/	A	B	C	D	α	H	J	K	L
3000	-3.434	-3.434	-6.751	22.58	0.125	0.07	0.95	3.42	1.26
3750	-8.7	-3.8	-11.9	45	0.111	0.09	0.52	2.52	1.03
4000	-11.51	-3.8	-14.26	56.99	0.111	0.10	0.61	4.61	1.01

The equation for the average stress-strain curve becomes

$$\sigma^2 + A_1\varepsilon_\ell'^2 + B_1\sigma\varepsilon_\ell + C\sigma + D\varepsilon_\ell + E\sigma^2\varepsilon_\ell + F\sigma\varepsilon_\ell^2 + G\sigma^2\varepsilon_\ell^2 = 0$$

$$\varepsilon_\ell = \frac{\varepsilon}{1 - \alpha\varepsilon}$$

$$\varepsilon = \frac{\varepsilon_\ell}{1 + \alpha\varepsilon_\ell}$$

$$A_1 = A + \alpha D$$

$$B_1 = B + 2\alpha\varepsilon$$

$$E = 2\alpha$$

$$F = \alpha B + \alpha^2 C$$

$$G = \alpha^2$$

Equation (1) can be solved for the stress:

$$\sigma = \frac{-Q_2 - \sqrt{Q_2^2 - 4Q_1Q_3}}{2Q_1}$$

$$Q_1 = 1 + E\varepsilon_\ell + G\varepsilon_\ell^2$$

$$Q_2 = C + B_1\varepsilon_\ell + F\varepsilon_\ell^2$$

$$Q_3 = D\varepsilon_\ell + A_1\varepsilon_\ell^2$$

Expression for unloading curves:

$$\sigma + H = \frac{J}{X}(\varepsilon - X)^2$$

$$X = \varepsilon_1 + \frac{\sigma_1 + H}{2J} - \sqrt{(\varepsilon_1 + \frac{\sigma_1 + H}{2J})^2 - \varepsilon_1^2}$$

σ_1, ε_1, are the coordinate values of certain known points in the stress-strain plane.

Expression for reloading curves:

$$\sigma + K = Y(\varepsilon + L)$$

$$Y = \frac{\sigma_1 + K}{\varepsilon_1 + K}$$

2.3 STEEL PROPERTIES

The bars used in this test program were number 4 and number 6 deformed reinforcement. In the first two tests 8 number 4 bars were used in each beam. In the tests number 3 to number 8 four number 6 bars were used in each beam. All of these bars were from the same shipment. In tests number 9 and number 10 four number 6 bars from another shipment were used in each beam. By special request the second shipment very closely matched the first order as verified below.

Twenty inch lengths were randomly cut from some of the bars to determine the stress-strain properties of the reinforcement. A 120 kip capacity hydraulically operated Tinius-Olsen Testing Machine was used to run the tests. Reference holes for the Demec Strain Indicator were drilled on opposite sides of the test specimens. Readings were taken until the range of the Demec was exceeded. The results of these tests are tabulated in Table 2.4. Figure 2.3 shows the stress-

strain diagram for the #6 reinforcements described above. The strain readings indicate that strain hardening started when the strain of 0.0066 inch/inch was reached. However the strain hardening of the steel was not taken into account in the analysis and the stress-strain diagram in the plastic region was assumed straight. An equation which describes both the elastic and the plastic portions of the stress-strain relationship is also given in Figure 2.3.

TABLE 2.4

PROPERTIES OF THE REINFORCING STEEL

SHIPMENT	BAR SIZE	NUMBER OF SPECIMEN	AVERAGE YIELD STRESS/KSI/	MEAN DEVIATION/KSI/	STANDARD DEVIATION /KSI/
1	#4	4	56	0.92	0.92
1	#6	6	60.2	0.97	0.99
2	#6	6	60.1	0.94	1.02

2.4 PREPARATIONS AND EQUIPMENT FOR BEAM TEST

This section briefly describes the procedures and equipment used to prepare the beam for testing. In addition, the test equipment and measuring devices are described.

2.4.1 FORMS AND STEEL REINFORCING CAGES

Forms for pouring the beams were prepared by rearranging existing steel forms used to fabricate two bay frame specimens.

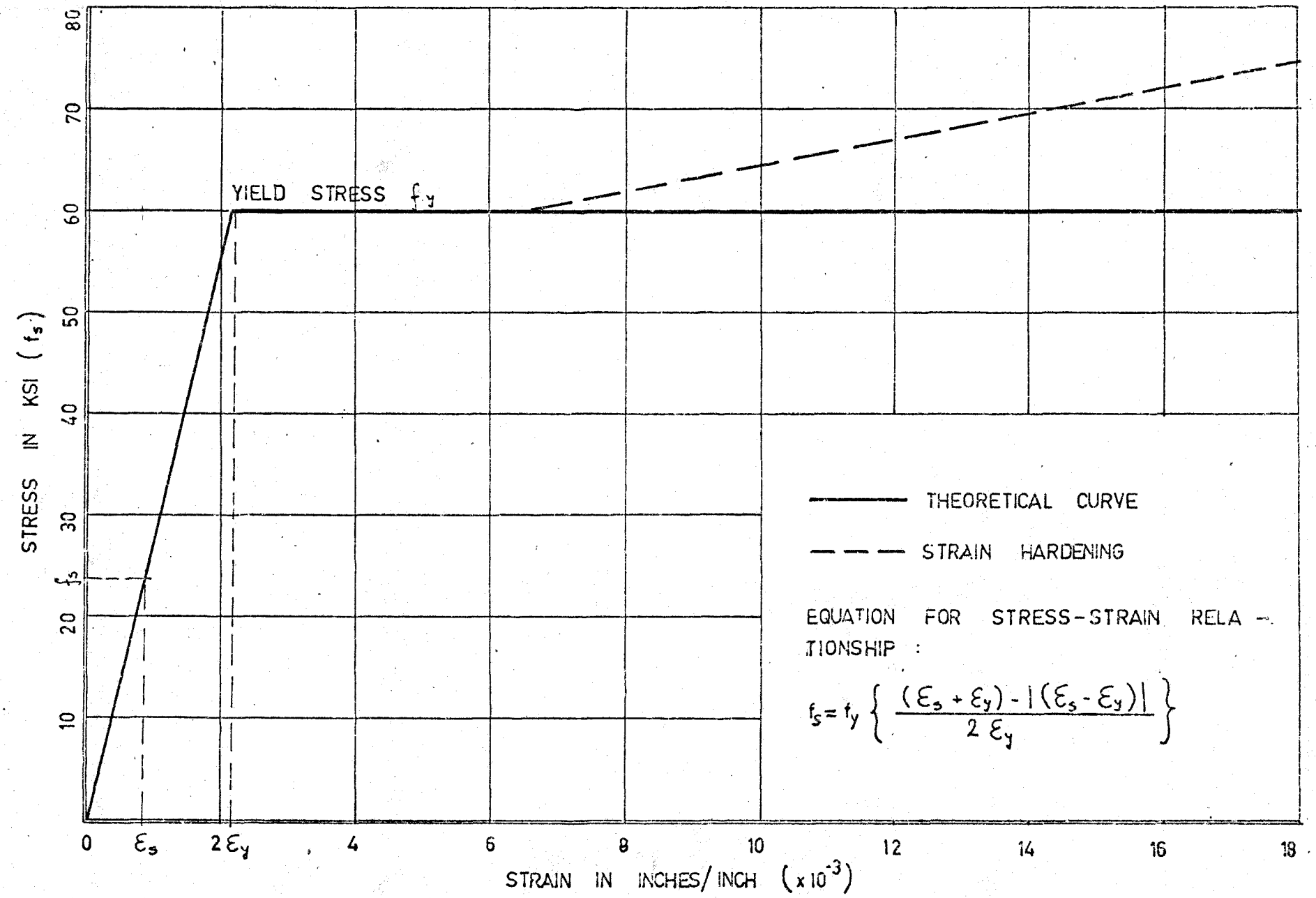

FIG. 2.3. STRESS-STRAIN RELATIONSHIP FOR STEEL

The steel forms were chosen because they were not easily damaged with re-use and because they were fabricated to closer dimensional tolerances. These forms were made by bolting 1 2 inch thick, 9 inch by 4 inch angles to a 1/2 inch thick base plate. The base plate was made from two pieces, 12 feet and 8 feet long. The two parts were put together, the angles were then clamped in place and bolt holes were drilled. in the components as a unit.

The reinforcing steel cages for the beams were made by tying the bars to 0.15 inch diameter ties spaced at 3 inch intervals. These ties were accurately produced on a specially designed bending device. The reinforcing was firmly wired into each corner of the ties. After the cage was completed, the spacing of the reinforcing steel was checked. If necessary, adjustments were made and the bars were re-wired to the ties. The position of the cage in the form was controlled by using 1 inch high steel chairs. The chairs were placed at the bottom of the steel form and after the reinforcement cage was in position, additonal chairs were installed at the sides of the form. Then during pouring of the concrete and by vibrating, the position of the cage could not be moved.

2.4.2 PREPARATION OF BEAMS FOR TESTING

After curing for 21 days under wet burlap, the beams were moved to the main test floor where they were prepared

for testing. The following steps were required to ready the beams for testing:

a) Position of the vertical load: Two hydraulic jacks were used to apply the load, their position between the bases and their clearance from the top of the beam had to be checked. The load was applied to the beam through the ball seat, which rested on a steel plate. The bearing stress was reduced by transforming the load through a 8 inch by 8 inch plate bearing devibly on the surface of the concrete. This part of the loading system is shown in Fig. 2.4.

b) Position of the bases and the roller supports: The bases were made from concrete poured into the form of an approximate dimensions 2 feet by 2 feet and 1 1/2 feet high. In the middle of the form was placed hollow steel 8 inch by 8 inch section. The hollow sections were cast in the concrete and their height over the concrete surface varied between 4 inches to 1 foot. At the top of the hollow section were steel plates 1/2 inch thick, welded to the hollow section. In order to have the beam placed in truly horizontal position, small adjustments were made by adding plates of various thicknesses to the tops of the bases. The whole set-up for the test is shown in Fig. 2.4. The beam was placed on the three bases. In the first 4 tests the bases were of the same height. Later it was decided to cut off the hollow section of two bases, in order to get enough space to insert the load cells. Installation of the additional load-cells under the supports was done in

order to provide comparative informations about the moment distribution as well as contribute to a better controlled loading system. Once the load-cells were installed to give information about the magnitude of the reactions, the structure was statically determinate and the magnitude of the applied load as well as calculation of the real bending moments throughout the beam could be easily done.

Due to the statical scheme, the outside supports for the beam were composed of a simple, 1 1/2 inch in diameter, 8 inch long roller, sitting on the steel plate. This arrangement enabled a small movement in the horizontal direction. In addition, the outside supports were required to resist upward movement. This arrangement was necessary because of an up-lift caused by loading with load on only one span. The construction of the hold down arrangement is shown in Fig. 2.4. The middle support was provided with roller bearing, which enables permitted rotation.

c) Strain measurement preparations: Demec strain gauge points were attached on one side of the beam at three levels spaced over the beam height. The spacing of the demec gauge points is shown in Fig. 2.5. The demec gauge points were fastened to the beam by using a drop of melted sealing wax. This wax hardened quickly and made a very durable connection.

d) Preparation for deflection measurements: The deflection was measured at the points of loading and near the outside supports. The measurements were taken using Dial Gauges.

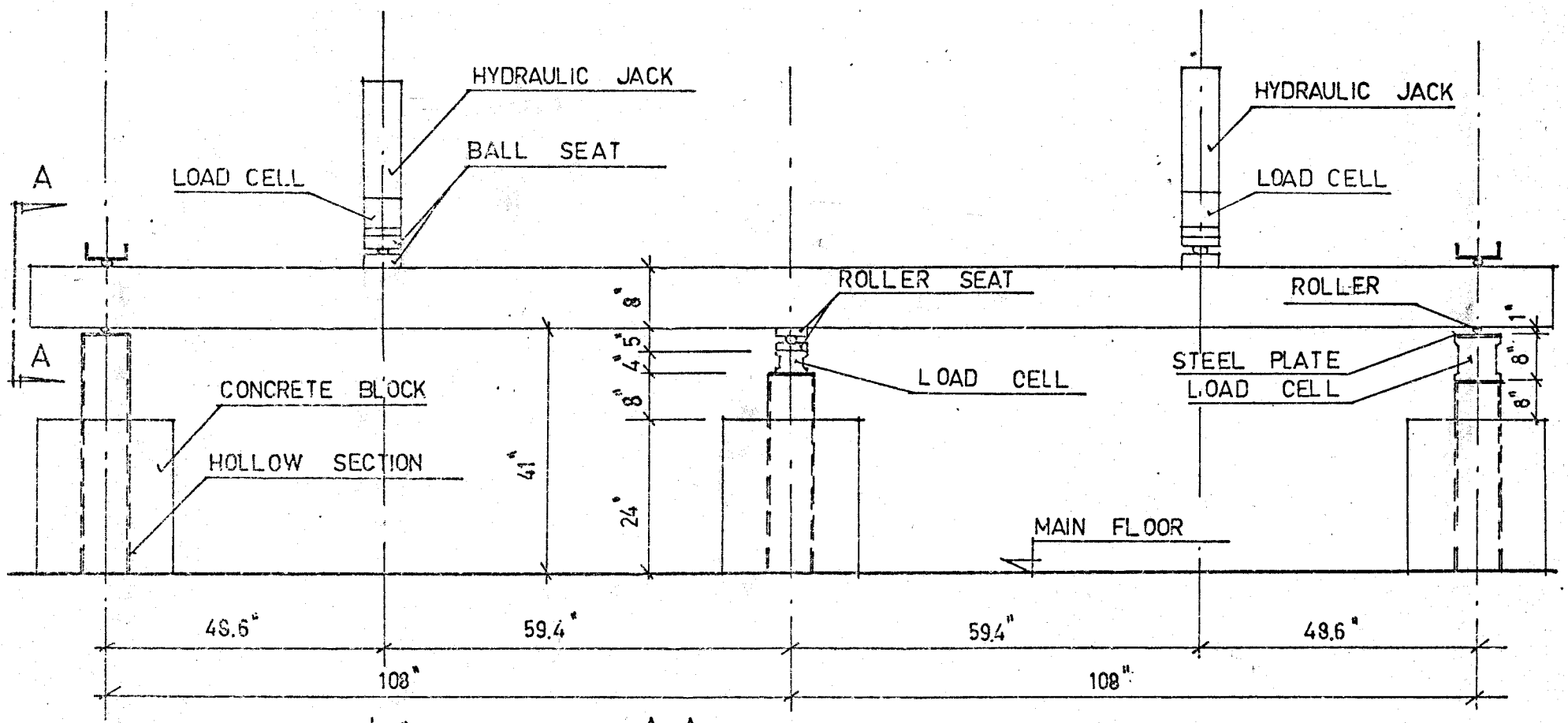

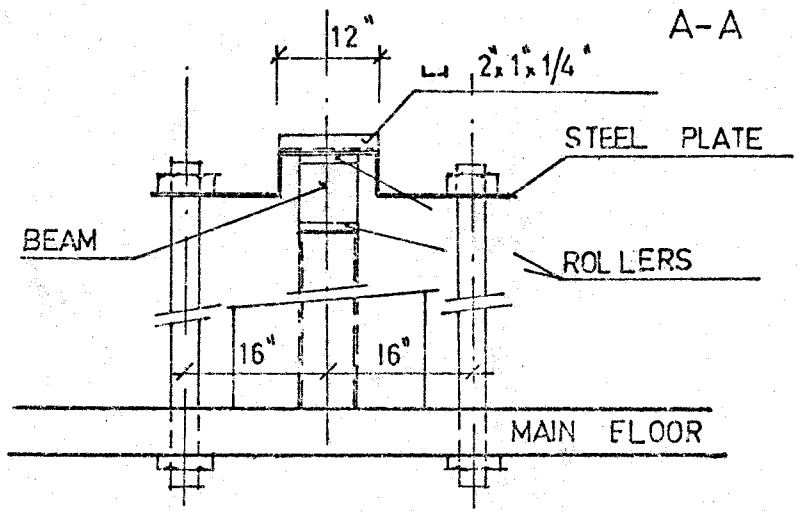

FIG. 2.4. SET UP OF THE TEST

The set-up is shown in Fig. 2.5.

e) Load sensing apparatus: The load was applied by two hydraulic jacks. The control and adjustment of the load was done by using load-cells, which were inserted between the bottom at loading platform and the steel plate on the beam. Similar load-cells were used for measuring the reactions. A full bridge of electrical resistance type metafilm strain gauges from Budd Instruments Limited, were glued to the load cells with GA-5 efoty cement. The load cells were calibrated in a 120 kip Tinius-Olsen Testing Machine. The calibration curves were very nearly linear. The load cells for all the beam tests were connected to balancing and switching boxes which in turn were connected to a strain indicator.

2.5 DEMEC POINTS AND DIAL GAUGES-DISPLACEMENT

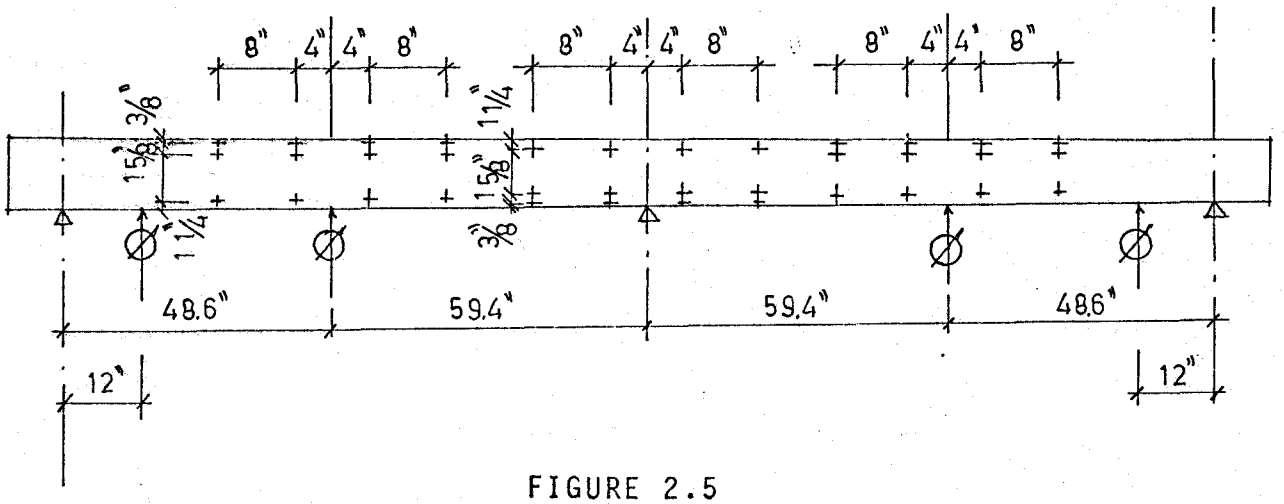

FIGURE 2.5

CHAPTER 3

BEAM ANALYSIS

3.1 INTRODUCTION

In conjunction with the beam tests which are described in Chapter 4, a method of analysis was sought which could accurately predict the behaviour of reinforced concrete beams under the conditions of repeating loading. The purpose of this chapter is to provide a detailed account of the numerical analysis evolved to facilitate prediction of the above mentioned behaviour.

The large number of important variables and the nature of repeated loading preclude the feasibility of an overall experimental type of analysis. Therefore, the choice of the beam testing program was orientated by the desire to eliminate most of the variables and to choose conditions which would serve as a relatively simple but meaningful test case for comparison with the analytical method.

To be able to provide cycle loading and create the conditions for building up the residual stresses and residual moments which can eventually result in forming a mechanism, there was a need to have an indeterminate structure. It was decided that all test beams and therefore all beams analysed will be continuous, with two equal spans. The single point loads on each span were applied symmetrically about the middle

support. Placing of the loads was 0.45L from the outside supports. This position of the loads was chosen to produce a reasonably high ratio of the proportional collapse load over the shake-down load.

The plastic analysis was worked out mostly on the principles of the behaviour of the mild steel. Because one of the objectives of this research program was to establish if the plastic theory can be directly applied also to reinforced concrete structures, it was necessary to have a cross-section which has the overall behaviour very close to that of the mild steel. This was the reason for choosing the underreinforced cross-section which has the moment-curvature relationship almost identical with the moment-curvature relationship for the mild steel. The underreinforced ratios also typifies normal design practise.

3.2 RANGE OF PARAMETERS

The range of parameters used in the analysis were very limited. However any of the parameters mentioned in this section could be varied without changing the method of analysis.

a) Beam Dimensions

All the beams analysed in this section have an overall length of 20 feet with two spans, each 9 feet long.

b) Cross-Section Dimensions

The beams have the same cross-section. The size used

was a 8 inch by 8 inch section with four number 6 reinforcing bars, or eight number 4 reinforcing bars. The dimensions of the cross-sections, position of the reinforced bars and also the spacing of the ties are shown in Fig. 4.1.

c) Concrete

In conjunction with each beam tested, tests were carried out on the standard cylinders to establish the stress-strain relationship for the concrete. This stress-strain diagram was than compared to the theoretical stress-strain relationship for the established concrete strength as introduced by SINHA[3] and HOGNESTAD and McHENRY[1]. The mathematical curve for the stress-strain relationship which matched up best with the cylinder test results was then used in the numerical analysis.

d) Steel

A concrete cover for the deformed reinforcing bars mentioned in (b) was 1 inch. There was a small variation in the yield stress as shown in Table 2.4 and the average yield stress was 60.2 ksi except for the bars #4, where the yield stress was 56 ksi. The idealized shape permitted a simplification of the calculations and was thought to be justified in that there is very little discrepancies between the real and the idealized stress-strain relationship.

e) Age of Loading

Because of some technical difficulties most of the tests were not carried out at the age of 28 days after

casting. However the stress-strain relationship for the concrete was measured in the same day and therefore the influence of the age of the concrete was eliminated.

f) Atmospheric Conditions

In general, the atmospheric conditions were relatively similar considering the curing period. Variations in the temperature and humidity in the laboratory where the tests were done occurred but hopefully the tests of the concrete stress-strain relationship accounted for any effect of these variations.

3.3 ASSUMPTIONS

Various assumptions were included in the analysis. The assumptions which are listed below can be divided into three groups. These are:

a) Assumptions which have been verified by the author and other investigators.

1. Strain Variation: Plane sections perpendicular to the axis of the member before loading remain plane after application of load and moment.
2. Effect of Ties: The effect of ties upon the strength of the section and the stress-strain relationship of the concrete may be ignored. Calculations show that even at yielding stress in the ties, very little confining influence could be exerted due to confining effect.

b) Many of the assumptions summarized in this group resulted from the lack of an absolute numerical evaluation of their influence. The effect of these assumptions cannot be expressed in a quantitative manner, but their general influence on the analysis is known. The method of analysis could be adjusted to handle variations in the assumptions.

1. Effect of Bond

   The effect of the change in the cross-section between cracks was ignored. This change of cross-section is caused by bond between the concrete and steel.

2. Concrete Stress-Strain Relationship

   The concrete stress-strain relationship expressions which are the results of the experiments of HANSEN, HOGNESTAD[1] and SINHA[3] were used. The equations were compared with the back-up tests. A more complete description of the deviation of these curves is shown in section 2.2.3. The concrete strength in tension was ignored. Calculations show that there is very little influence of concrete strength in tension on the moment-curvature diagram. Tension in concrete was considered as a significant factor only for unloading of the cross-sections. It was assumed that the cracking strain for concrete in tension was 200 micro-inches per inch.

3. Steel Stress-Strain Relationship

The, ideal, elastic-plastic experimentaly verified steel stress-strain relationship shown in Fig. 2.3 was used. The strain-hardening of steel was not included in the analysis in order to obtain the, ideal, stress-strain relationship. Also the Bauschinger's effect, which could be described as a reduction of the yield limit for plastic flow in one sense, when there already had been a plastic flow in the opposite sense, was also ignored. The Bauschinger's effect would cause a slight change in the magnitude of the elastic range of the bending moment by variable repeated loading. It would be possible to do some additional tests to establish the real effect. However, it was felt that this small change in the magnitude of elastic moment would not be significant in the further analysis. Therefore the effect was ignored.

4. Plastic Moment (MP)

It was assumed that the value of the MP is the highest magnitude of the moment in the moment-curvature diagram (Fig. 3.1) and that this value of MP stays unchanged throughout the cycles of loading.

MOMENT – CURVATURE DIAGRAM

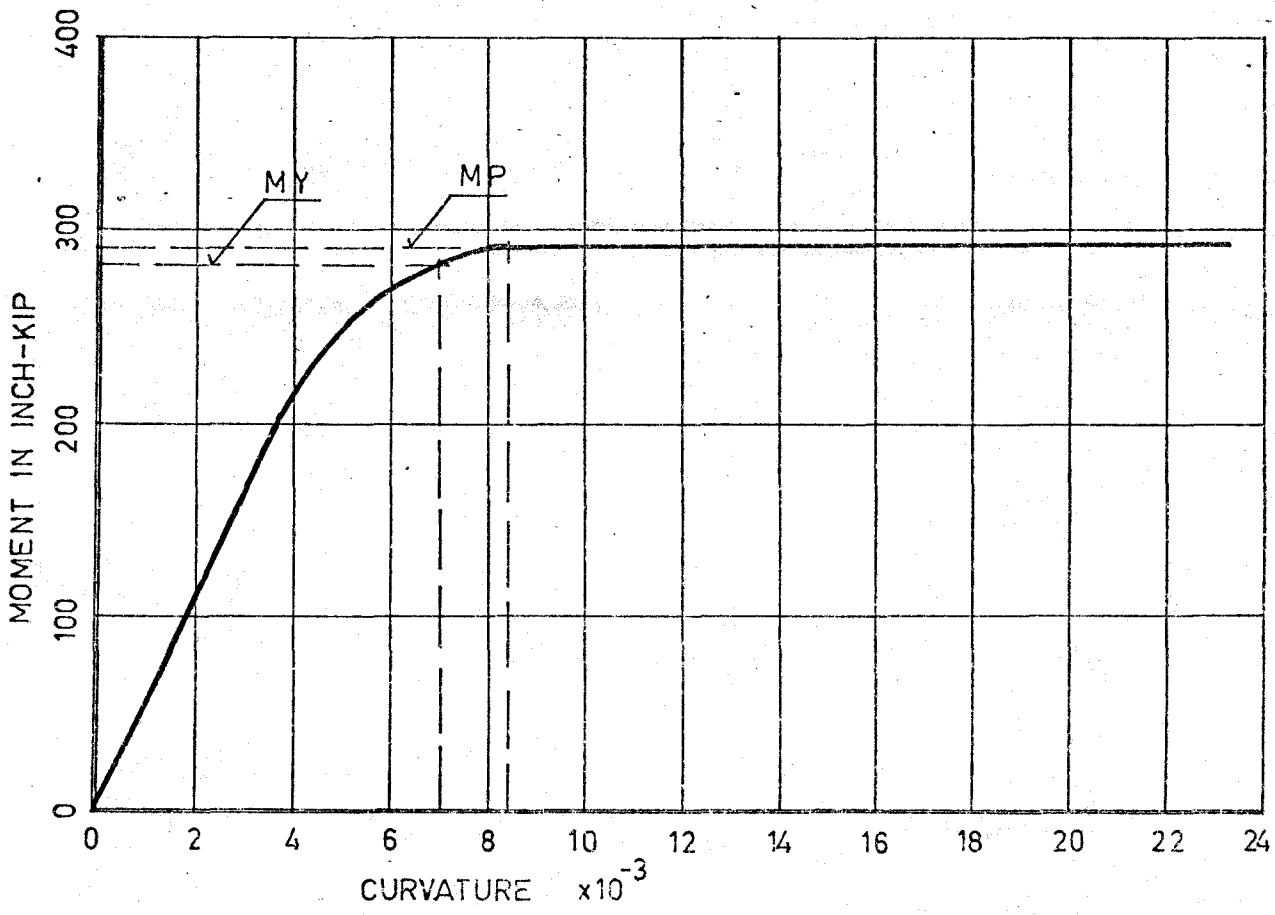

VALUES OF MP AND MY

FC	3 000	3 400	3 750	TEST 1, 2 3 100
MP	289	291	293	249
MY	272	274	276	230

FIG. 3.1. THEORETICAL VALUES OF MP AND MY

5. Plastic Hinge

When a section has developed the full plastic moment capacity then a hinging action can occur at this section. This plastic hinge rotation takes place while the bending moment transmitted across the hinge remains constant. A plastic hinge can undergo rotation of a certain magnitude provided that the bending moment stays constant at the fully plastic value. The reinforced concrete beams tested in this research program had a symmetrical cross-section. The amount and position of the reinforced steel was equal on the top and bottom. This arrangement of reinforcement makes it impossible to reach at the same time a high stress in concrete, yield stress in the tension steel and yield stress in the compression steel. Therefore, in this numerical analysis, the reinforced concrete cross-section in which concrete is in the inelastic region, tension steel is at the yield stress and the compression steel has not reached the yield point is considered as fully plastic.

6. Length of the Plastic Hinge

As the length of the plastic hinge is assumed to be the length of the beam on which the applied bending moment is equal to or greater than the bending moment MY (Fig. 3.1). The curvature in

the cross-sections throughout the hinge length is assumed to be equal to average curvature, which is calculated from the rotation of the hinge over the hinge length.

7. Shrinkage

The effect of shrinkage was not included in this analysis. It has been shown by calculation that its effect is not significant.

c) The following assumption is of the type which have facilitated the computer application of this analysis.

Weight of the Beam

The weight of the beam is small when compared to the applied load, therefore it was ignored in this analysis.

3.4 ANALYTICAL METHOD

The analysis of a continuous reinforced concrete beam with two equal spans will be discussed in detail in this section. Two of the tests, #1 and #10, were done as the tests for proportional loading. The analyses for these tests were done by adding a small adjustment to the analysis for variable repeated loading. The proportional loading tests were helpful in the establishing of the fully plastic moment for the given cross-section as well as in the establishing of the collapse load.

3.4.1 CALCULATION

The numerical solution of the beam analysis was carried out on an CDC 6400 Computer. The computer program is reproduced in Appendix.

The length of the beam was divided into 26 small segments. The cross-sections along the beam length could be spaced so closely that the distance between them would be infinitely small. Then the calculation of the change in slope between sections and the displacement could be very accurately performed by using the average of the curvatures between adjacent cross sections. The practical solution required that the beam be divided into a limited number of segments. Dividing the length into 26 segments produced reasonably correct deflected shapes. The time required for calculation was nearly directly proportional to the number of beam segments used. Dividing the beam into a fewer segments will cause decreasing accuracy in the prediction of the deflected shape of the beam. The calculation employes the average curvature over the segment length and by increasing the length of the segment the average curvature becomes less and less accurate. When the number of segments will establish the length of a segment to be more than 15 inches, the iteration procedures which used to calculate the deflected shape tend to become inefficient due to slow convergence. An increase in the number of segments provides more accurate calculation, but the number of variables in computer program increases so

rapidly that it can result in exceeding the computor memory capacity and the increase in the ratio of accuracy is very small.

a) Input Information for the Computer Program: For the computer solution of the problem the following information was given as an input. The information was either read as variable data or were given a constant value in the program.

1) Beam Characteristics

11) Dimensions of the length, width and thickness of the beam.

12) Number and length of the segments also the distance of each cross-section from the left hand support.

13) Information about the position and the magnitude of the load.

14) Area and location of longitudinal reinforcing steel.

15) Value of the fully plastic moment MP for the given cross-section and the value of the moment when the tension steel starts yielding (MY).

2) Material Properties

21) Stress-strain relationship for steel indicating a modulus of elasticity, yield strain and yield stress.

22) Concrete stress-strain relationship. Given were a set of three equations. One was the equation of the envelope of the stress-strain curves for a given concrete. One was for unloading and one for reloading. Along with the equations, a set of the coefficients was given. These are different for every strength of concrete.

3) Program Limits and Range

31) Set limits for iterative cycles for calculating strain to balance load and moment at a cross section.

32) Assign limit to cycles for converging on the correct deflected shape.

33) Let the number of load cycles for incremental collapse.

b) Initial Estimates and Iterative Procedures

ba) Moment Distribution: The evaluation of the fixed end moments for the given load gives us the initial estimate of the values for the balancing computations. The result of this iteration in the calculation of the moment over the middle support. Then the structure becomes statically determinant and the rest of the bending moments over the length of the beam can be calculated. Because the moment distribution method employs an unchanged stiffness throughout the beam, the method is only an approximate estimate. The correction of the bending moment diagram is the next step in the iteration. In the case that the loading conditions produce at any place bending moment which is higher or equal to MP then the adjusted B.M. diagram is known because the frame becomes determinant. This is facilitated by the properties of the plastic hinge.

When the moment diagram does not reach at any point the value of MP, an estimate of the correct moment diagram is made by using the moment-curvature relationship.and satisfying compatibility of displacements and equilibrium. This process is continued through a certain number of converging cycles until

the correct deflected shape of the beam is known and therefore a correct bending moment diagram. These iteration cycles are more particularly described in section (bc).

bb) Balancing the Cross-Section

Each cross-section is divided into 20 strips. First the strain in the top fibres and the centroid of the cross-section for the initial loading are estimated. From the geometry of the section the strain at each strip and also at the centroid of the tension and compression steel is known. Using the equations for the stress-strain relationship both for concrete and steel the values of stresses throughout the cross-section are calculated. Simply by multiplying the area of each strip by the average stress in the strip and then adding these values for all strips the magnitude of compression force in the concrete is obtained. Because the point of application of the compression force in each small strip is near the centroid of each strip, the resultant of the compression in the concrete can be computed. Also the magnitude and the position of the tension and the compression forces in the reinforcing steel are known. The first condition for a balanced section is that the sum of the internal and external axial force is equal to zero. When this condition is not satisfied, the centroid of the cross-section has to be moved until the condition is fulfilled to within a certain accuracy. This accuracy limit was for practical reasons set at 100 lb.

When the section is balanced for the first condition the

internal moment is computed and compared to external moment. In this second step in the iteration the initial estimated strain is changed to a strain which produces an internal moment of a magnitude and sign closer to the external moment. The satisfactory accuracy limit for this step was set at 0.5 inch-kip difference between internal and external bending moment. Once the section is balanced for both conditions, all informations about the strains and stresses throughout the cross-section are stored in the computer's memory. For unloading and reloading the section the important information is the strains and the stresses from previous loading stages. Using the equations for the stress-strain relationship for unloading and reloading, the same iteration steps as are mentioned above are followed. When the section is in the unloading stage, the residual strain at zero stress is calculated and added to the stored information for each strip as well as for the reinforcing steel. The equation for the reloading stress-strain relationship for concrete is an equation of a straight line and by alteration can happen that values of stress beyond the range of stress-strain curve could be taken into further calculation. Therefore a limit was set to this equation so that the values of stress could not exceed the values given by the original stress-strain curve.

bc) Deflected Shape of the Beam

Using the applied load and the assumed bending moment diagram, the strain distribution required to provide

resisting moments was computed as described in section (bb). From these strain values the curvature was found. Assuming the average curvature over the segment length the value of the average curvature is calculated. Calculation of the deflected shape is illustrated in Fig. 3.3.

The result of this calculation is a deflected shape of the beam shown in Fig. 3.4. This calculation is started from the left hand support. To get the real deflected shape for an estimate moment diagram the curve which represents the deflection must be rotated to lie on the right hand support (Fig. 3.4.b). This curve represents the real deflected shape for the assumed moment diagram. If the moment diagram was correct, then the curve has zero deflection over the middle support. If the magnitude of the deflection at the middle support is not equal to zero, then the assumed moment diagram was incorrect. The first iteration step is to choose a new magnitude for the moment over the middle support, then compute the new moment diagram and from this the new deflected shape. When finally the deflection at the central support reaches zero, the moment diagram is correct. A limit for this iteration step in the computor program was chosen for deflection at the central support. It was assumed that a value of less than ±0.01 inch deflection is sufficiently accurate. This limit corresponds to a change in the moment at the middle support of ±2 inch kips.

In the case that bending moment either reaches the

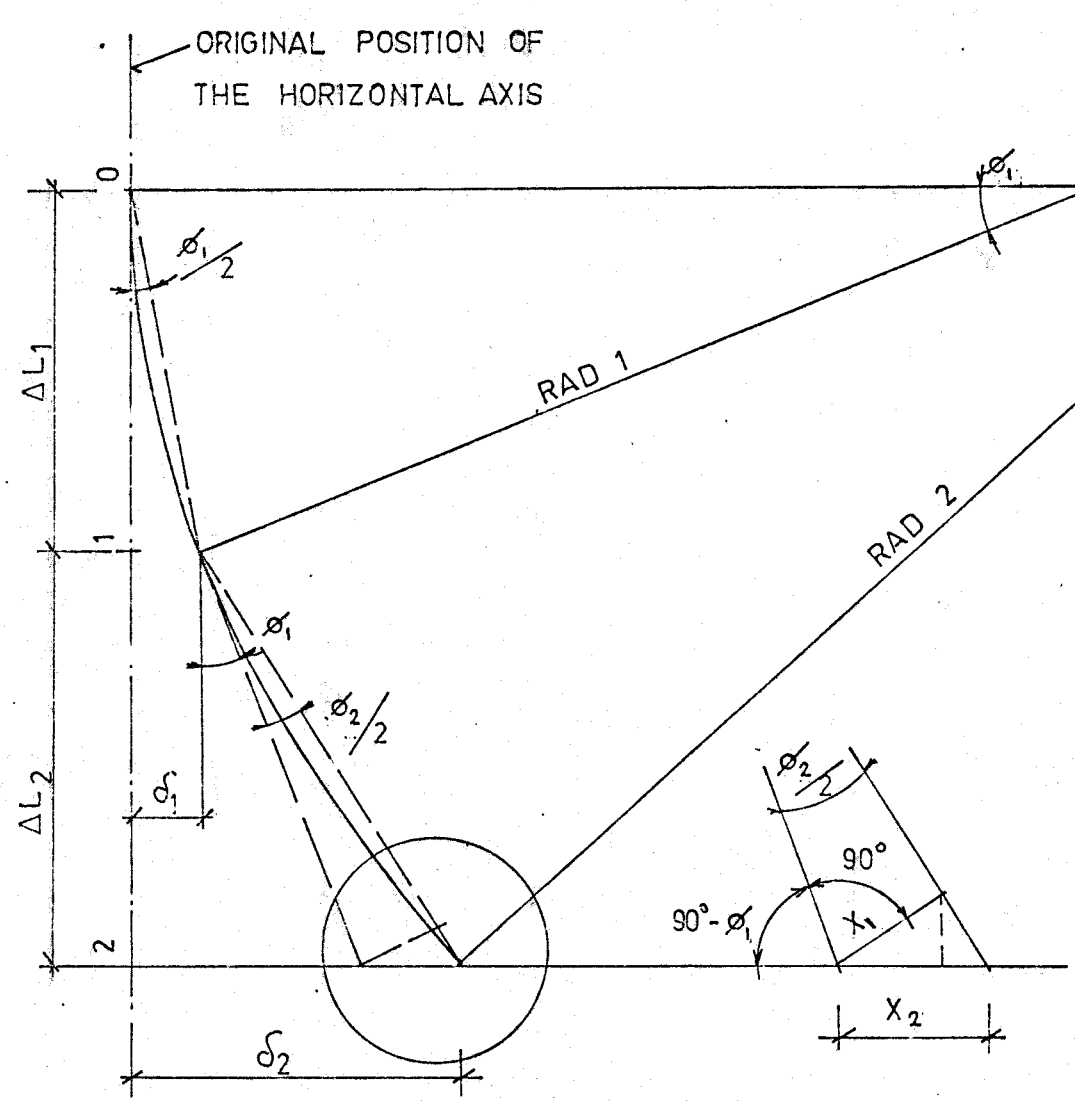

$$RAD\,1 = \frac{2}{CURV\,0 + CURV\,1}$$

$$RAD\,2 = \frac{2}{CURV\,1 + CURV\,2}$$

$$\phi_1 = TAN^{-1}\left(\frac{\Delta L_1}{RAD\,1}\right)$$

$$\phi_2 = TAN^{-1}\left(\frac{\Delta L_2}{RAD\,2}\right)$$

$$\delta_1 = \Delta L_1 \times TAN\left(\phi_1/2\right) - \frac{\Delta L_1^2}{RAD\,1}$$

$$\delta_2 = \delta_1 + \phi_1 \times \Delta L_2 + \frac{\Delta L_2^2}{RAD\,2}$$

$$X_1 = \frac{\Delta L_2^2}{RAD\,2}$$

$$X_2 = \frac{X_1}{\cos(\phi_1)} \doteq X_1$$

FIG. 3.3. BEAM DEFLECTION CALCULATION

a) ASSUMED MOMENT DIAGRAM

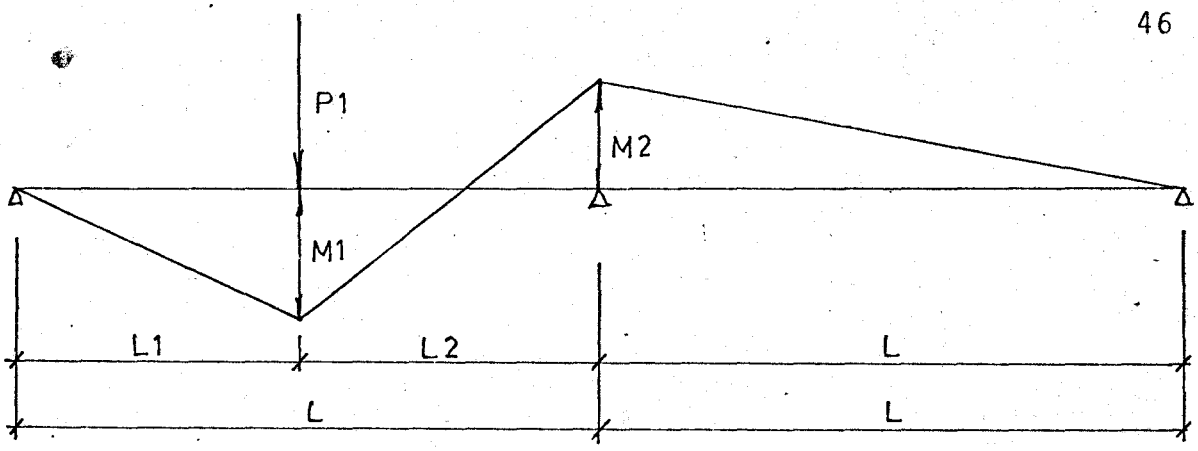

b) DEFLECTED SHAPE OF THE BEAM

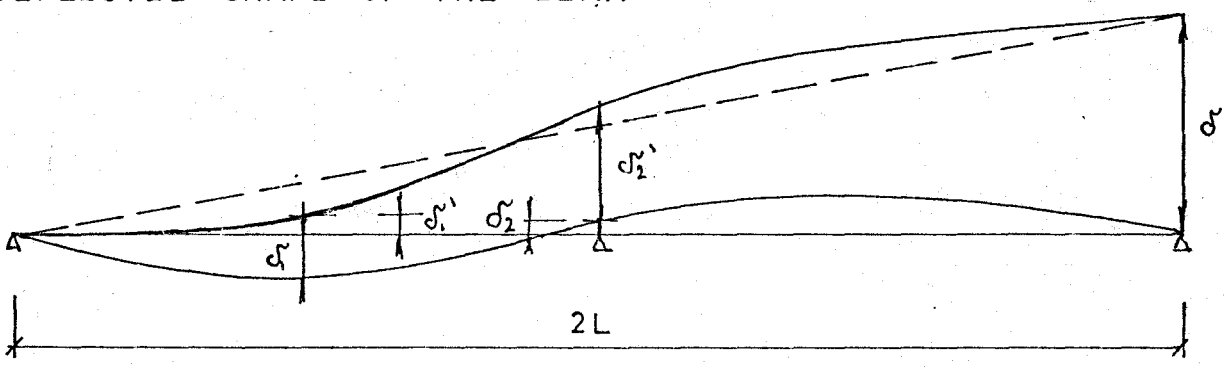

$$\delta_1 = \frac{\delta}{2L} \times L1 - \delta_1'$$

$$\delta_2 = \frac{\delta}{2} - \delta_2' \neq 0$$

c) CORRECTED MOMENT DIAGRAM

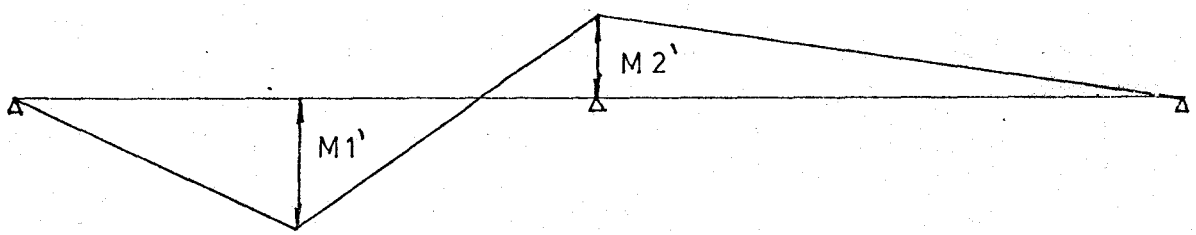

d) NEW DEFLECTED SHAPE OF THE BEAM

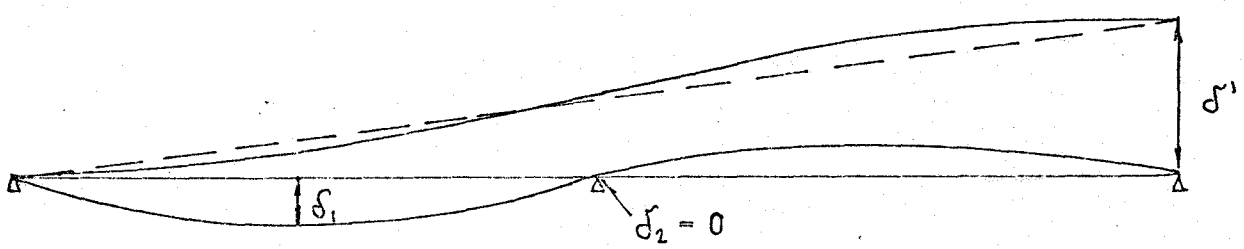

FIG.34. CALCULATION OF DEFLECTION WHEN BM ≤ MP

value of MP or is greater than MP, the exact moment diagram is known and therefore it is possible to compute the correct deflected shape of the beam. There are three possible cases for the development of plastic moments:

1. Fully plastic moment is in the left span.
2. Fully plastic moment is in the right span.
3. Fully plastic moment is at the middle support.

In the first case the calculation of the deflected shape of the beam uses the radii of curvatures for each segment starting from the right support (see Fig. 3.5). Using the assumption that the length of the plastic hinge is equal to the distance between the two moments MY, then the length and position of the plastic hinge are known. The deviation of deflections are evaluated as was described above up to the segment where the segment length containing the beginning of the plastic hinge - where the first MY is located. Because it is known that the moment diagram is correct and hence so are deviations of deflections, the procedure is to simply rotate this part of the deflection curve until it goes through the middle support. This step establishes the magnitude of deflections over the length from one end of the beam to the beginning of the plastic hinge. The deflections under both extremities of the plastic hinge are assumed to be the same. The next computation consists of the same calculation from the other end of the beam. This time the length of the deflection curve is rotated until it matches up with the

BENDING MOMENT DIAGRAM

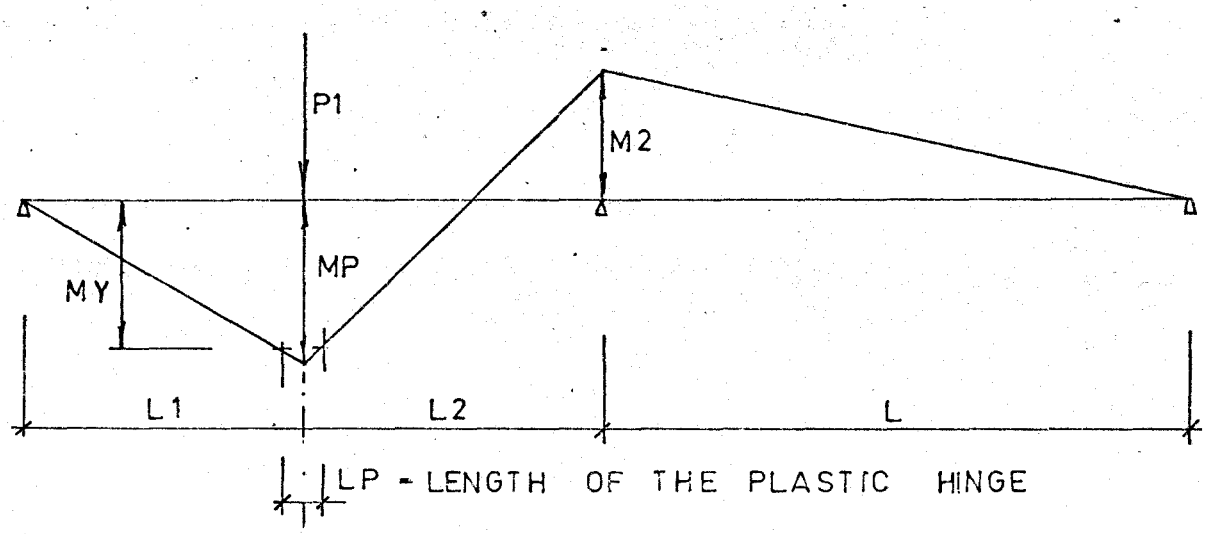

DEFLECTED SHAPE

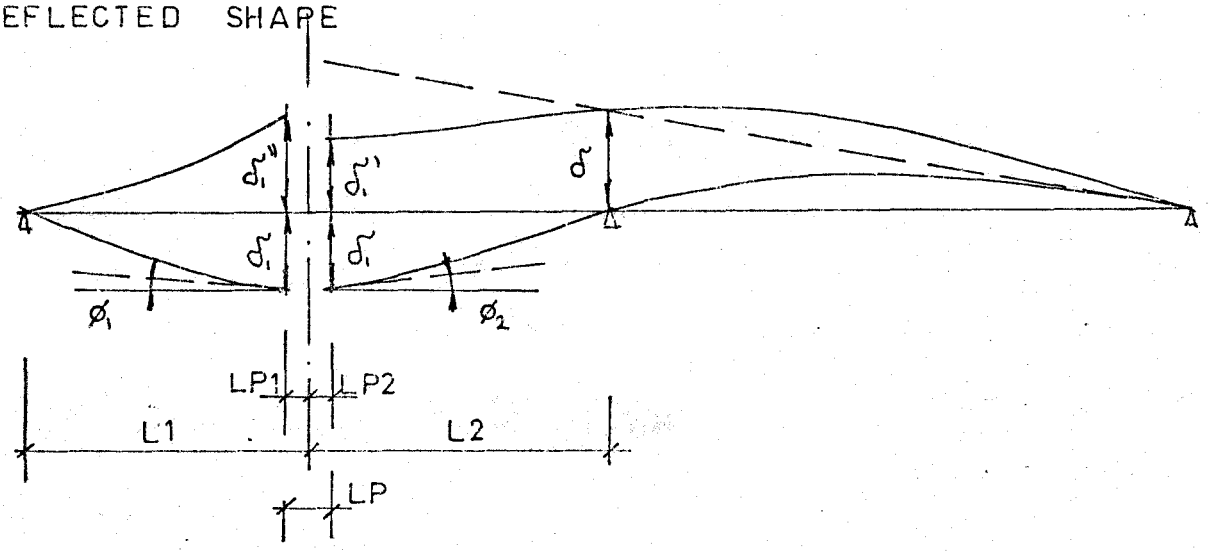

$$\delta_1 = \frac{\delta}{L} \times (L + L2 - LP2) - \delta_1'$$

THE AVERAGE CURVATURE OVER THE PLASTIC HINGE LENGTH =

$= (\phi_1 + \phi_2) / LP$

FIG. 3.5. CALCULATION OF DEFLECTION WHEN M1=MP

magnitude of deflection at the other side of the plastic hinge.

To accomodate compatibility of deflections the plastic hinge has to undergo a certain rotation. This rotation is defined as the sum of angles ϕ_1 and ϕ_2 which is equal in magnitude to the angle between the tangents to the deflection curve at the extremities of the plastic hinge (Fig. 3.5). Once the rotation which occurs at the plastic hinge is calculated, then it is possible to compute the strain distribution over this cross-section using the average curvature over the plastic hinge length. This average curvature is equal to the value of hinge rotation divided by the hinge length.

In the second and third case, when MP is in the right span or at the middle support, the same procedure is followed except that the calculation for the deviation of deflections starts from the left hand support.

c) Loading Cycles and Residual Moments: One loading cycle consists of three loading stages and three unloading stages. The loads are applied in the following sequence:

1. Load on the left span
2. Unload the left span
3. Load on the right span
4. Unload the right span
5. Load on both spans
6. Unload both spans

The loading cycle is shown in Fig. 3.6.

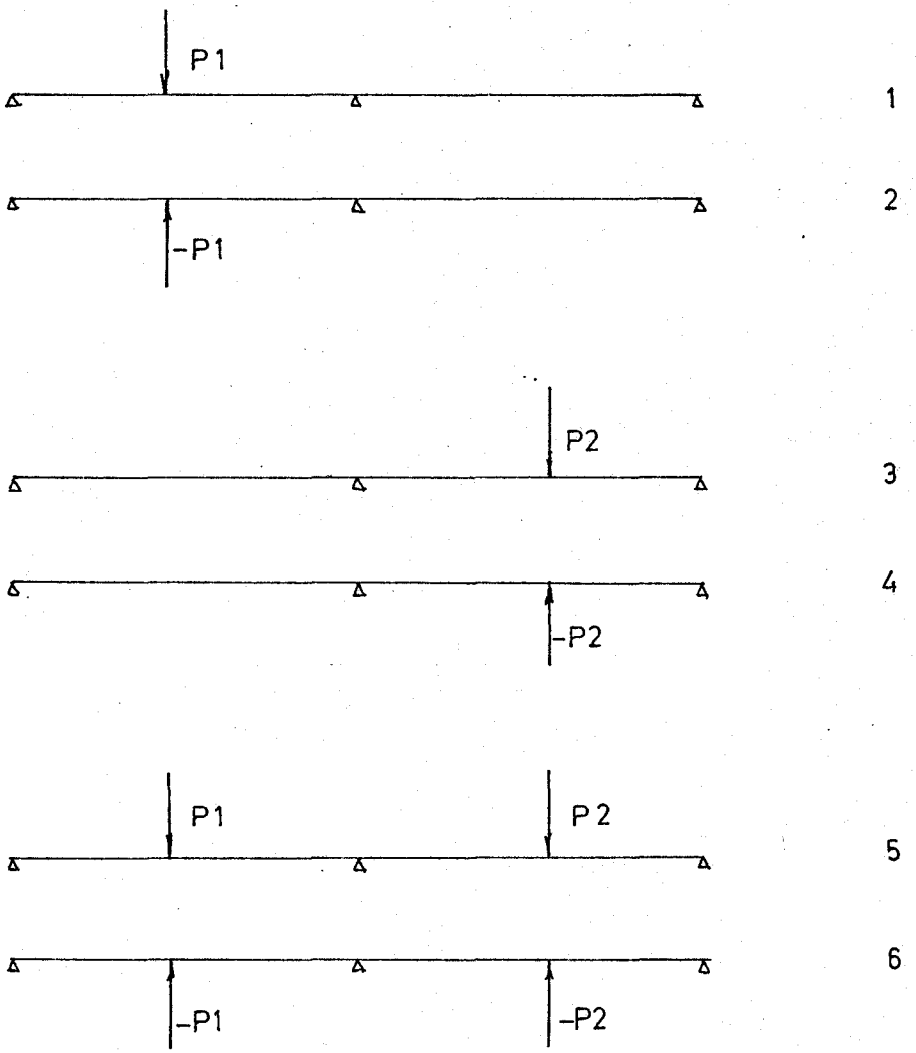

FIG. 3.6. LOADING CYCLE

In the three loading stages the moment diagrams are computed by using the moment distribution method and in the case where the bending moments do not reach the value of fully plastic moment the diagram is corrected by iteration procedures as was described in section (bc). After these

procedures the distribution of bending moments throughout the beam length are known and the magnitude of deflection in each chosen segment and all necessary informations about the chosen cross-sections are calculated. When a plastic hinge forms, from compatibility of deformations the hinge rotation is determined and the length of the plastic hinge is calculated from the shape of the bending moment diagram.

The shape of residual B.M. is known, because the beam is statically inditerminate to one degree & it is necessary only to estimate the magnitude.
After a few converging iteration cycles when the curve which represents the deflected shape of the unloaded beam sits on all three supports, the correct residual moment diagram has been found. These residual moments are important for the next loading stage where these moments are added to those calculated by the moment distribution method as a first trial. The residual strains and stresses in all the strips of the cross-sections are recorded and used for balancing the sections for a new set of bending moments from the next loading stage. The magnitudes and positions of loads used in the analytical program are the same as specified in the tests.

3.5 MORE GENERAL APPLICATION OF THE METHOD OF BEAM ANALYSIS

The finite element method has proven to be a valuable tool for the analysis of various members and structures. The less sophisticated form used here seemed very satisfactory for beam analysis. The basic principles involved may be programmed

to provide solutions for a wider range of boundary conditions. The iterative techniques were highly specialized and would require adjustments for a wider application. Even with the use of high speed computers, the CDC 6400 in this case, the method developed here was very time consuming and would be impractical for design purposes. The analysis does however provide an alternative and complimentary means for studying shake-down effects. The computer program can be used up to a magnitude of the load close to that of collapse load. The program stops as soon as the collapse mechanism has developed. The loads which produce a distribution of bending moment with one plastic hinge and one or two values very close to MP can easy stop the computor program because due to iterative technique, the magnitude of the moments close to MP might be changed into MP and create an apparent collapse mechanism.

CHAPTER 4

THE RESULTS OF THE BEAM TESTS AND THE NUMERICAL BEAM ANALYSIS

4.1 INTRODUCTION

This chapter provides complete information about the test data which are compared with the results of the numerical analysis. In the first part there are the descriptions of the proportional loading tests which were done on two test specimens with different cross-sections. The results are compared with the results of the adjusted numerical analysis. The second part contains the test results of 8 test specimens subjected to variable repeated loading. Plotted are data of deflection, strain measurements and curvatures along with interpretation of some typical strain history readings in the tension steel by using the idealized stress-strain relationship. The test data are compared with the datas obtained by using the numerical analysis which was explained in Chapter 3. In the last part of this chapter all the datas from the tests and the analysis for each critical cross-section at each critical loading stage are accumulated to facilitate comparison.

The fabrication and instrumentation of the test beams, the material used, the properties of materials and the test equipment were described in Chapter 2. The test procedure is described in this chapter.

4.2 RANGE OF THE BEAM TESTS

The beam testing program concentrated on only one type of beam. The beam dimensions, material properties and testing methods were standardized as well as possible. The dimensions of the test beam are shown in Figure 4.1.

A concrete mix with a designed 28 day cylinder strength of 3750 psi was used throughout the tests. Naturally, even though a standard mix was used, variations in strength occurred for each test. The discussion of the causes and the methods for handling concrete strength variations was included in Section 2.2. Four of the beams (#3, #4, #5, #6) tested with variable repeated loading are shown in Fig. 4.2.a and b.

The position, percentage and type of reinforcing steel as shown in Fig. 4.1, were the same in test beams #3 to #10 inclusive. The other type of reinforcing steel with a different yield point was used in the test beams #1 and #2.

All the beams were tested with the same equipment. The position of the load and program of the loading cycles remained constant throughout the tests. The tests #1 and #10 were proportional loading tests and their purpose was to determine fully plastic moment as well as the value of the proportional collapse load. In these tests the load was applied in both spans at the same time and the magnitude of the load was gradually increased until the collapse occurred. The rest of the beams were subjected to the previously specified program of load cycles to determine shake-down load. The number of

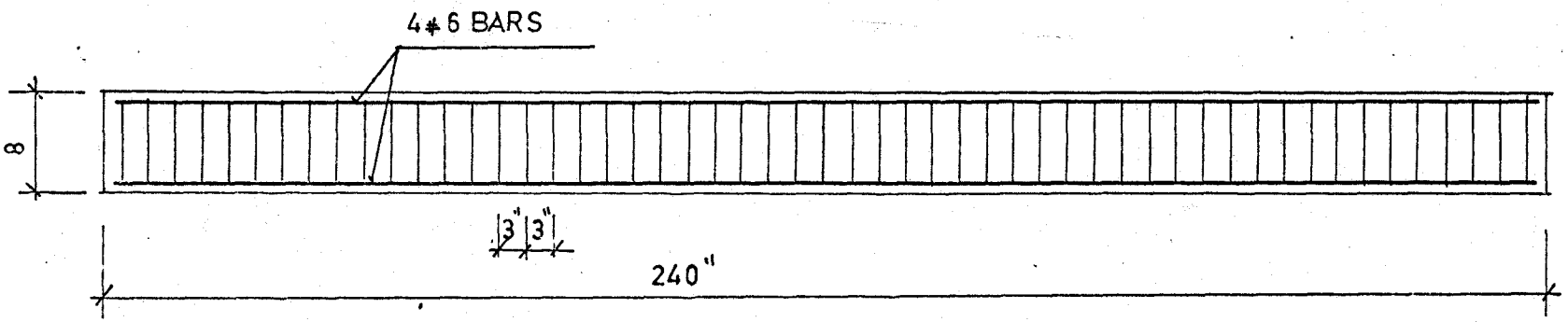

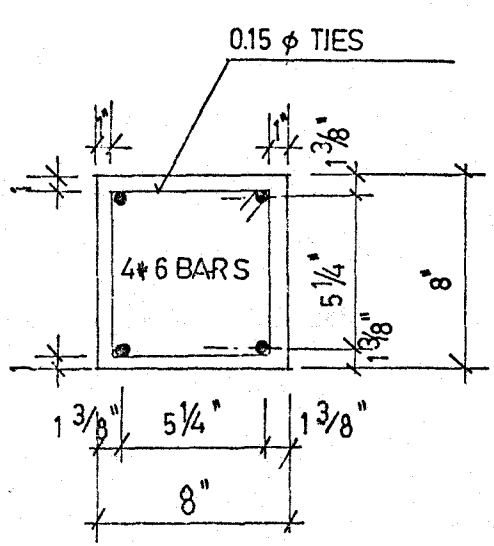

A – CROSS SECTION
BEAMS # 3 – 10

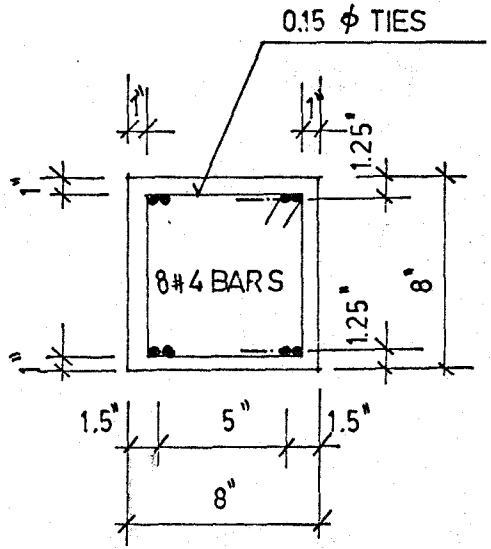

B – CROSS SECTION
BEAMS # 1-2

FIG. 4.1. DIMENSIONS OF THE BEAM

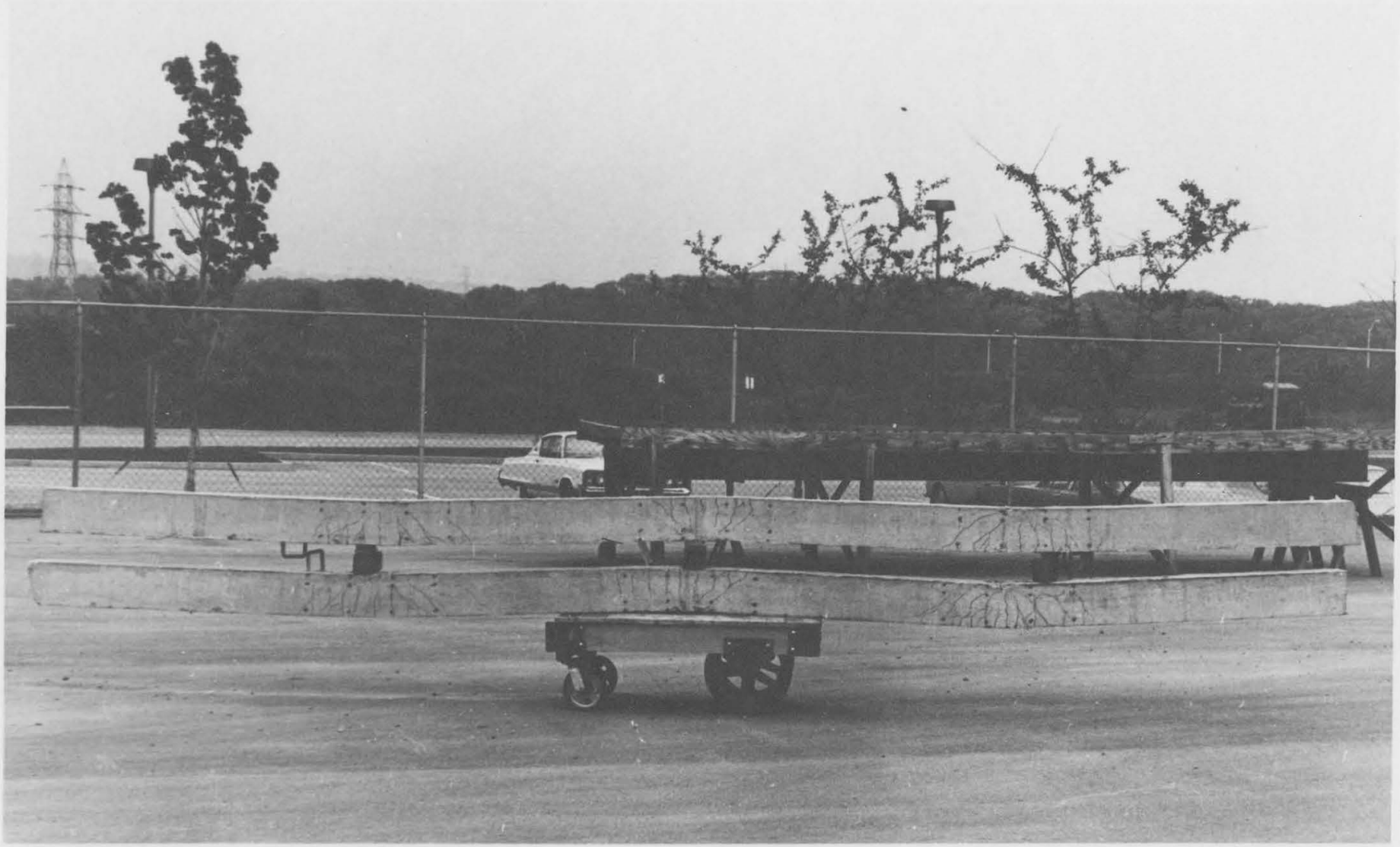

FIG. 4.2a. BEAMS # 3 AND # 4 AFTER TEST

FIG. 4.2.b. BEAMS #5 AND #6 AFTER TEST

cycles of load varied from 2 to 23 in this test program. The magnitude of the load throughout any single test remained constant. A test was stopped when failure occurred or when after a number of load cycles the deflections and strain measurements reached a stable state.

4.3 EVALUATION OF THE TEST RESULTS

One evaluation of the test results was done by using the second computer program. The program calculates from the geometry of the cross-section and from the strain readings the curvature and strain distribution throughout the cross-section.

A) Input Information to the Second Program

The following information was either read as data or was set at a constant value in the program:

1) dimensions of the cross section
2) location of the reinforcing steel
3) number of cross-sections where the strain measurements were taken
4) location of the demec-points or strain measurements along the side of the beam
5) the magnitude of the load
6) strain measurements at three levels in each section

B) Program Limits and Range

From the geometry of the cross-section and the strain measurements the program was designed to calculate the centroid of the section, the strains at the top and the bottom of the section, the strains in the level of reinforcing steel and the curvature of the cross-section. The calculation employed only the test strain readings in the compression zone of the cross-section. The third strain reading which was taken at the level of tension reinforcing steel was not accurate enough mainly due to the distribution of cracks.

The errors which were due to the strain reading including positioning of the demec points described in more detail in Chapter 5. Chapter 5 also contains descriptions of possible errors associated with the position of the load and the magnitude of the load.

4.4 PROPORTIONAL LOADING BEAM TESTS

Two of the 10 beams were tested on proportional loading. The purpose of these tests was to establish the fully plastic moment for a given cross-section as well as the value of proportional collapse load. The load was applied in both spans as is shown in Fig. 4.2 and was gradually increased until the collapse occurred. The load was applied slowly and maintained at constant values during the times required for taking deflections and strain readings.

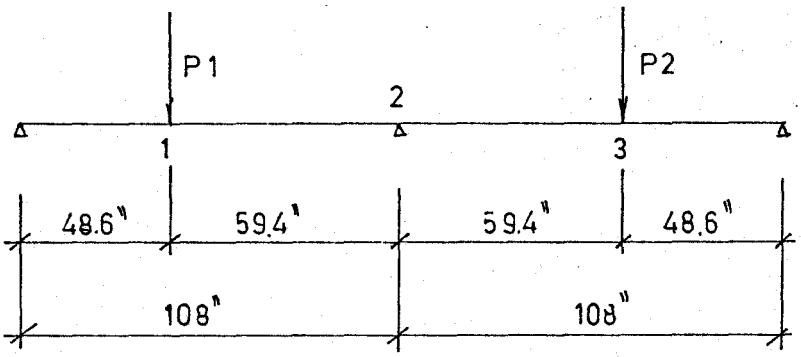

FIG. 4.2. PROPORTIONAL LOADING TEST

The evaluation of a theoretical internal moment was done by using the strain readings in the cross-section from the demec-points and then calculating the stress in the concrete and the steel using the stress-strain equations described in Section 2.2.3. By knowing all the forces in the cross-section the value of the bending moment was calculated. In addition to this theoretical moment-load and moment-curvature relation-ship in the test #10 also calculated and plotted were the actual moment-load and moment-curvature relationship, using the readings from the load-cells under the supports.

The computor program designed for variable repeated loading was adjusted so that it could be run also for proportional loading. Unfortunately the program was designed for a beam which has formed only 1 plastic hinge at any particular loading stage. Therefore by the critical loads of magnitude 13^K and 15^K the program stopped. As loads near those required to form additional plastic hinges were neared, the iterative

methods would not converge.

4.4.1 BEAM #1

The magnitude of the load was in the range 0 to 20 kip. The history of loading as well as the theoretical moment-load and moment-curvature relationship are shown in Fig. 4.3.

From the moment-load diagram it is evident that the critical load, when the creation of plastic hinges is taking place is 12^K - 16^K. The first plastic moment forms over the middle support, critical section #2, and is reached at a load of 12^K. Then the value of bending moment reaches the value of MP at the critical sections #1 and #3 at a magnitude of applied load of 12^K to 16^K. Then even if the magnitude of the load is increased the values of theoretical fully plastic moment remains constant. The further increase in load magnitude was enabled by increase in value of real plastic moment due to the strain hardening of reinforcing steel.

4.4.2 BEAM #10

In this proportional loading test the cross-section was slightly changed. The dimensions are the same as in the beam #1, but different reinforced steel with a higher yield stress was used.

The load was again in the range of 0 to 20 kips. The history of loading and the theoretical and actual moment-load diagram and the moment-curvature diagram are shown in Fig. 4.5.

MOMENT – LOAD RELATIONSHIP

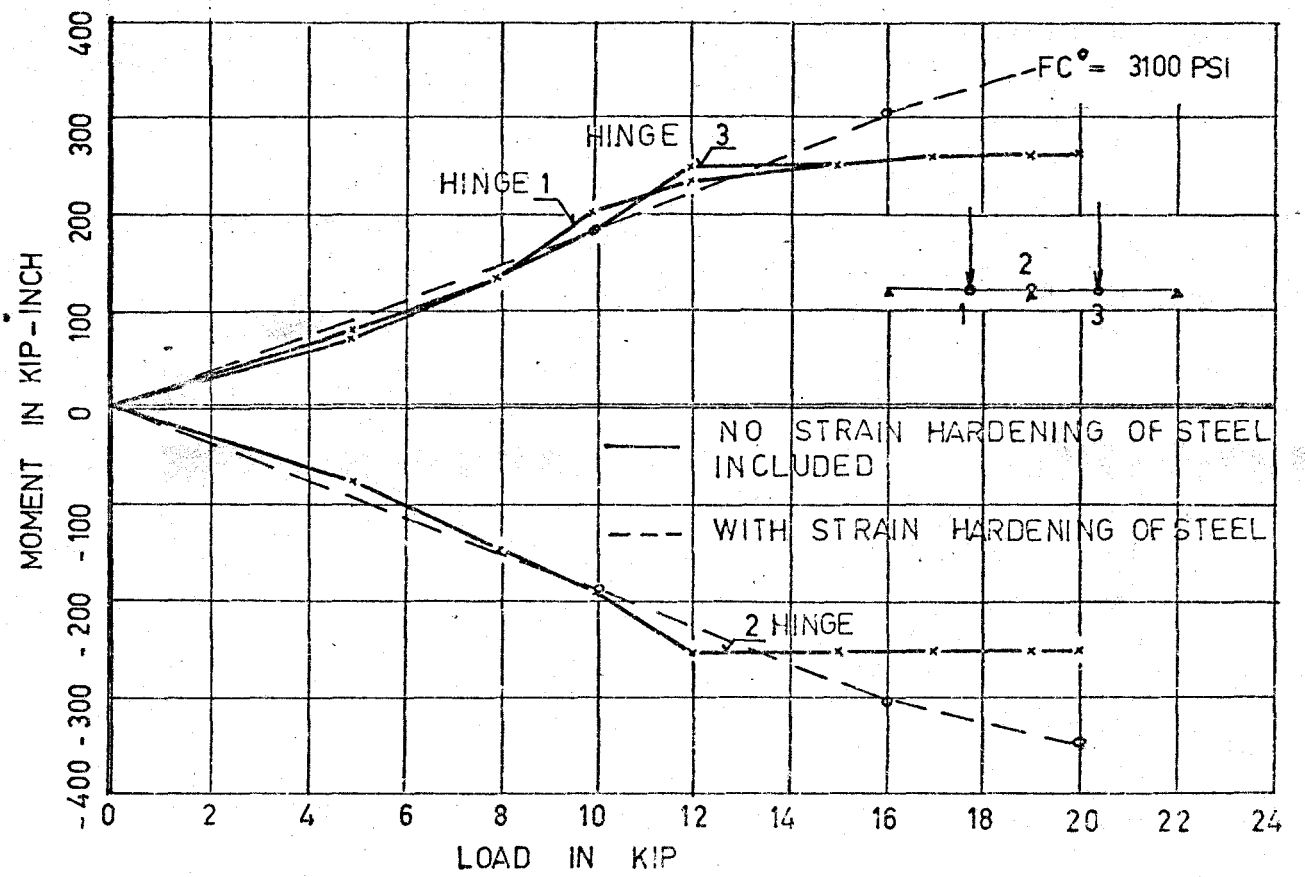

MOMENT IN BOTH DIAGRAMS IS CALCULATED FROM MEASURED STRAIN

MOMENT - CURVATURE RELATIONSHIP

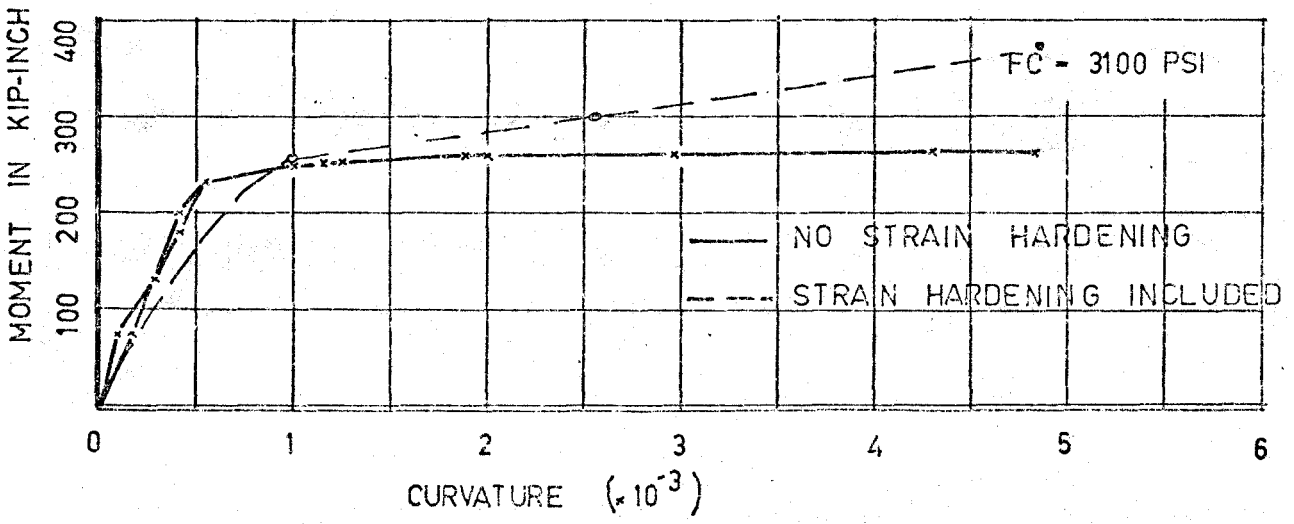

FIG. 4.3. MOMENT VERSUS LOAD AND CURVATURE - TEST # 1

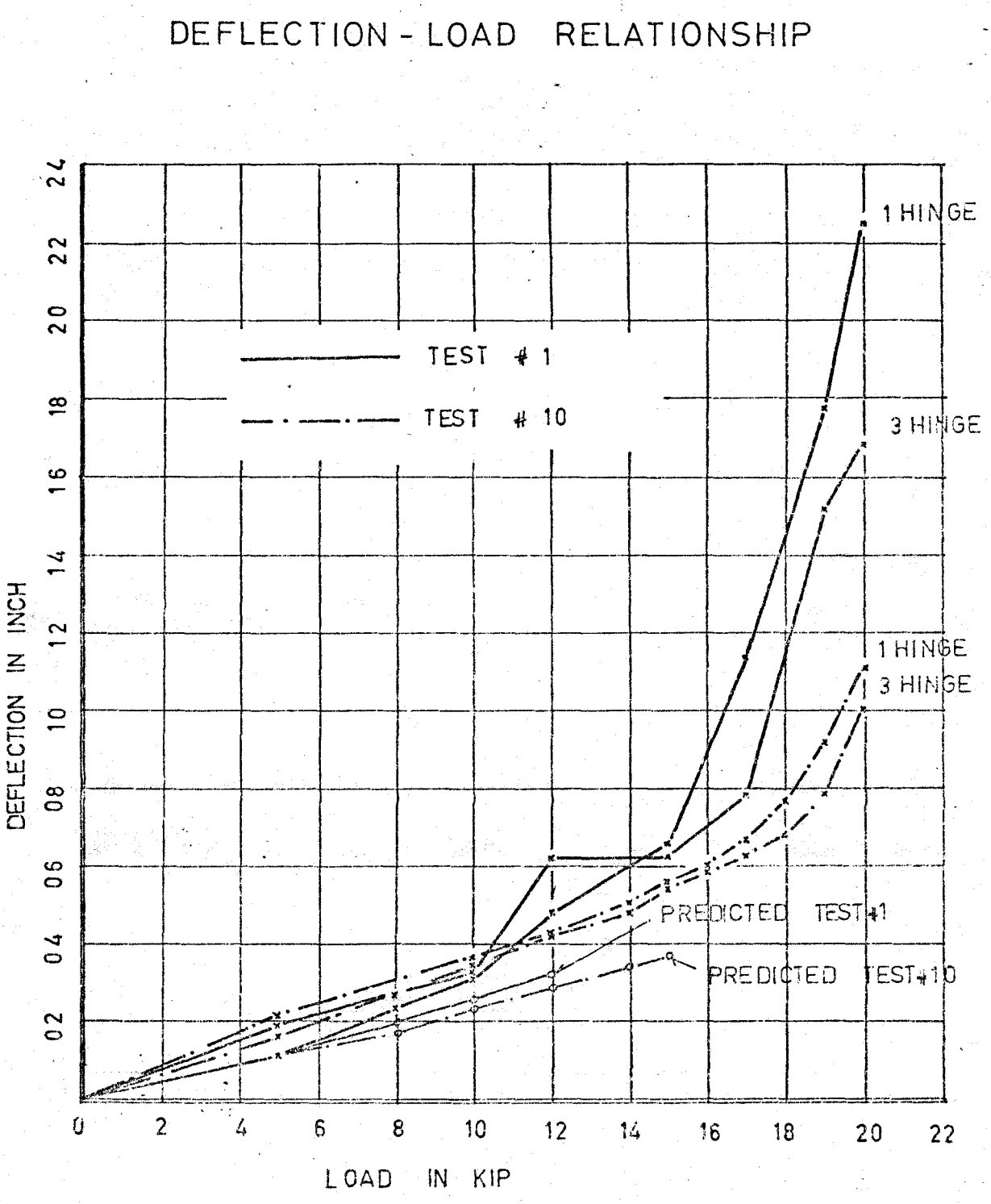

FIG. 4.4. DEFLECTION – LOAD RELATIONSHIP

MOMENT - LOAD RELATIONSHIP

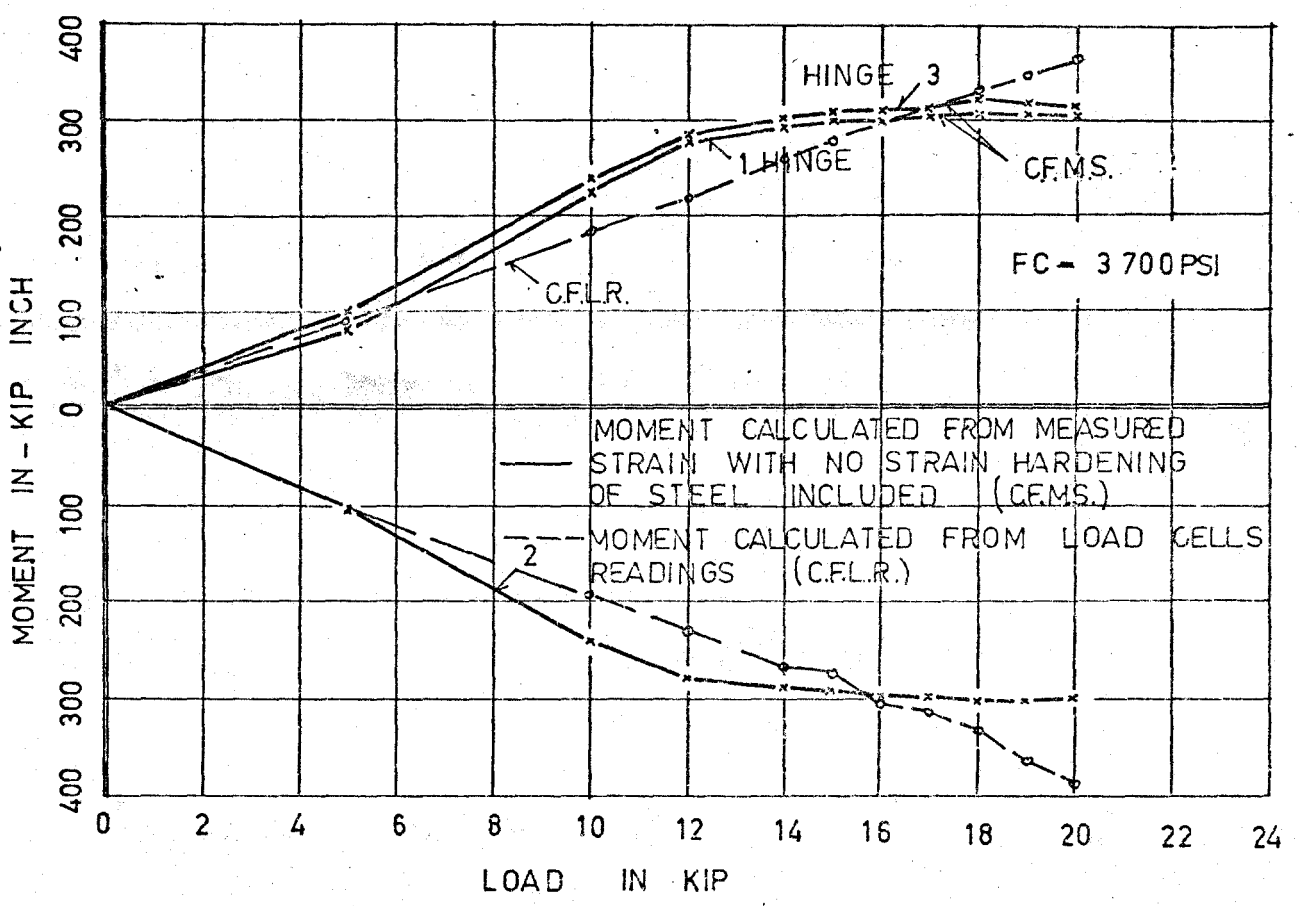

MOMENT - CURVATURE RELATIONSHIP

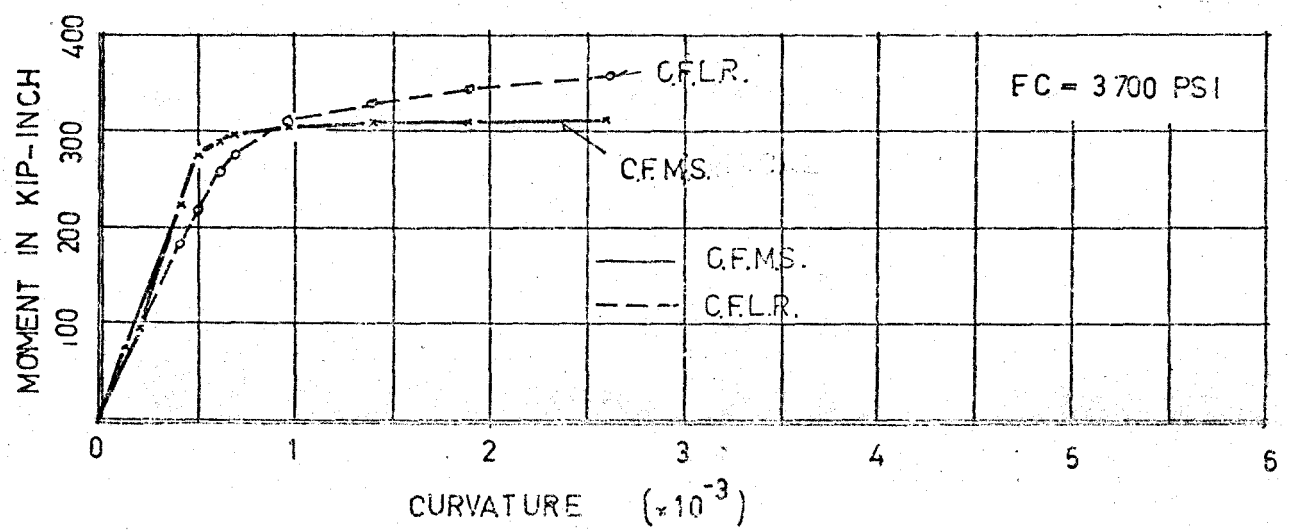

FIG. 4.5. MOMENT VERSUS LOAD AND CURVATURE TEST # 10

The load-deflection relationship is compared with the theoretical results of the numerical analysis in Fig. 4.4. The critical load P_C in this test was 18^K. The theoretical MP reached higher value than in the first test. This was due to the higher yield point as well as the greater amount of reinforcing steel in the cross-section. The first plastic hinge was created over the middle support when the load had the magnitude of 16^K. The plastic hinges in the critical sections #1 and #3 were created simultaneously at the 18 kip load.

The actual moment-curvature and moment-load diagrams, which were plotted by using the readings from the load-cells, are not following very well the theoretical diagrams. The most important discrepancy is that even after reaching the predicted value of MP the actual MP is further increasing. This effect is mainly due to strain-hardening in the reinforced steel which was neglected in the theoretical analysis.

4.5 INCREMENTAL COLLAPSE BEAM TEST

Eight of the ten beams were tested with variable repeated loading. The test specimen #3 to #9 had the same dimensions (Fig. 4.1a) and material properties. There were only slight changes in the concrete strength. The regime of loading cycles was the same. The load magnitude was adjusted from test to test. The test specimen #2 had a different type of steel reinforcing with a different yield stress (Fig. 4.1b).

The loading cycle is shown in Chapter 3, Fig. 3b.

This section contains the test results and the corresponding comparison results from the numerical beam analysis.

4.5.1 DEFLECTION MEASUREMENTS

The deflection measurements were taken at the points of application of loads (critical section #1 and #3) using the Dial Gauges as was described in Chapter 2, Section 2.4.2d. When the test beams failed after less than 10 loading cycles, the readings were taken at each stage of the loading cycle. In the tests where 23 loading cycles were applied, the readings were first taken at each loading stage and then after 8 or 9 cycles only at the end of each cycle. The deflection diagrams are presented in the same order as the beams were tested.

Each cross-section, where the development of a fully plastic moment was expected, is drawn separately. The tests where the magnitude of the applied load was greater than 16^K are not compared with the numerical analysis results because according to the analysis, applied loads of magnitudes greater than or equal to 16^K form a plastic collapse mechanism. The program was not designed for this type of failure.

All the predicted deflections are drawn as dotted lines. P_1 is the applied load in the left span, P_2 is the applied load in the right span. $P_1 = P_2$ means that the both loads are applied at the same time and $P_1 = P_2 = 0$ in the

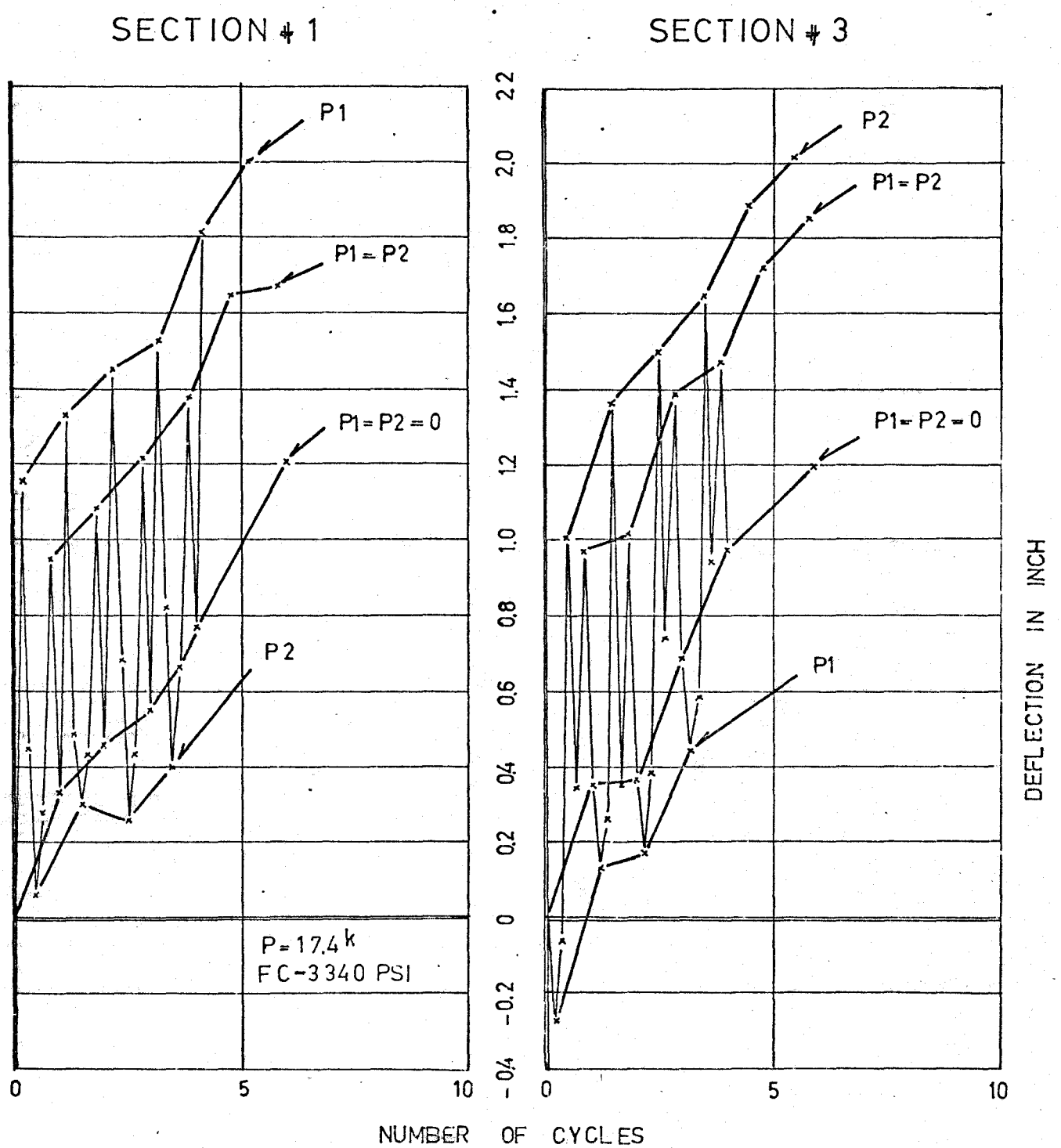

FIG. 4.6. DEFLECTION VERSUS CYCLES TEST # 2

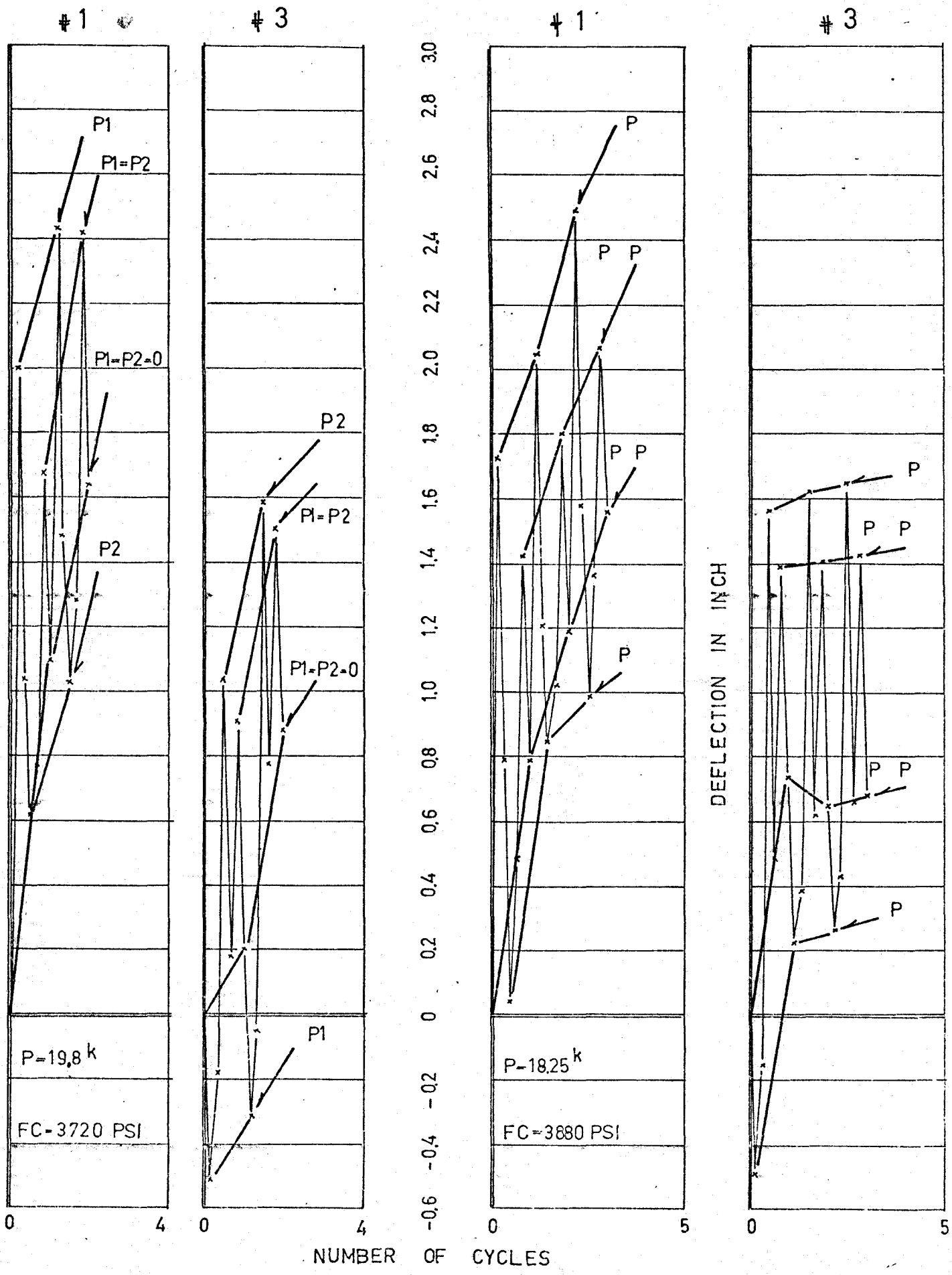

FIG. 4.7. DEFLECTION VERSUS CYCLES TEST #3 AND #4

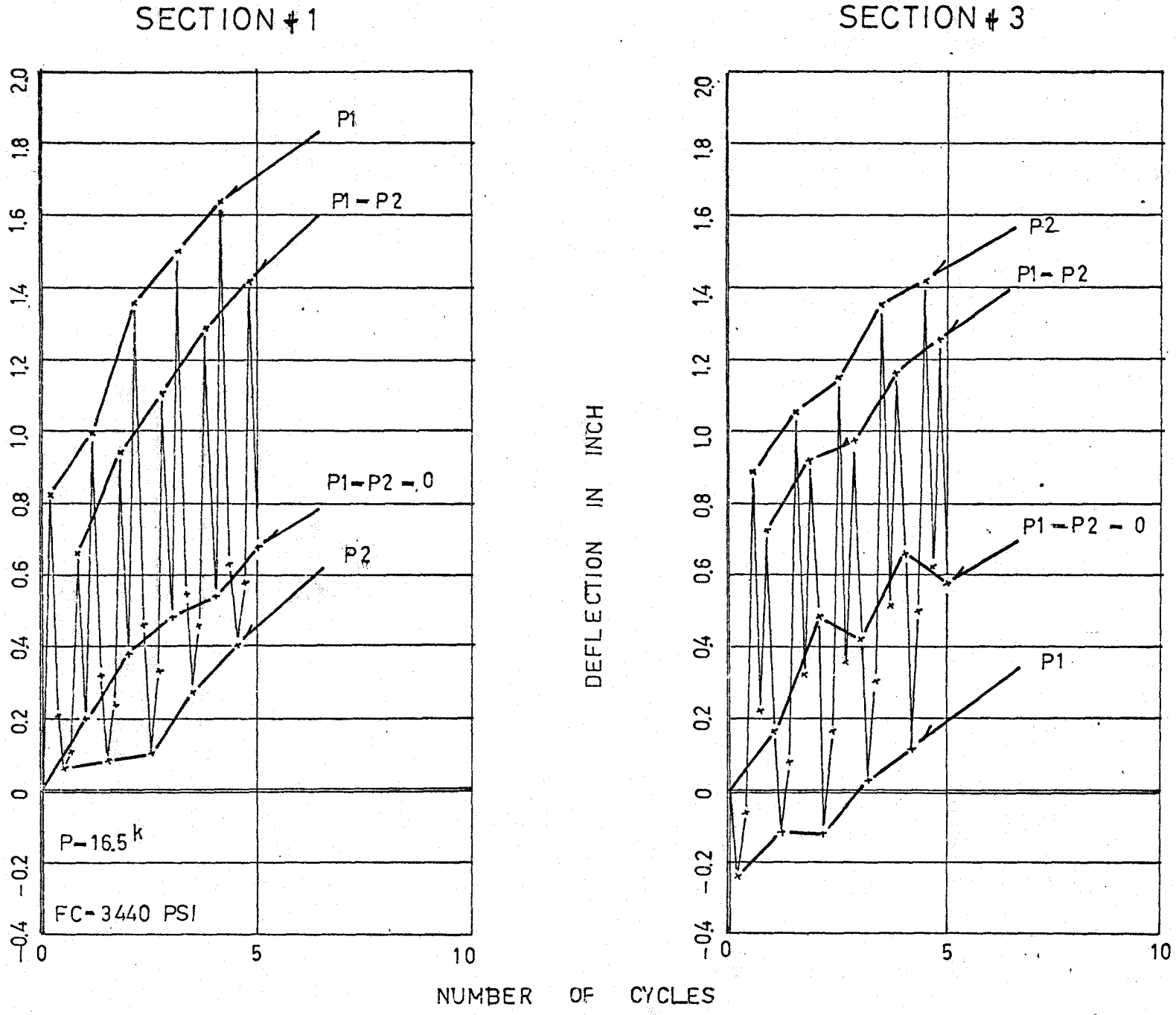

FIG 48 DEFLECTION VERSUS CYCLES TEST # 5

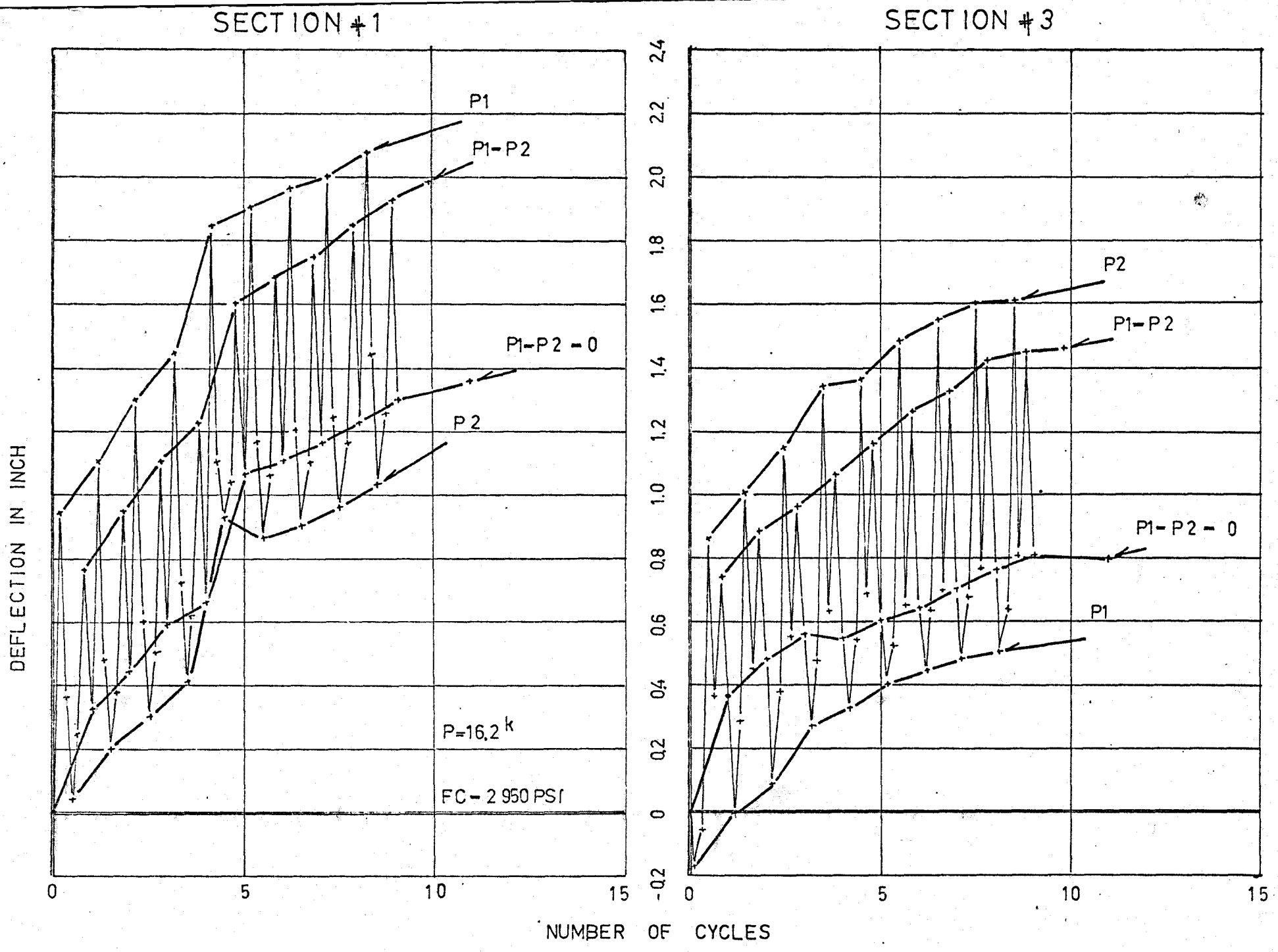

FIG 4 9 DEFLECTION VERSUS CYCLES TEST #6

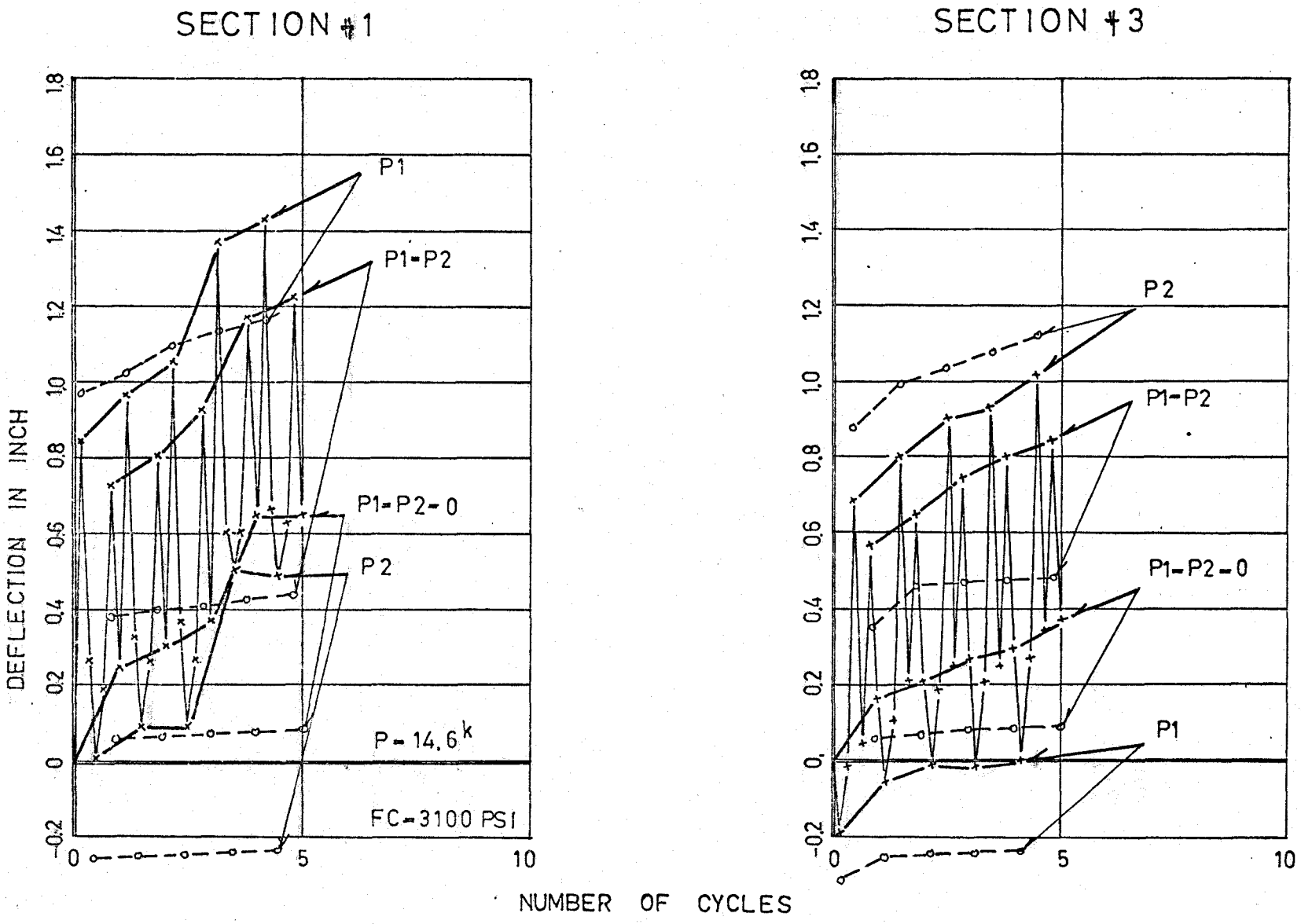

FIG. 4.10. DEFLECTION VERSUS CYCLES TEST # 7

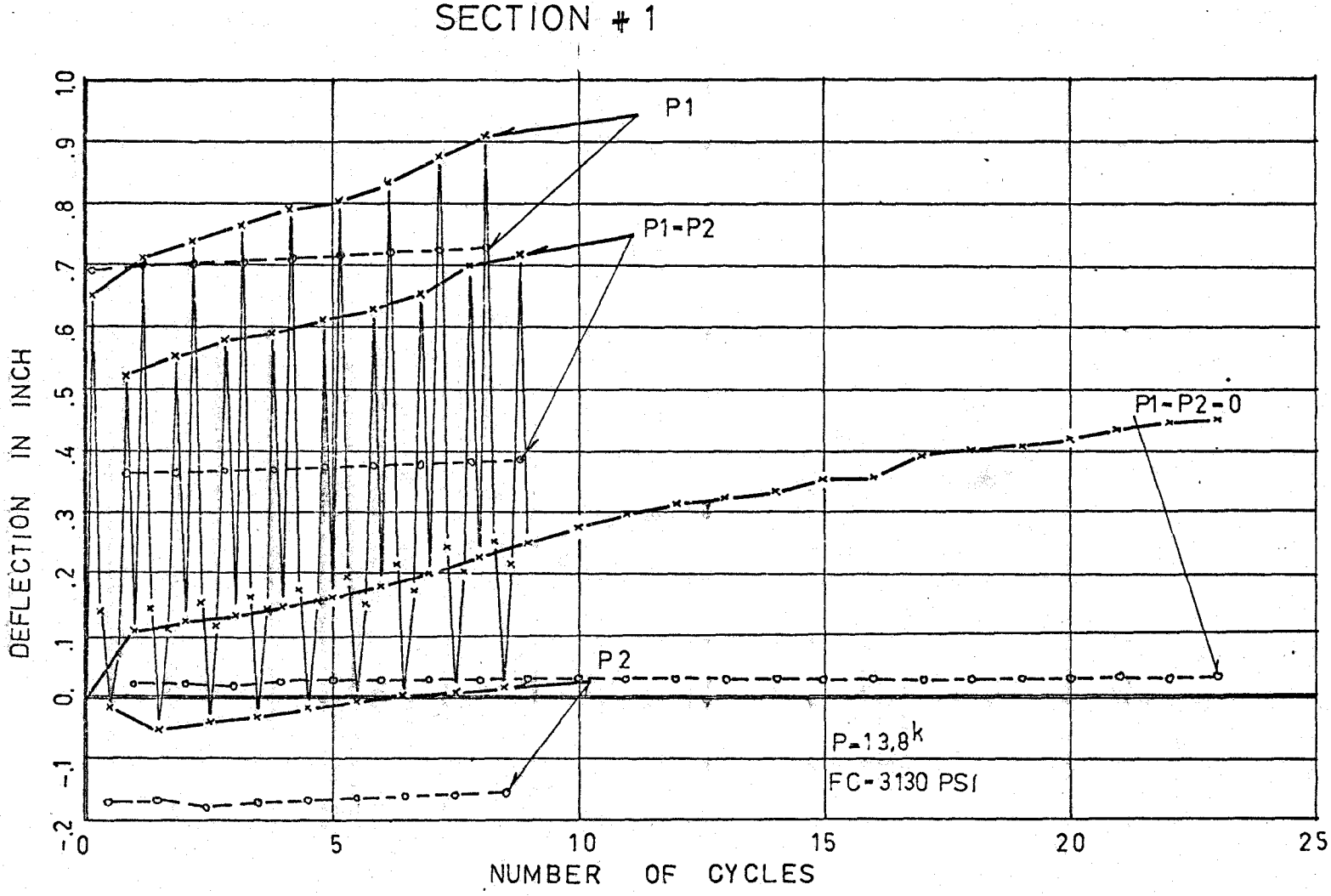

FIG. 4.11.a. DEFLECTION VERSUS CYCLES TEST # 8

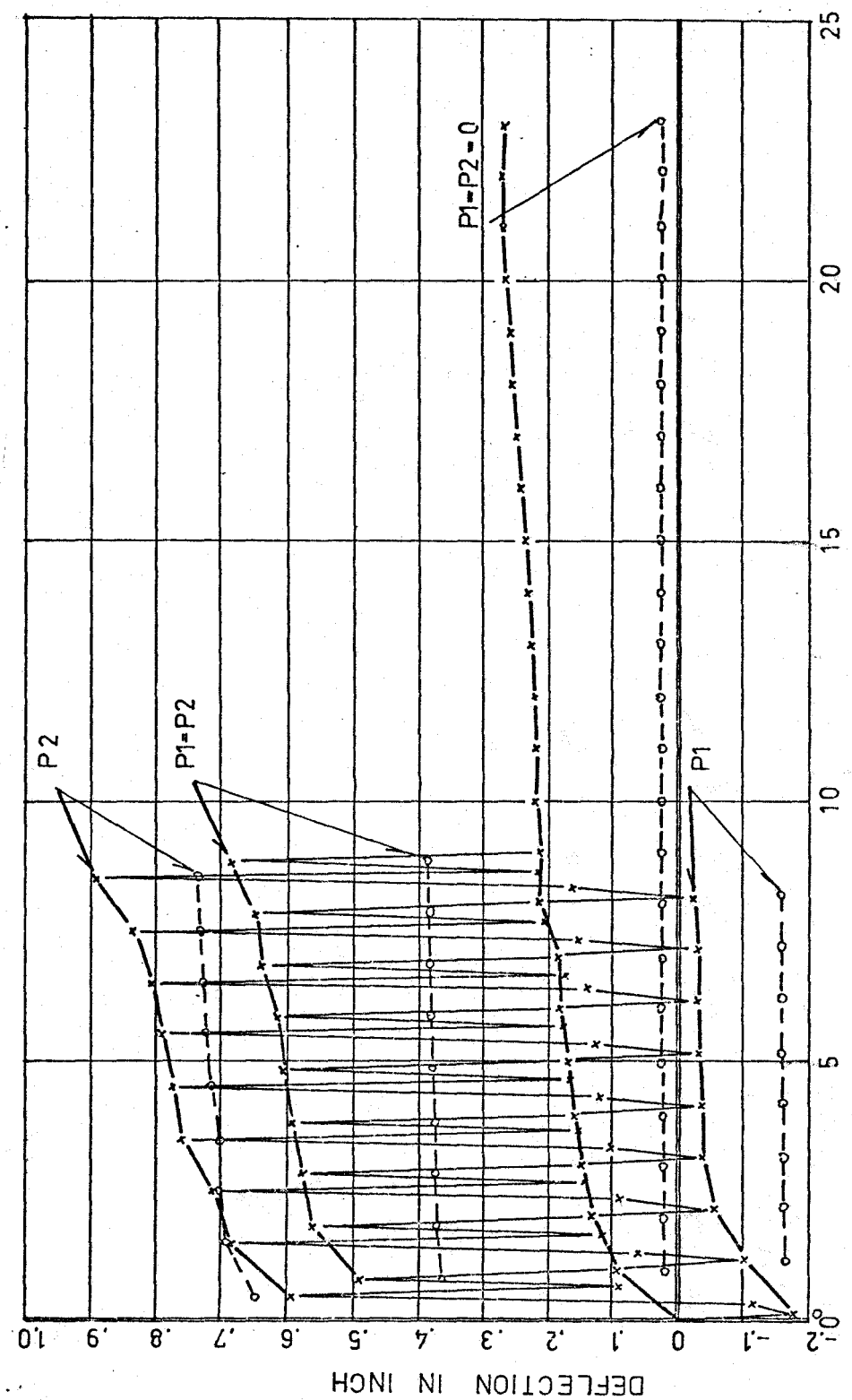

FIG. 4.11.b. DEFLECTION VERSUS CYCLES TEST # 8

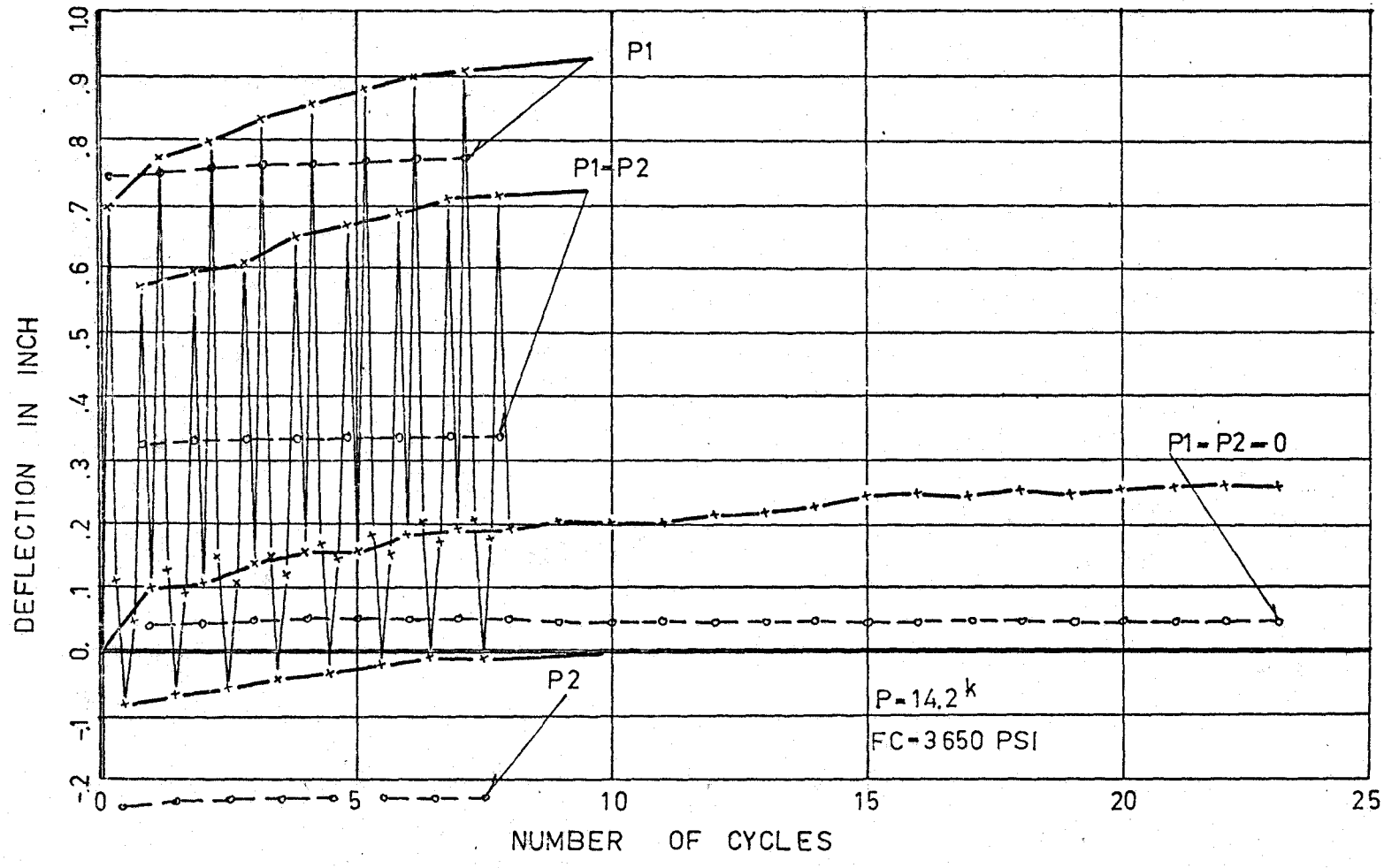

FIG. 4.12.a. DEFLECTION VERSUS CYCLES TEST#9

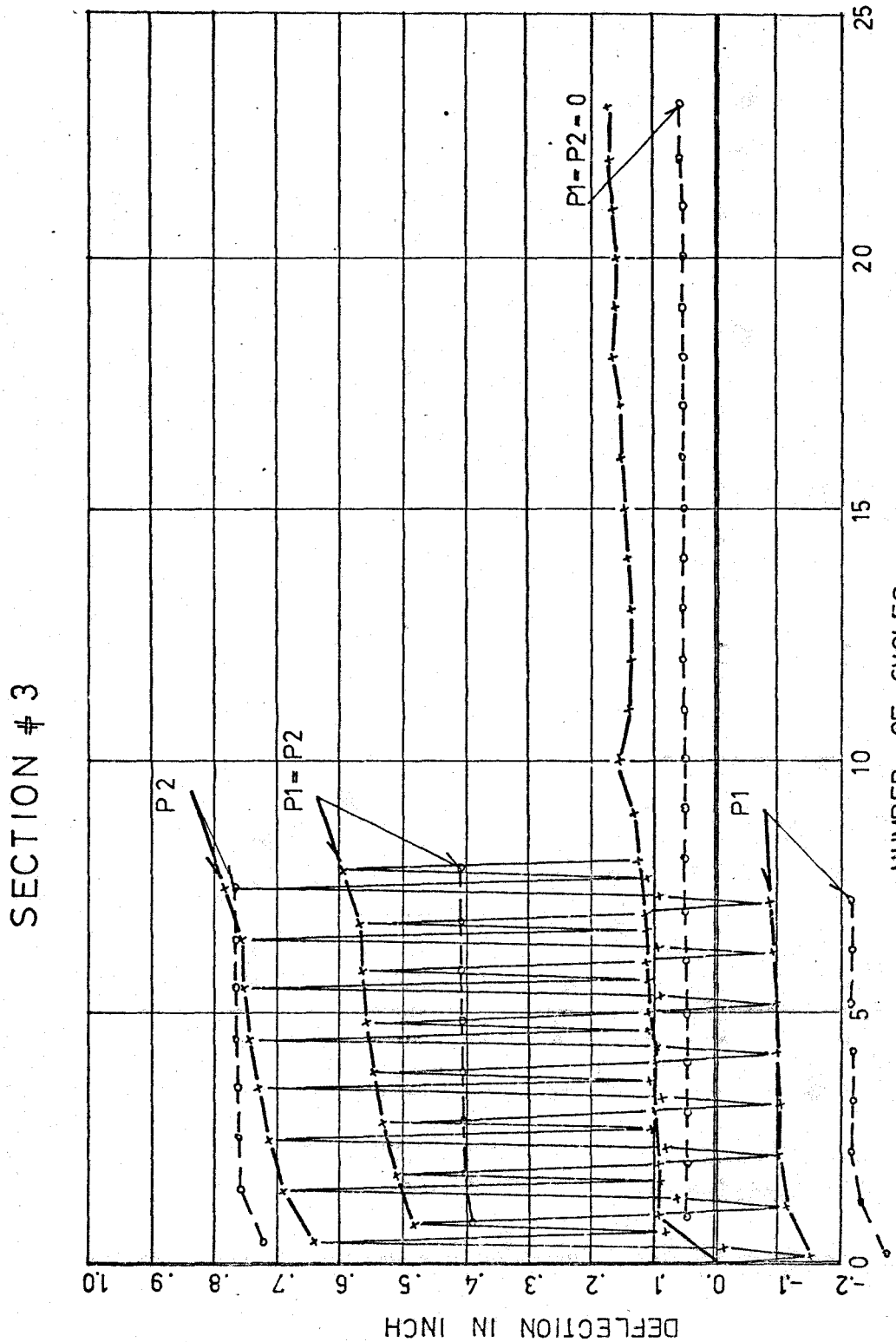

FIG. 4.12.b. DEFLECTION VERSUS CYCLES TEST #9

unloading stage after the loading cycle.

4.5.2 STRAIN MEASUREMENTS

A demec mechanical strain indicator was used to measure the strains at three levels in the cross-section. The spacing of the demec-points is shown in Chapter 2, Fig. 2.5. Readings were taken until the range of the strain indicator was exceeded. When the number of loading cycles was greater than 8, only the residual strain readings at the end of each cycle were taken.

The strain diagrams are reproduced for all three critical cross-sections, where the formation of a plastic hinge was repeated. Unfortunately there were no strain readings in test #3, where the magnitude of the applied load was 19.8^{K}. When the load was applied, the strain in the critical cross-sections had exceeded the range of the mechanical strain indicator. For the same reason there were only a very few readings taken in test #4, where the magnitude of the load was 18.25^{K}.

In addition to the strain history of the section either in the top or bottom fibres and curvature of the cross-section, also shown are the stress-strain diagrams for the reinforcing steel in the critical cross-sections. The values of the strain in the steel were computed using the second computer program (Section 4.3).

Assuming the idealized stress-strain relationship and knowing the yield stress and the yield strain, the values of

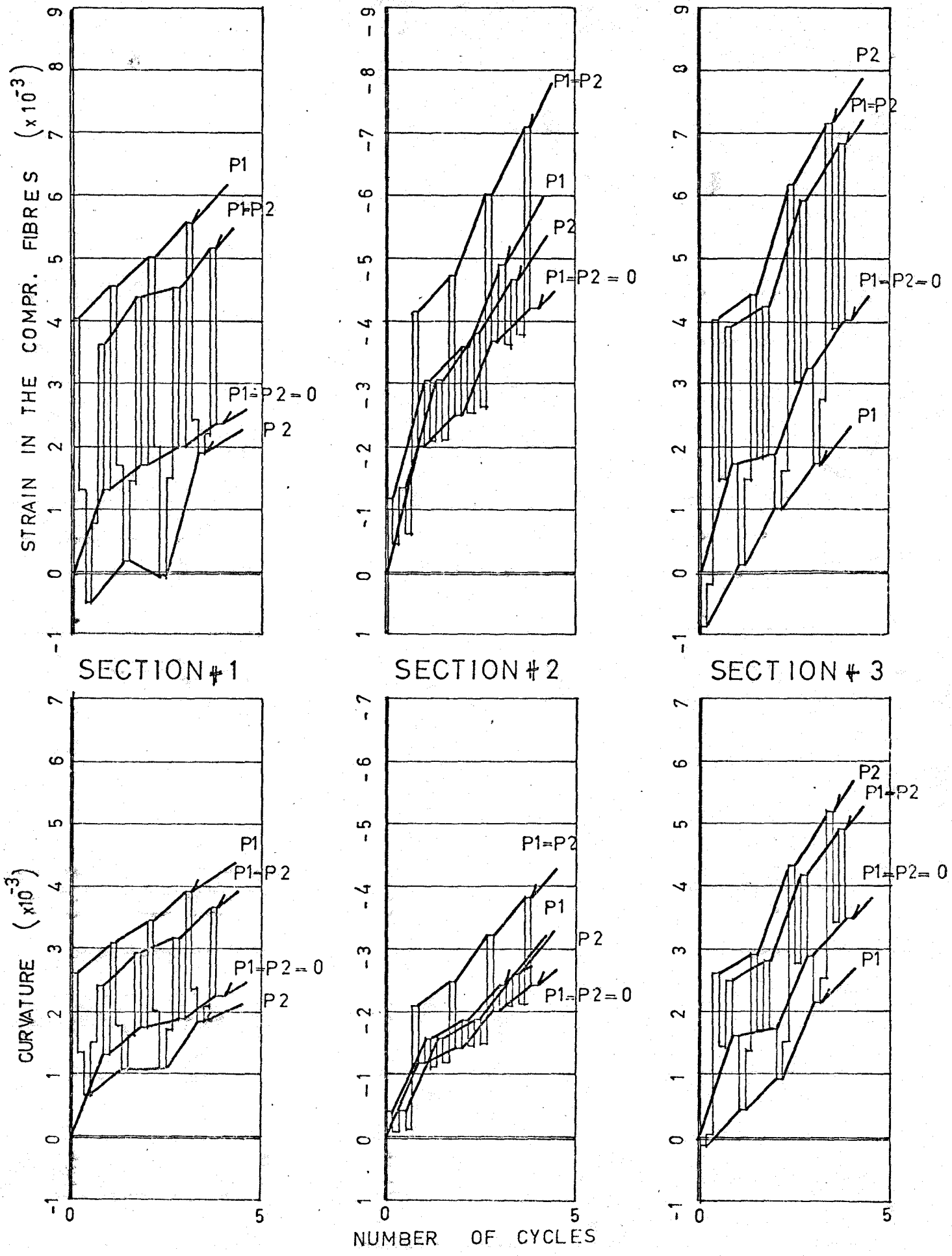

FIG. 4.13. CYCLES VERSUS STRAIN AND CURVATURE
TEST # 2

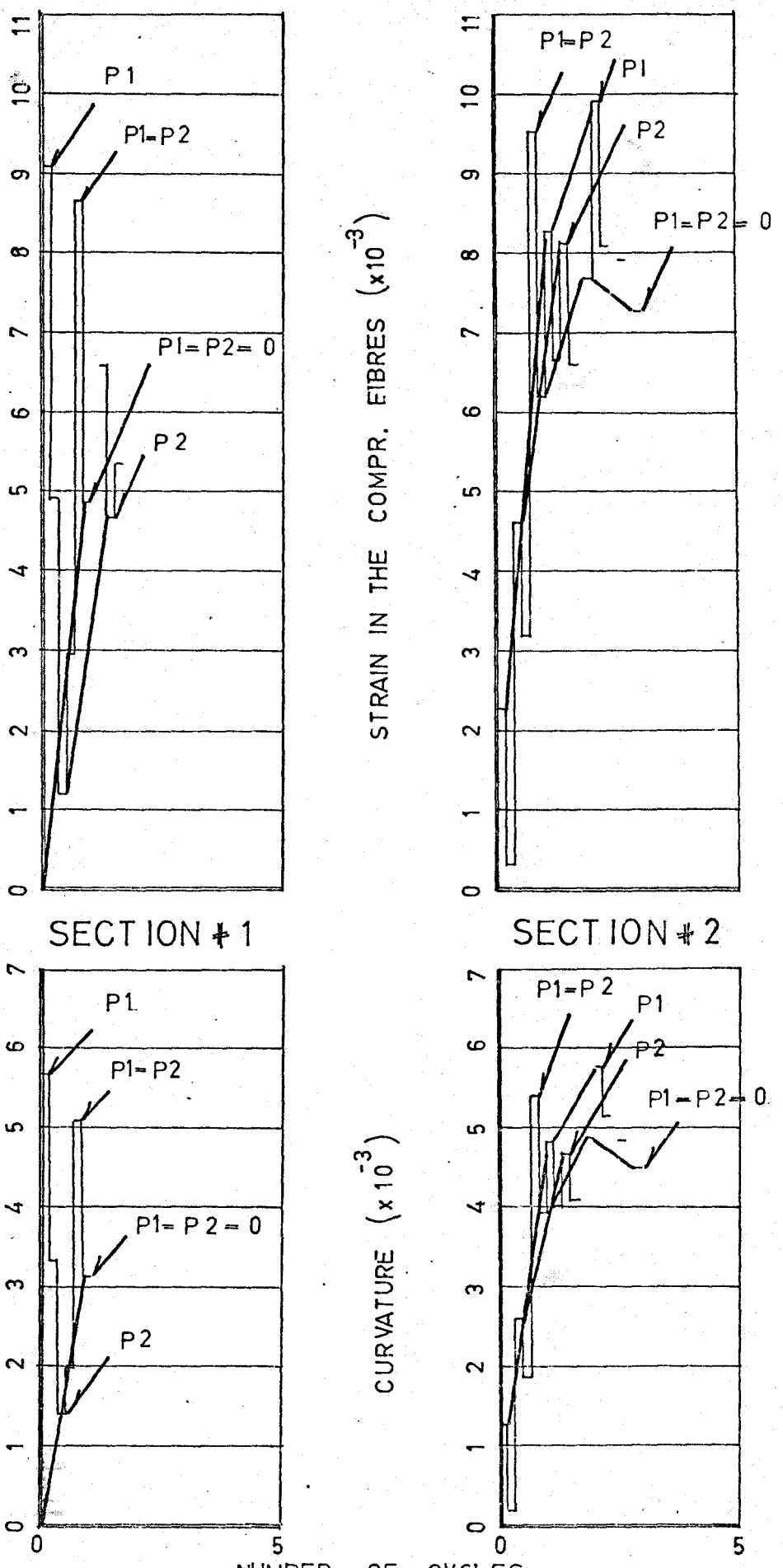

FIG. 4.14. CYCLES VERSUS STRAIN AND CURVATURE

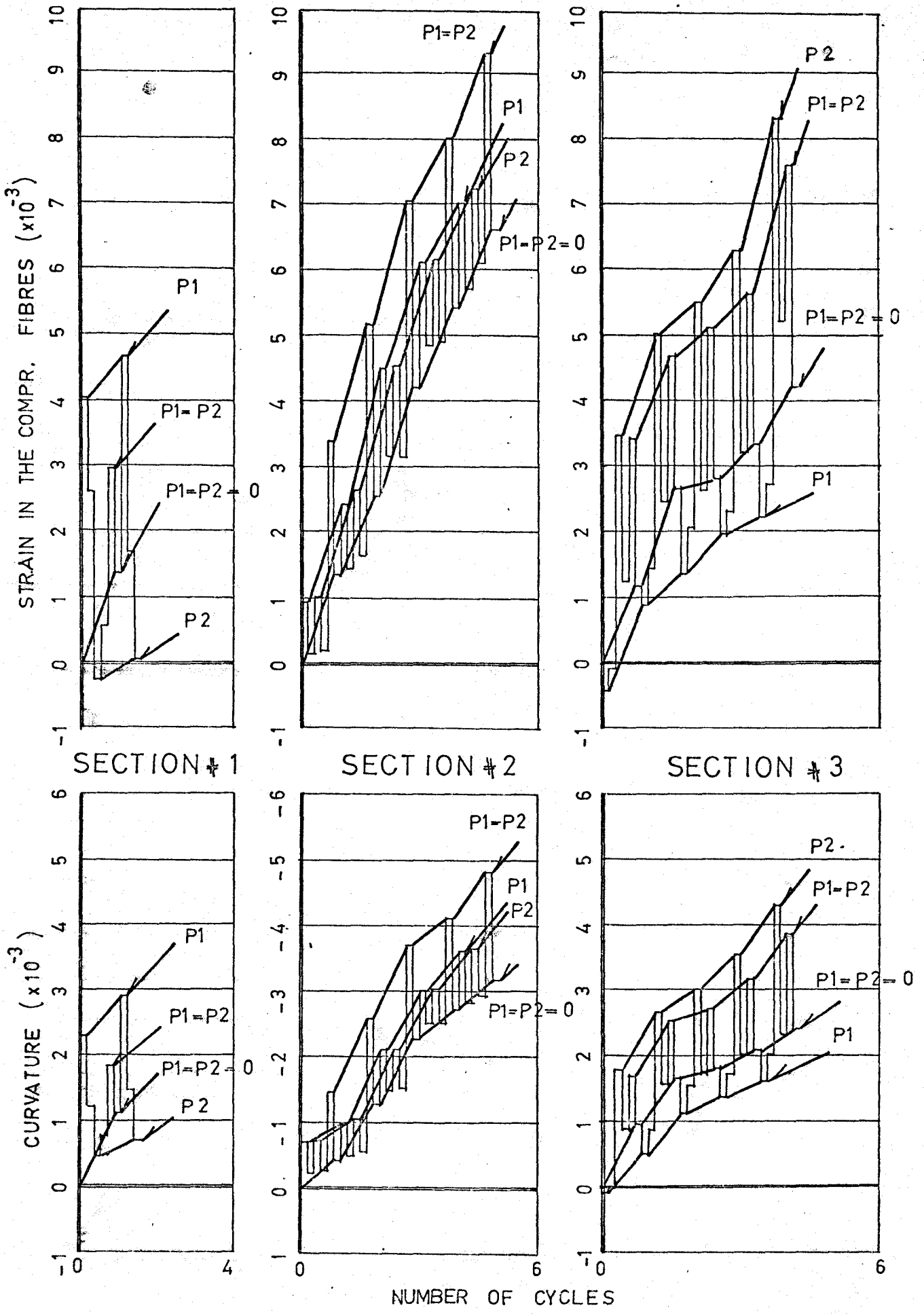

FIG. 4.15. CYCLES VERSUS STRAIN AND CURVATURE TEST # 5

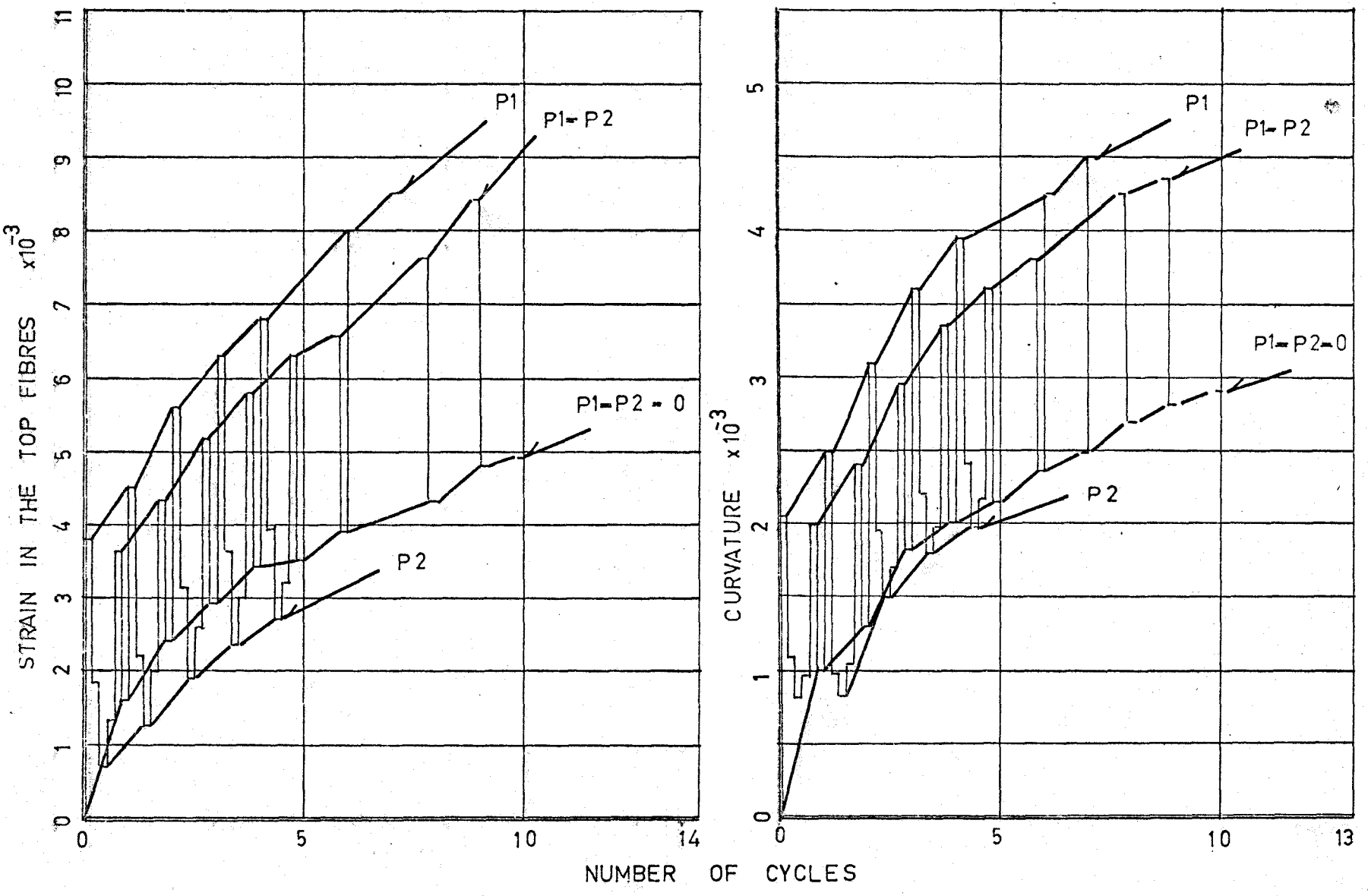

FIG. 4.16. CYCLES VERSUS STRAIN AND CURVATURE TEST # 6

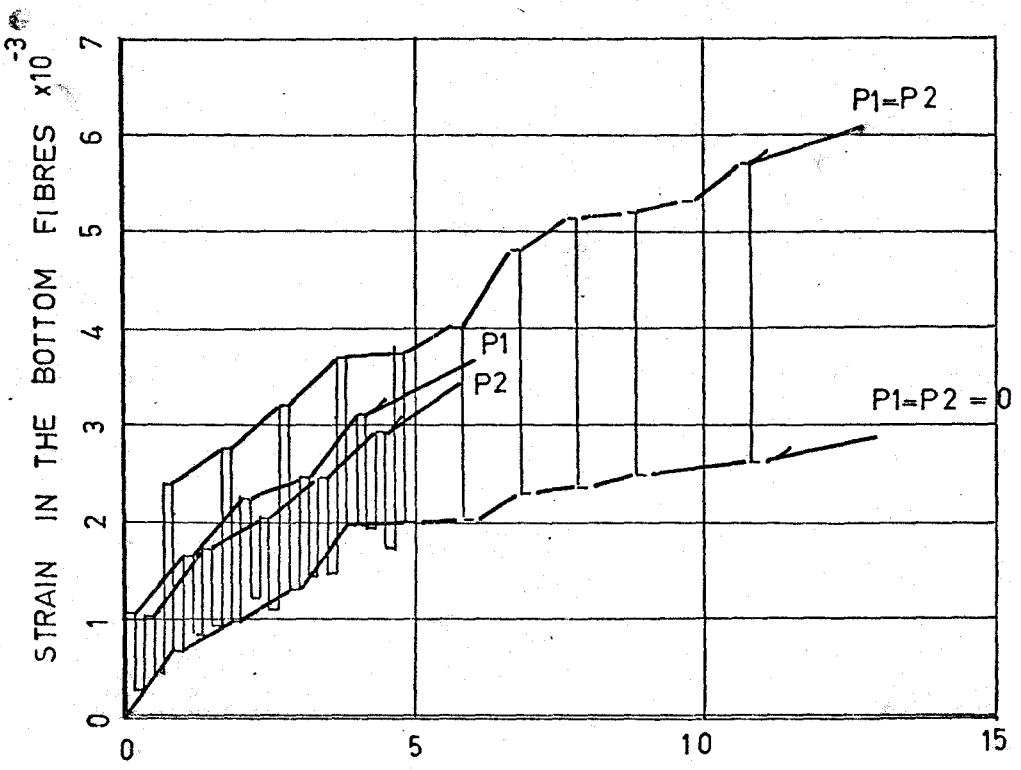

SECTION # 2

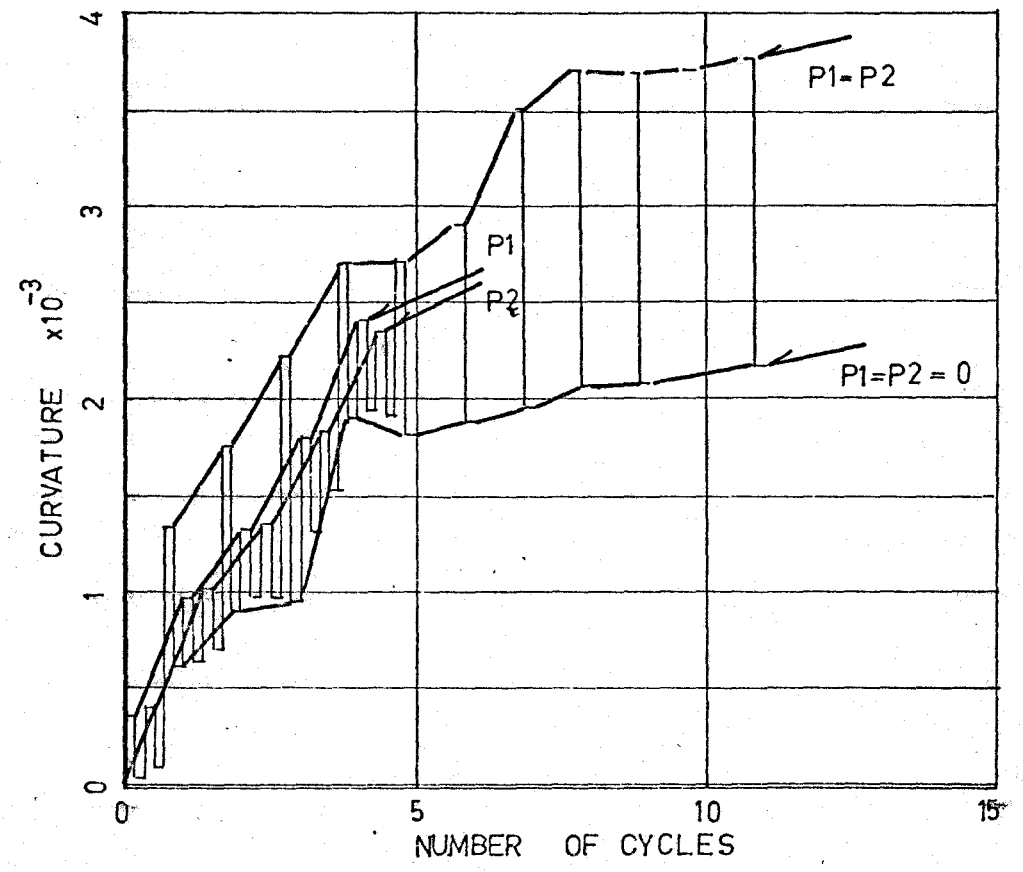

FIG. 4.17. CYCLES VERSUS STRAIN AND CURVATURE TEST # 6

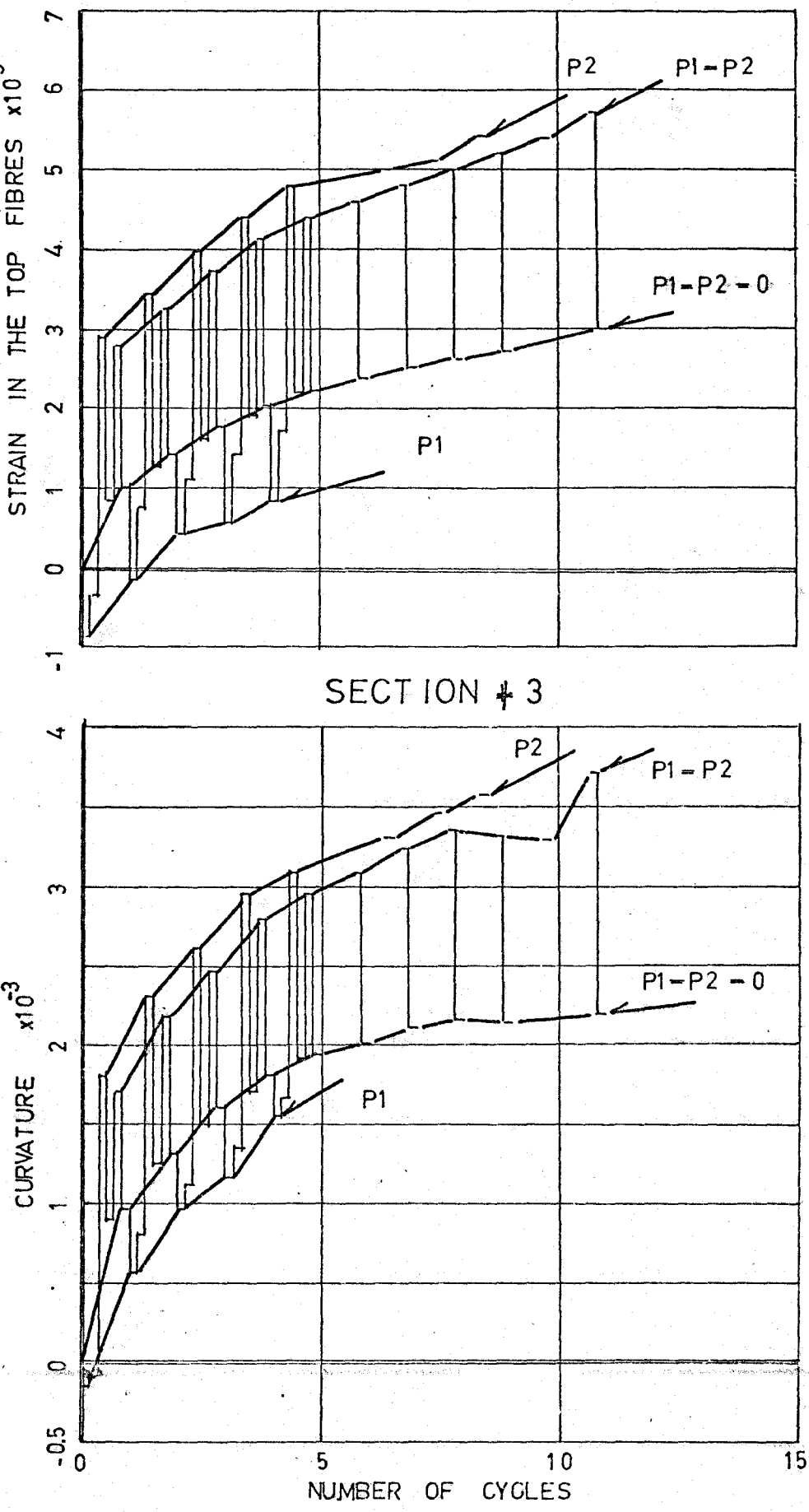

FIG. 4.18. CYCLES VERSUS STRAIN AND CURVATURE

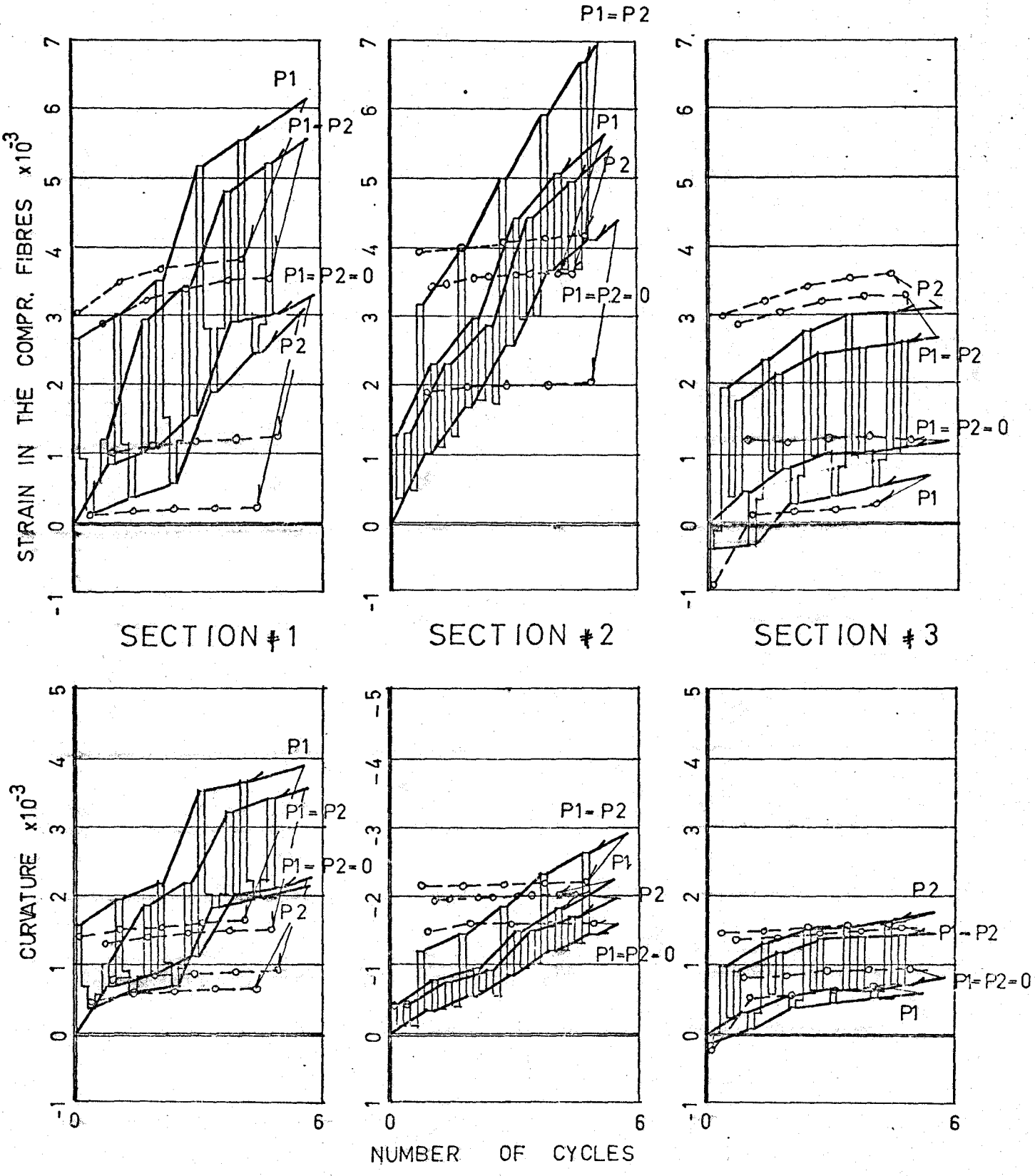

FIG. 4.19. CYCLES VERSUS STRAIN AND CURVATURE TEST #7

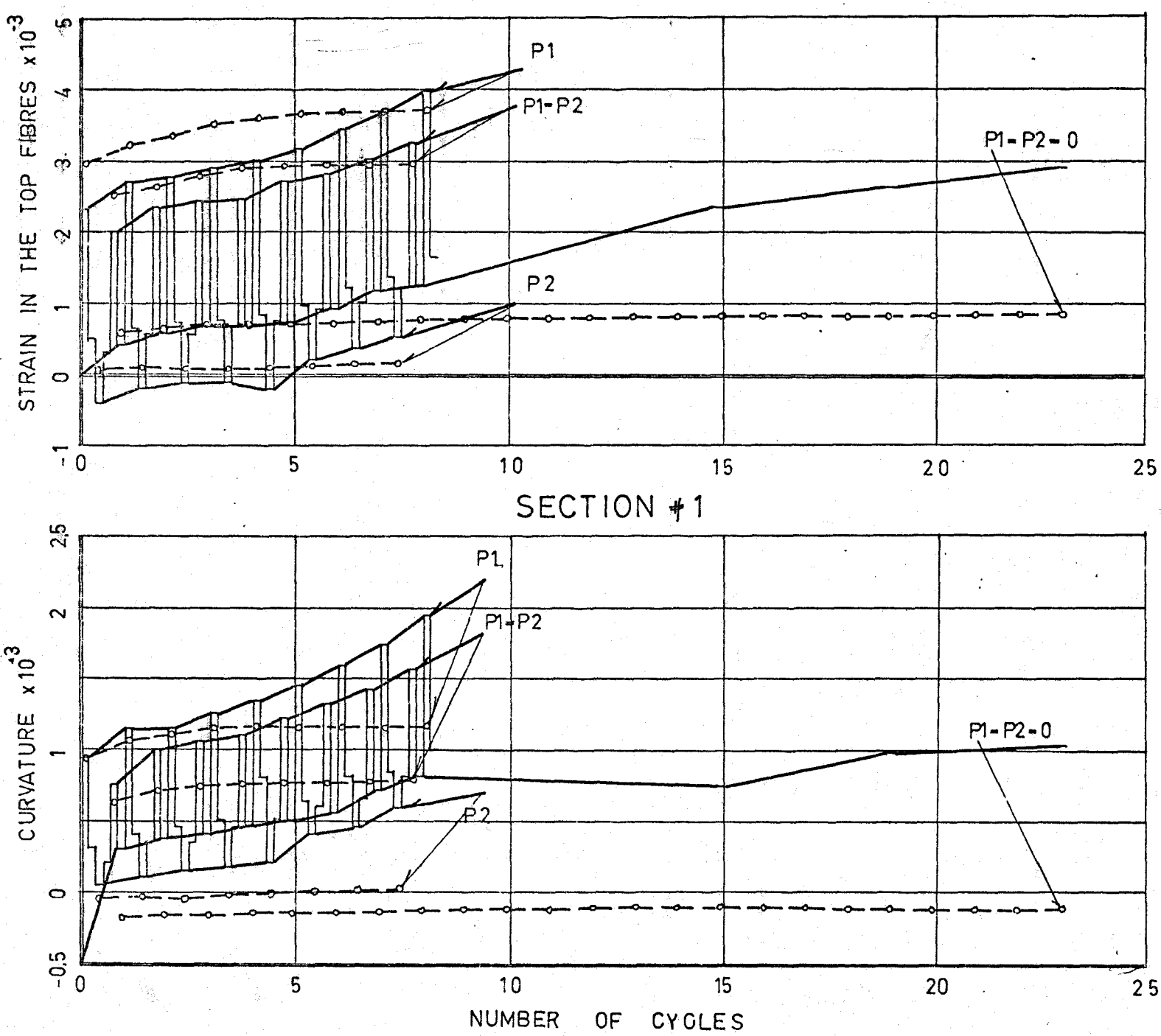

FIG. 4.20, CYCLES VERSUS STRAIN AND CURVATURE TEST #8

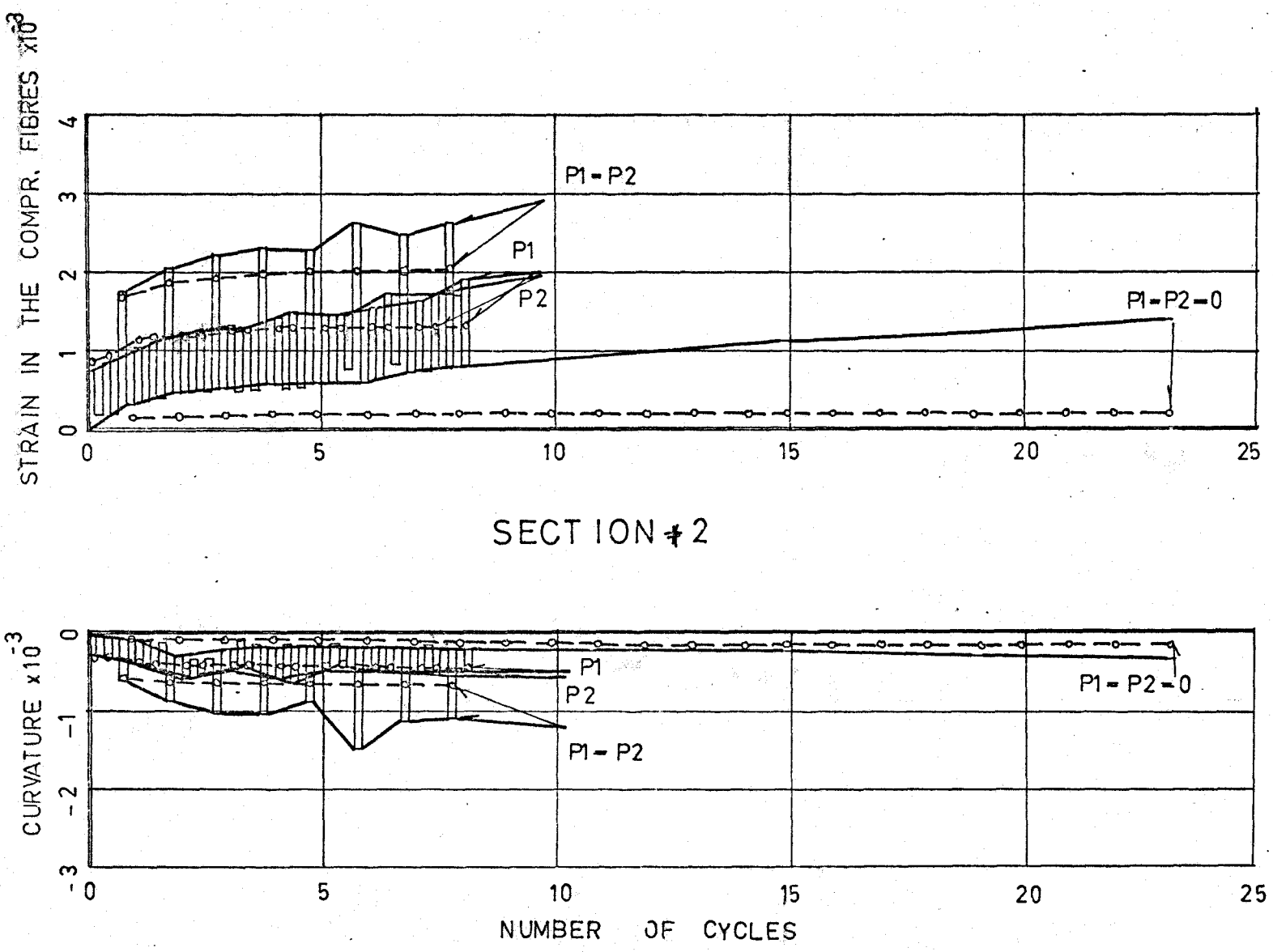

FIG. 4.21. CYCLES VERSUS STRAIN AND CURVATURE TEST # 8

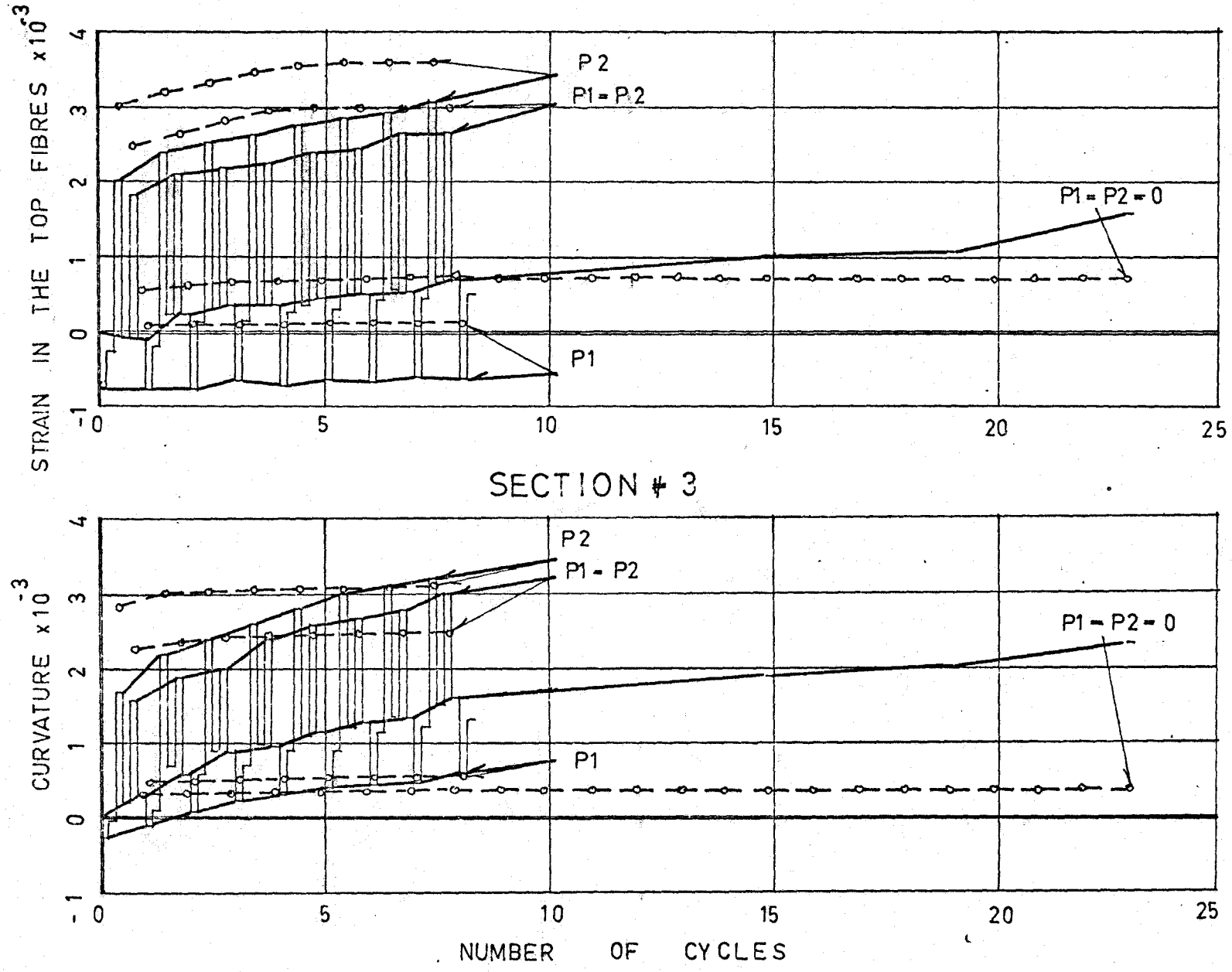

FIG. 4.22. CYCLES VERSUS STRAIN AND CURVATURE TEST # 8

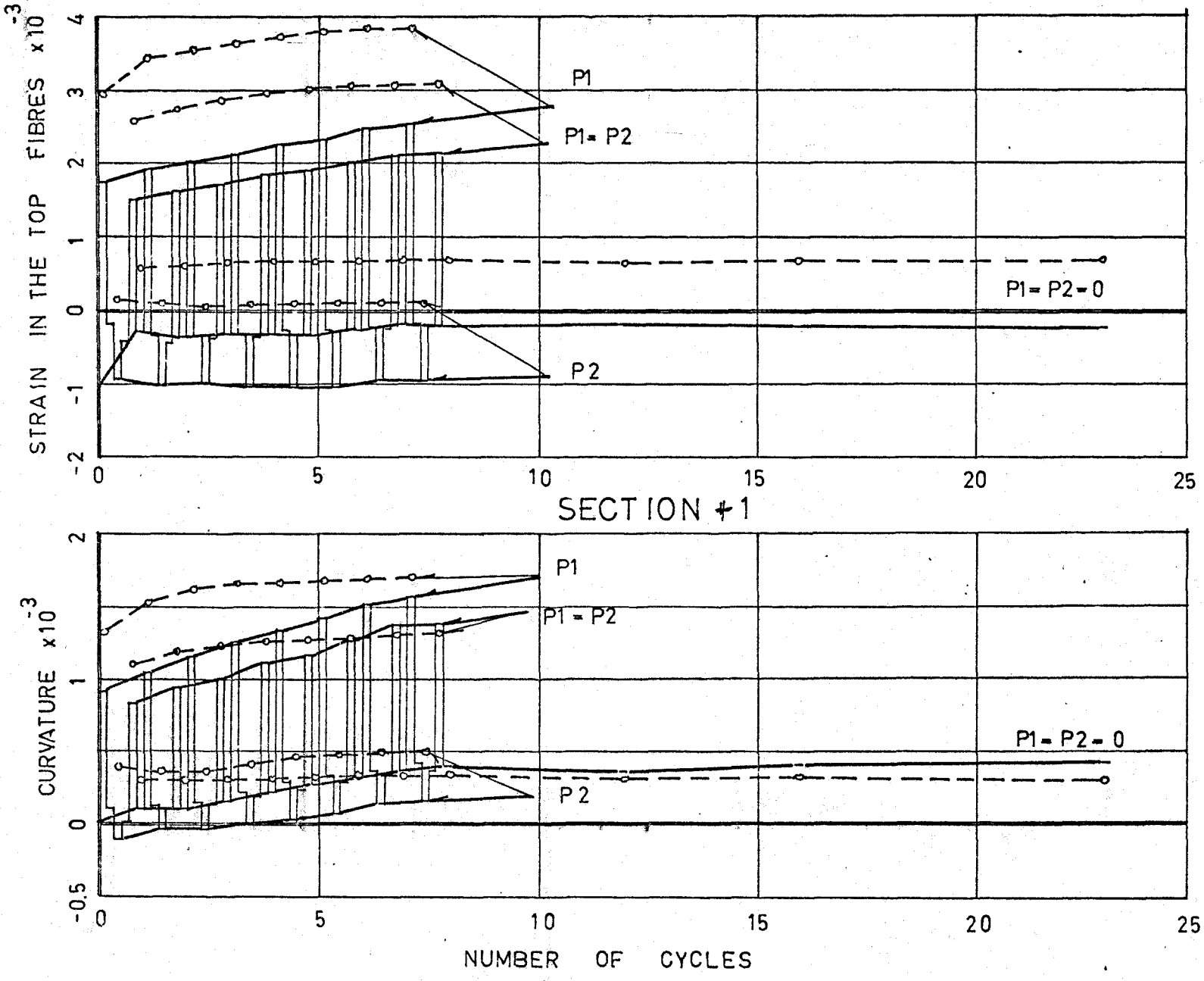

FIG. 4.23. CYCLES VERSUS STRAIN AND CURVATURE TEST # 9

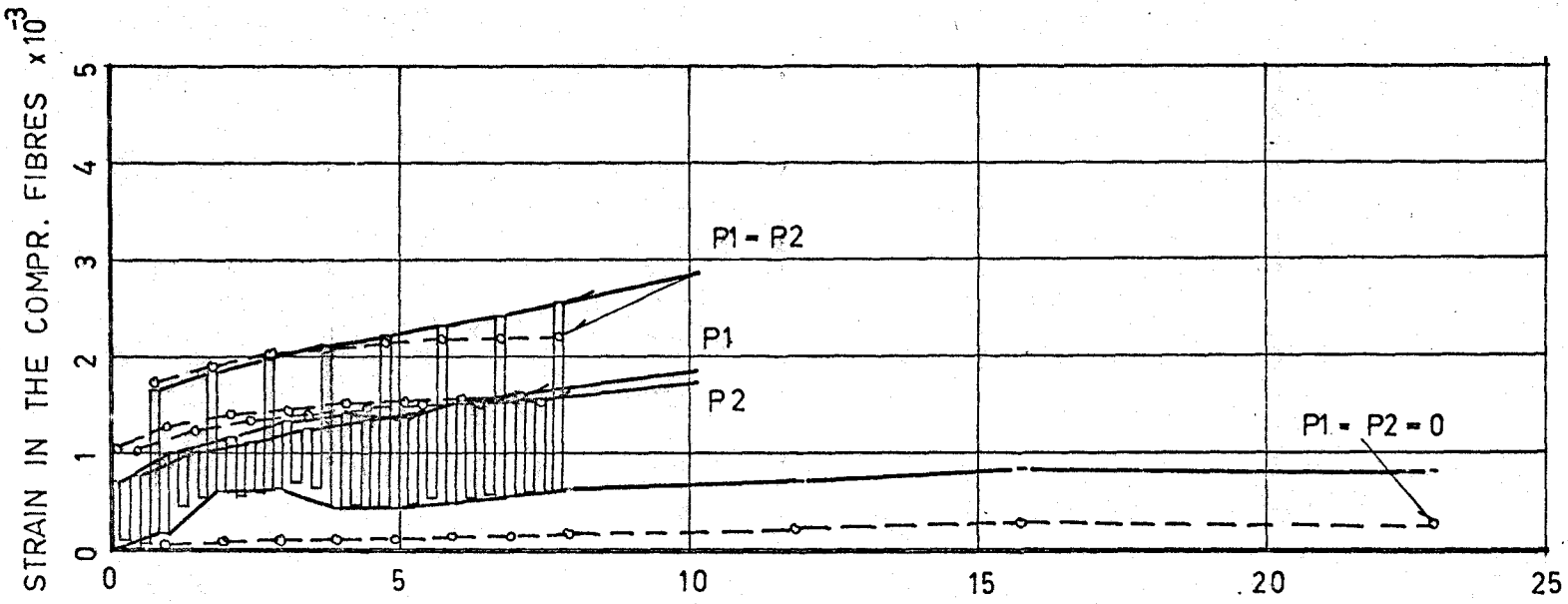

SECTION # 2

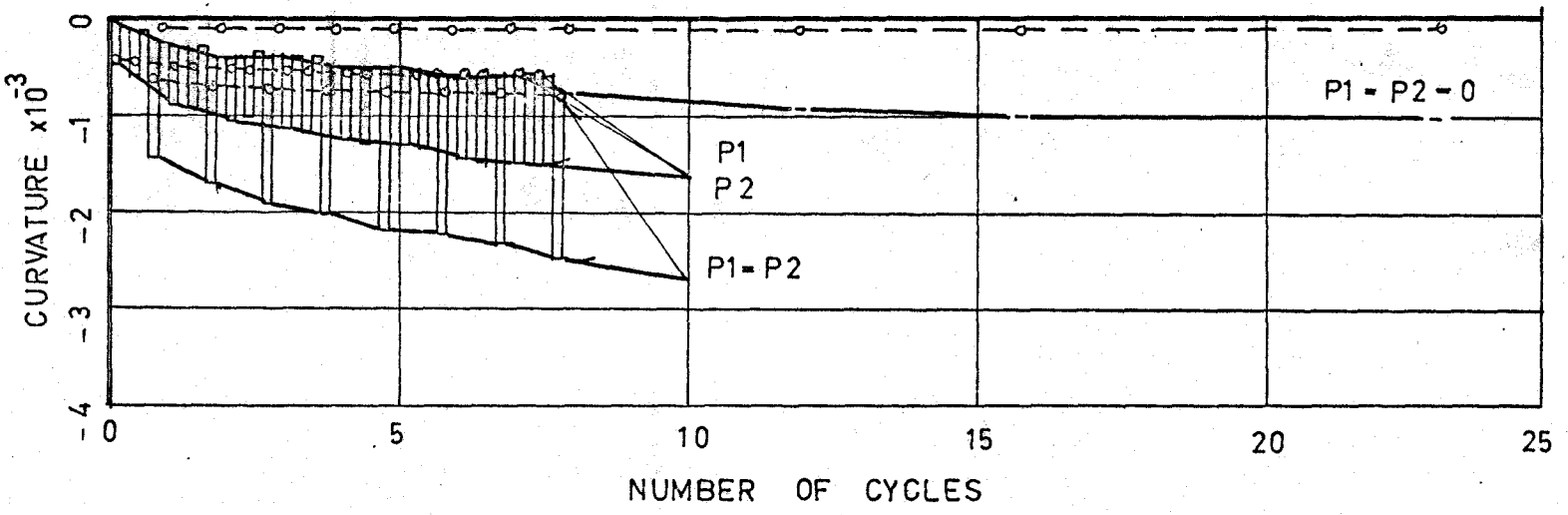

FIG. 4.24. CYCLES VERSUS STRAIN AND CURVATURE · TEST # 9

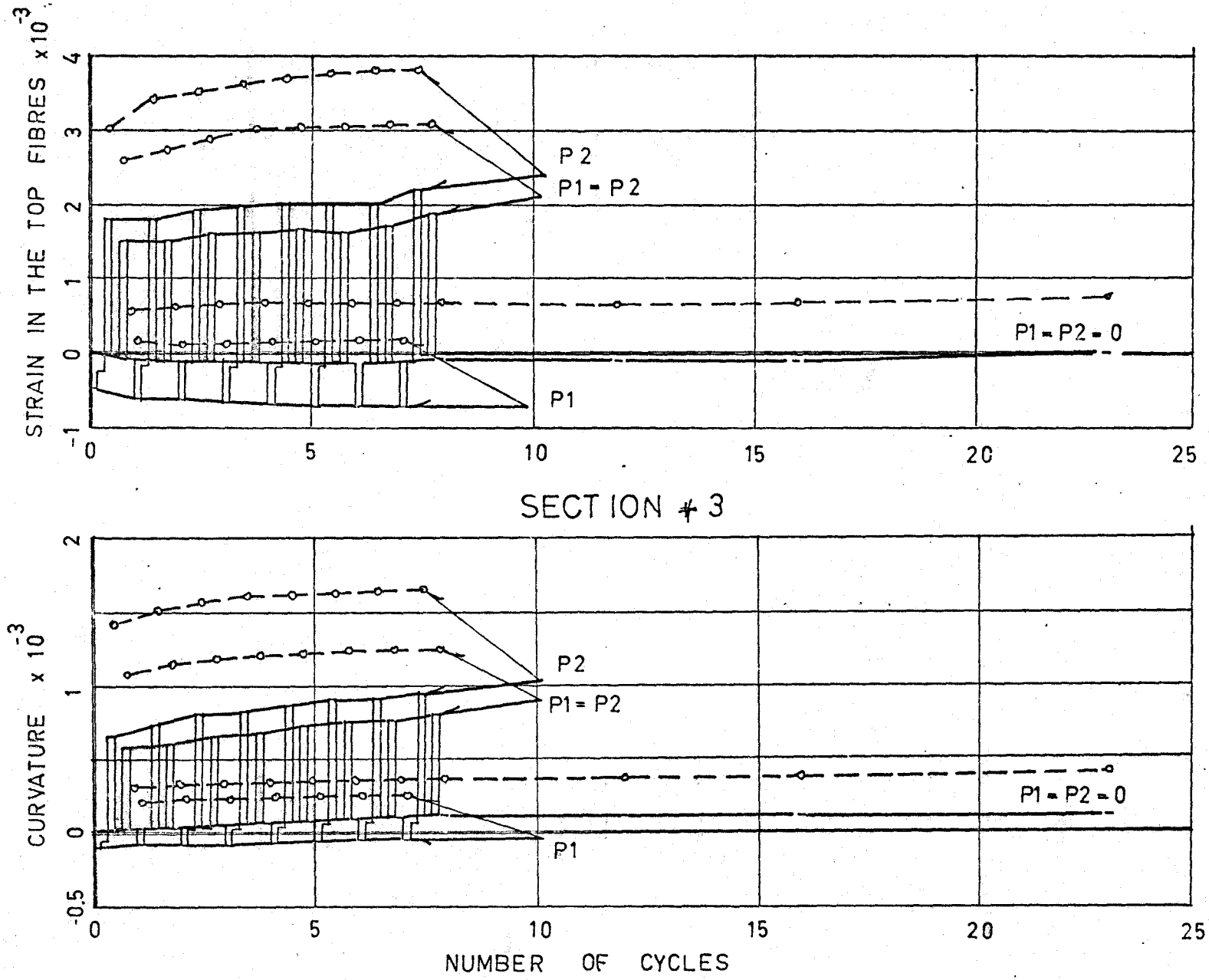

FIG. 4.25. CYCLES VERSUS STRAIN AND CURVATURE TEST # 9

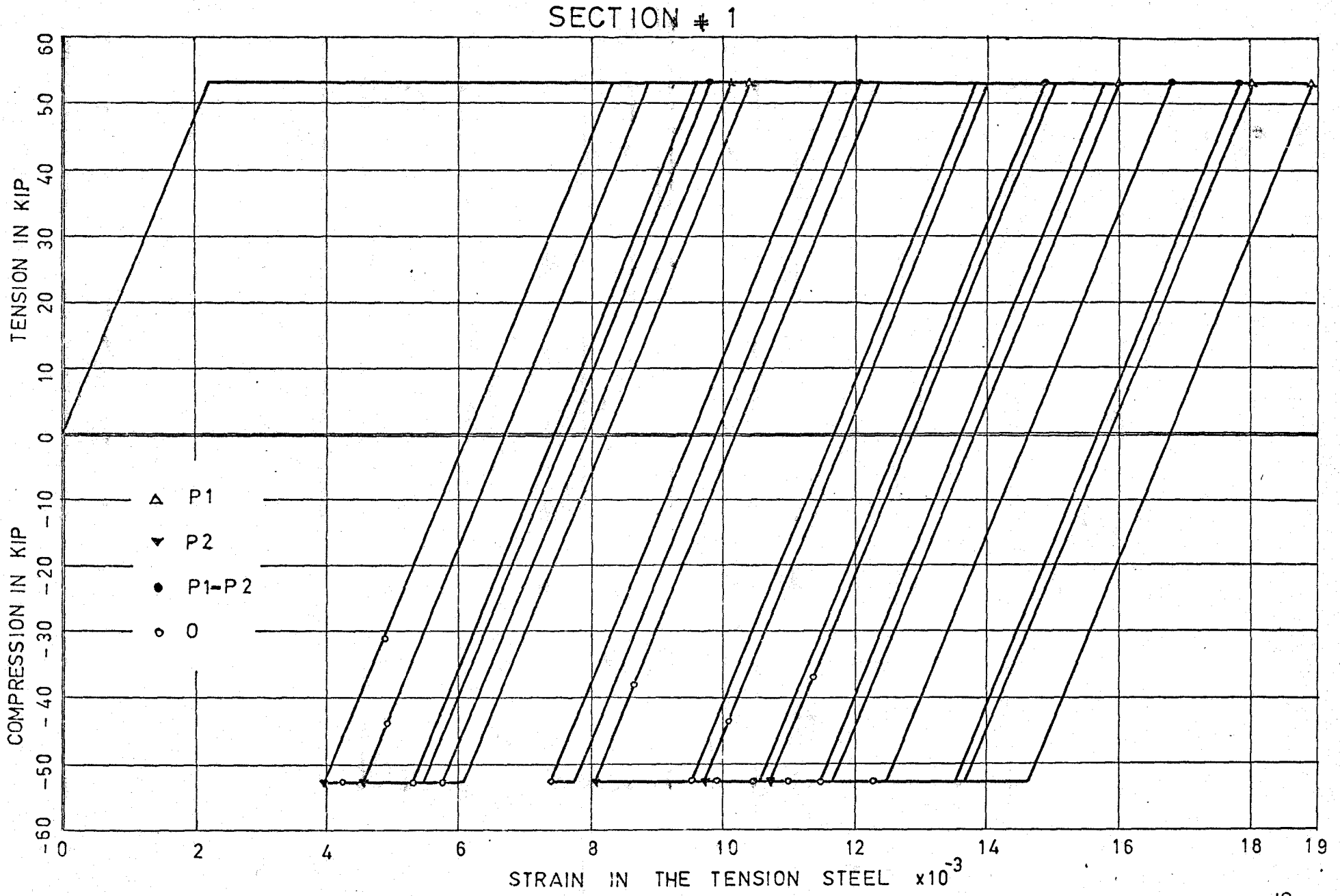

FIG. 4.26. STRESS VERSUS STRAIN IN TENSION STEEL TEST # 6

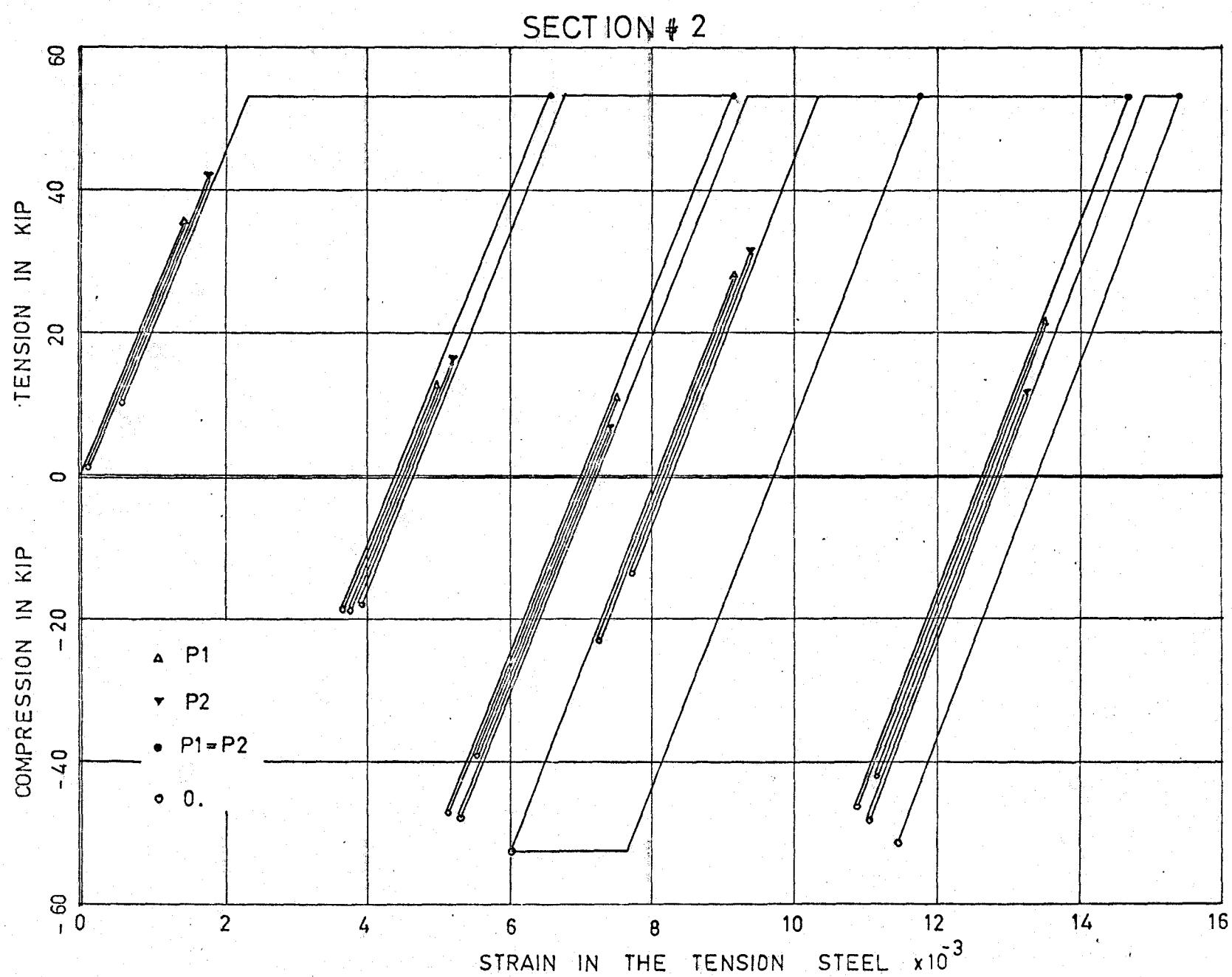

FIG. 4.27. STRESS VERSUS STRAIN IN TENSION STEEL TEST # 6

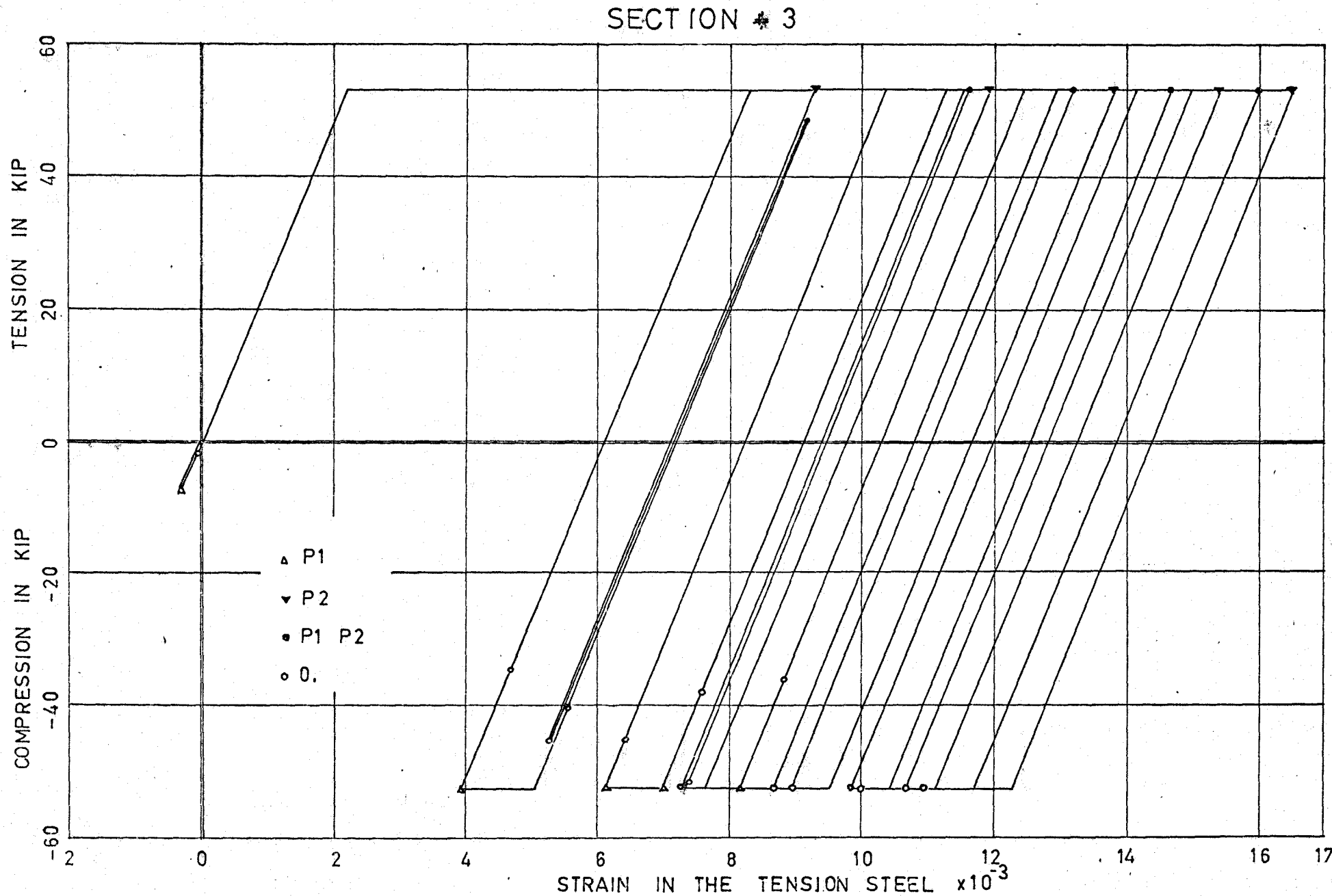

FIG. 4.28. STRESS VERSUS STRAIN IN TENSION STEEL TEST # 6

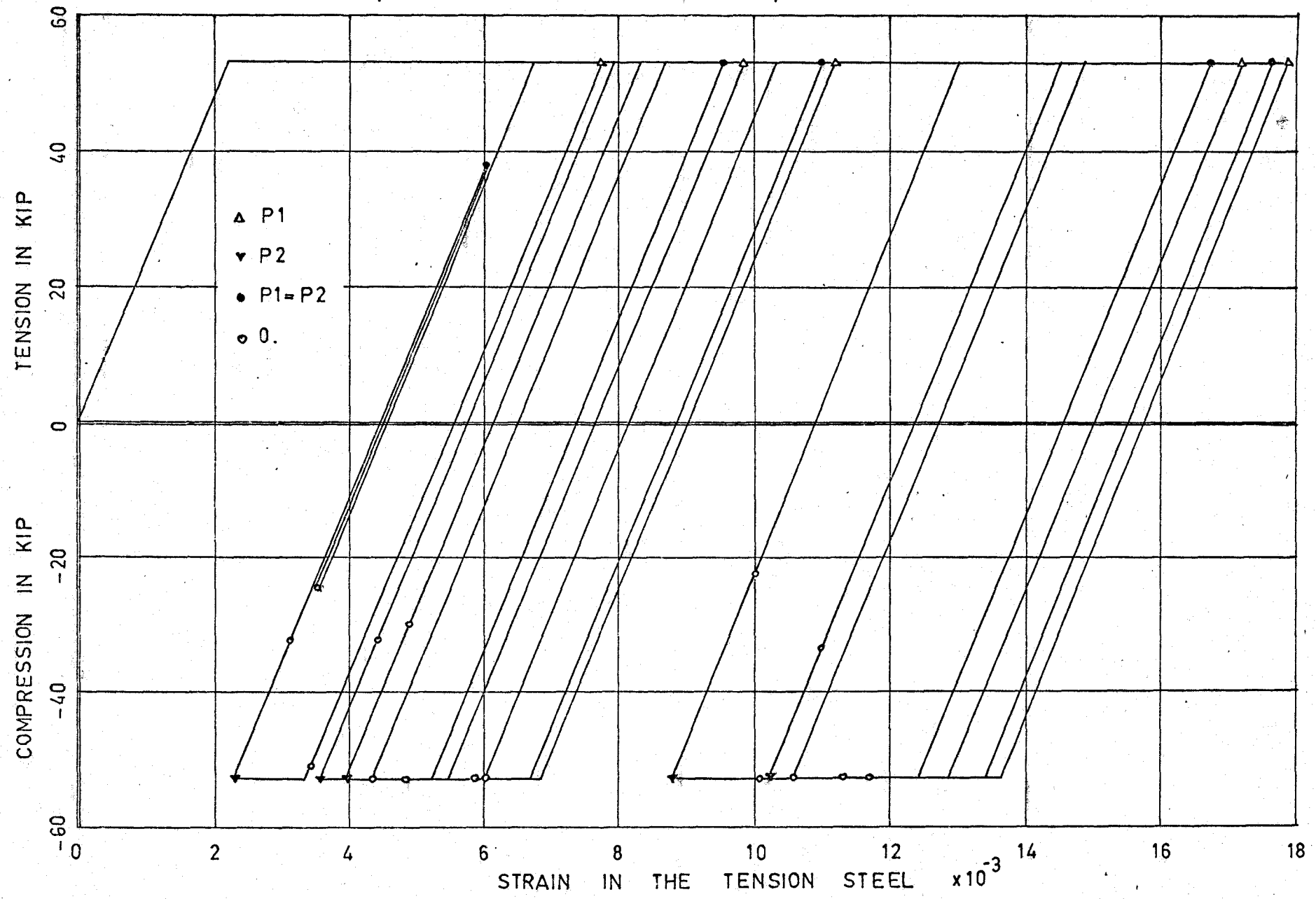

FIG. 4.29. STRESS VERSUS STRAIN IN TENSION STEEL TEST # 7

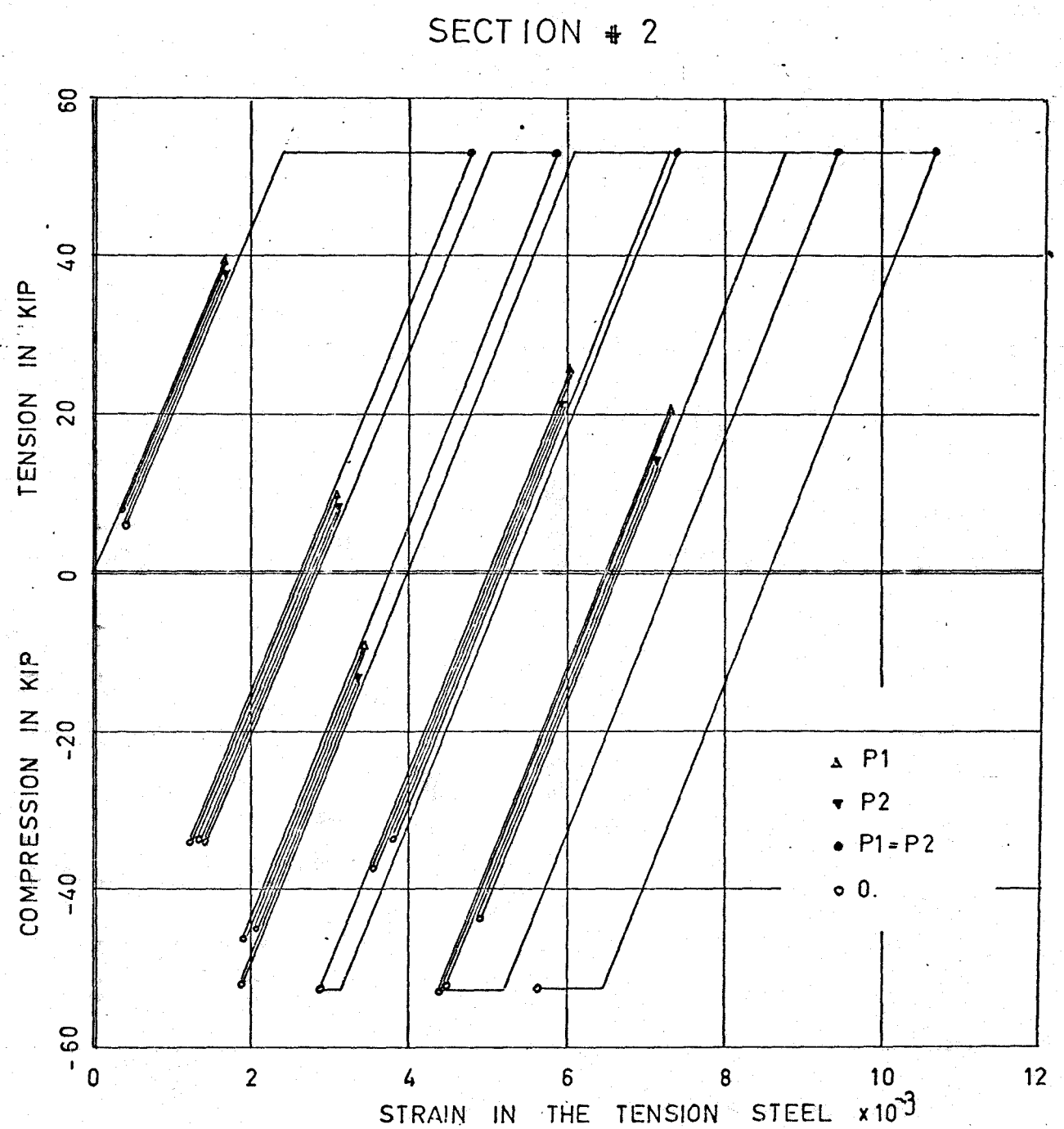

FIG.4.30. STRESS VERSUS STRAIN IN TENSION STEEL TEST # 7

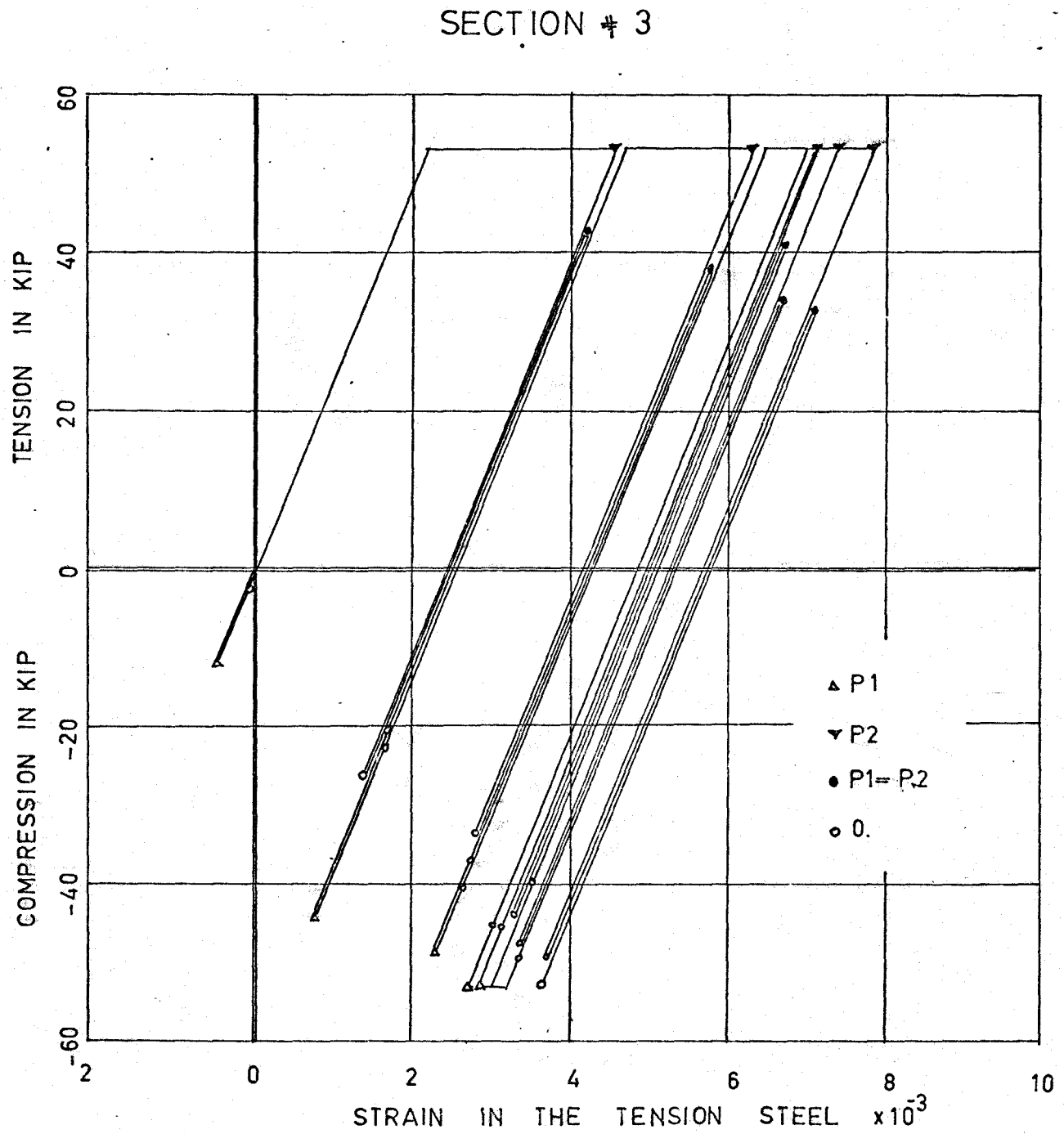

FIG. 4.31. STRESS VERSUS STRAIN IN TENSION STEEL TEST # 7

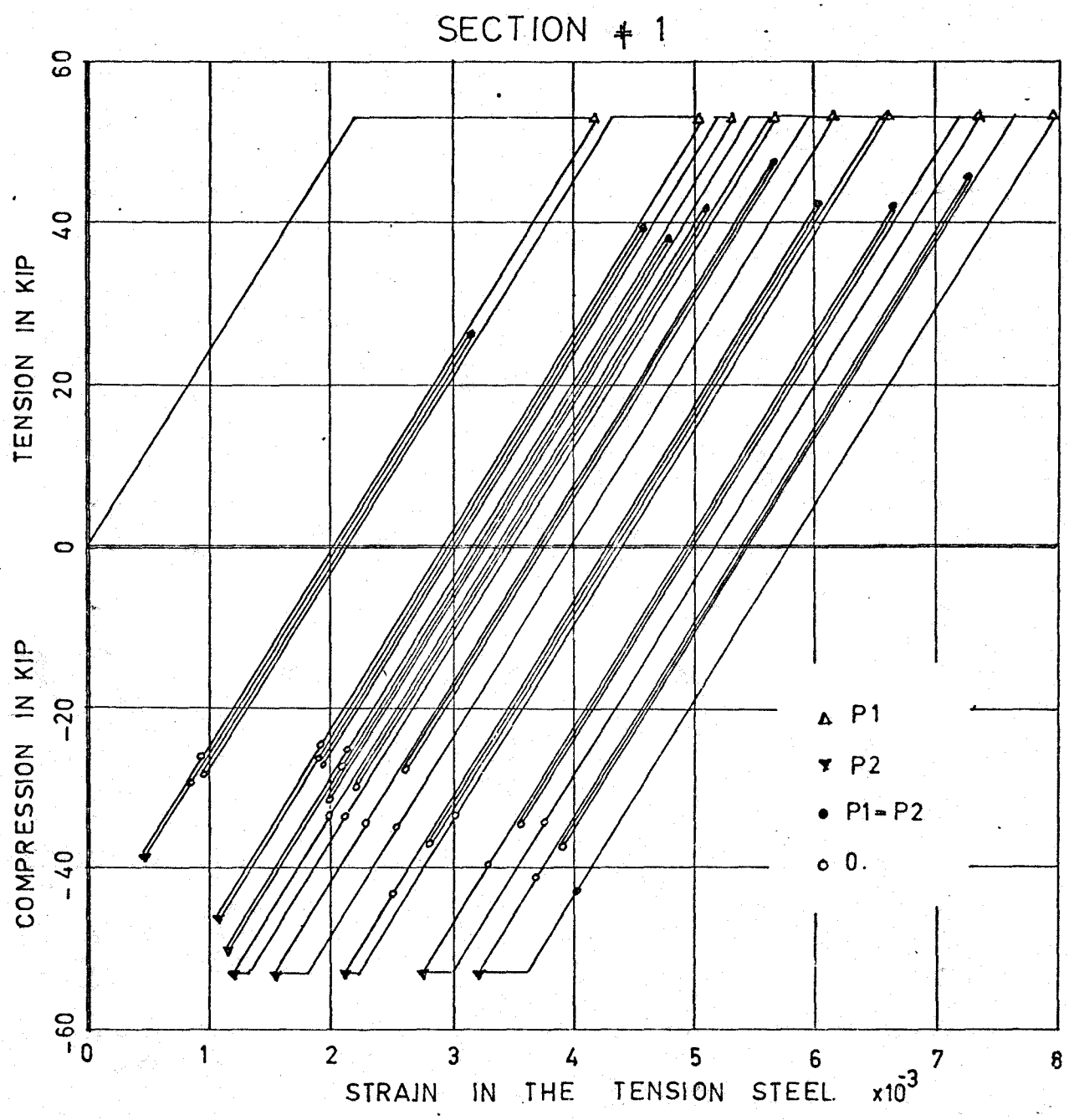

FIG. 4.32. STRESS VERSUS STRAIN IN TENSION STEEL TEST # 8

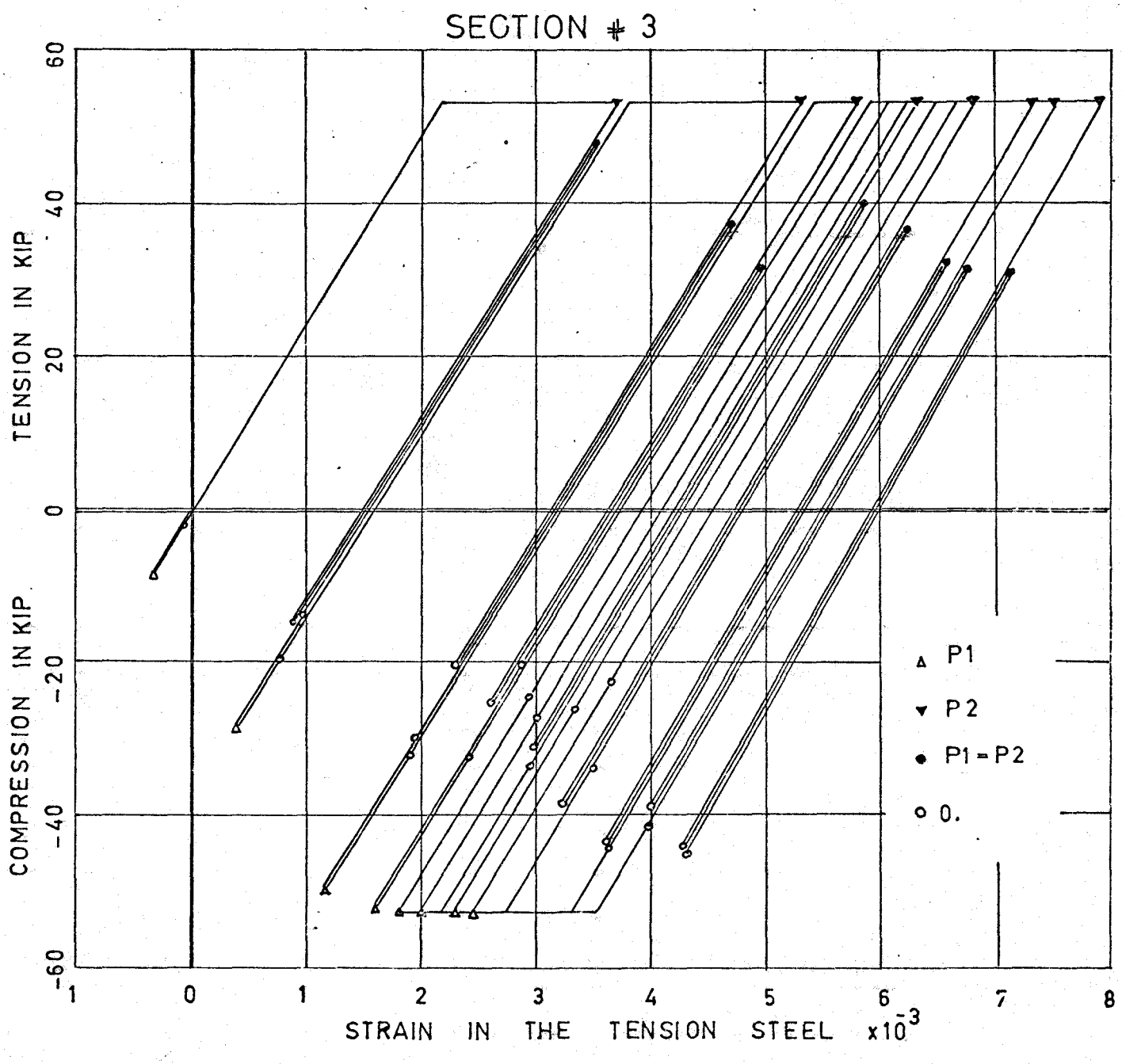

FIG. 4.33. STRESS VERSUS STRAIN IN TENSION STEEL

TEST # 8

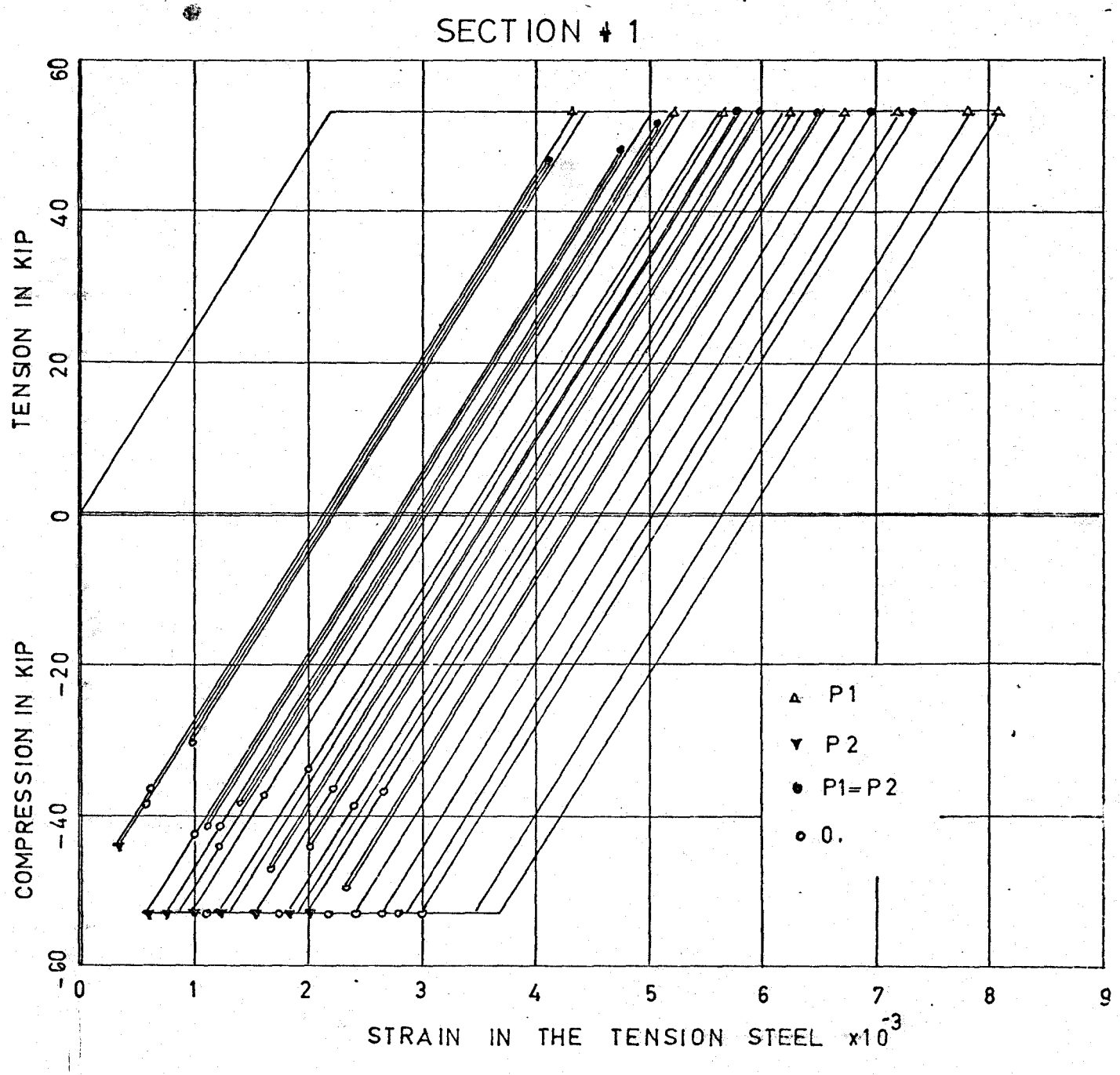

FIG. 4.34. STRESS VERSUS STRAIN IN TENSION STEEL TEST # 9

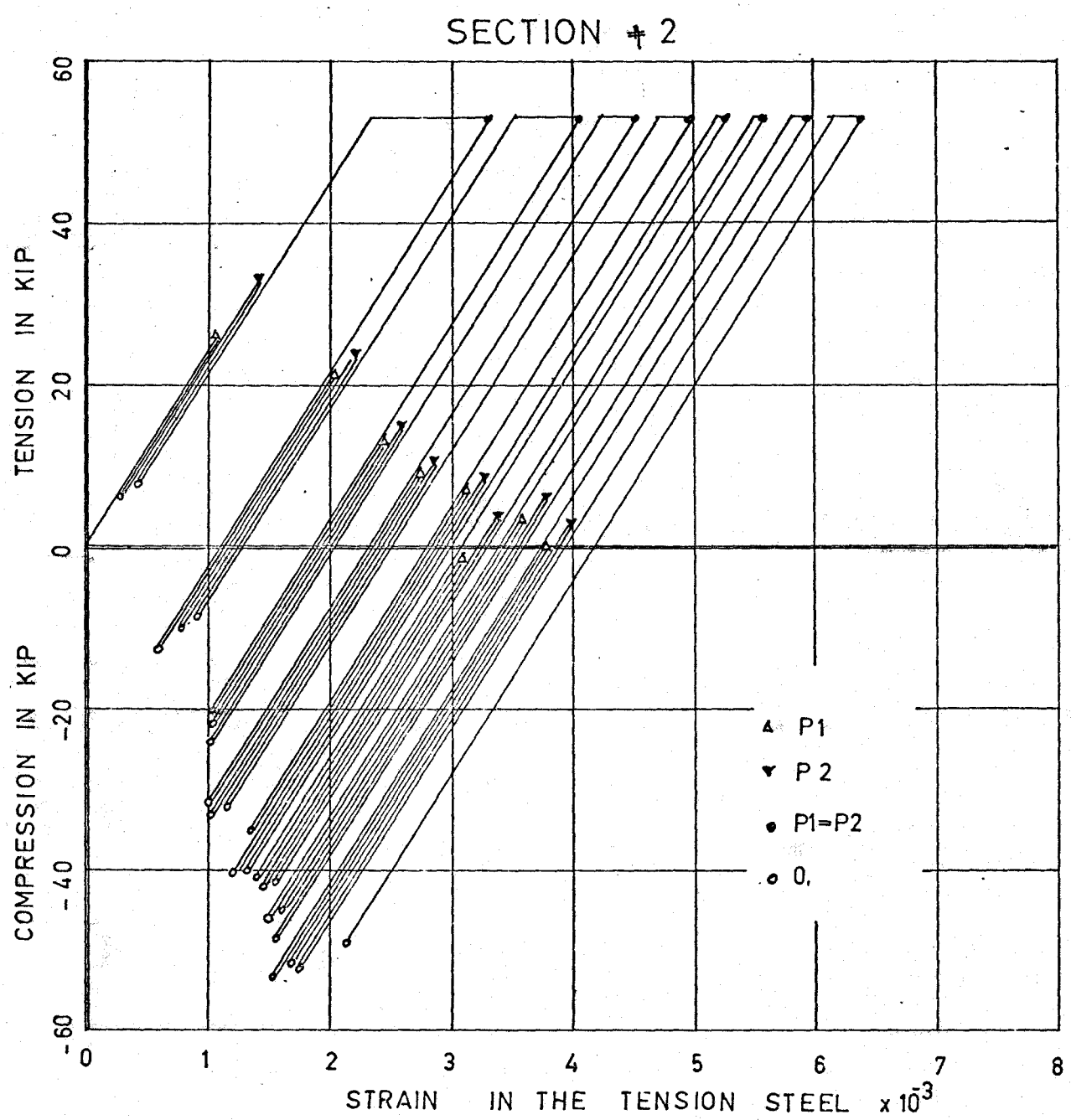

FIG. 4.35. STRESS VERSUS STRAIN IN TENSION STEEL

TEST # 9

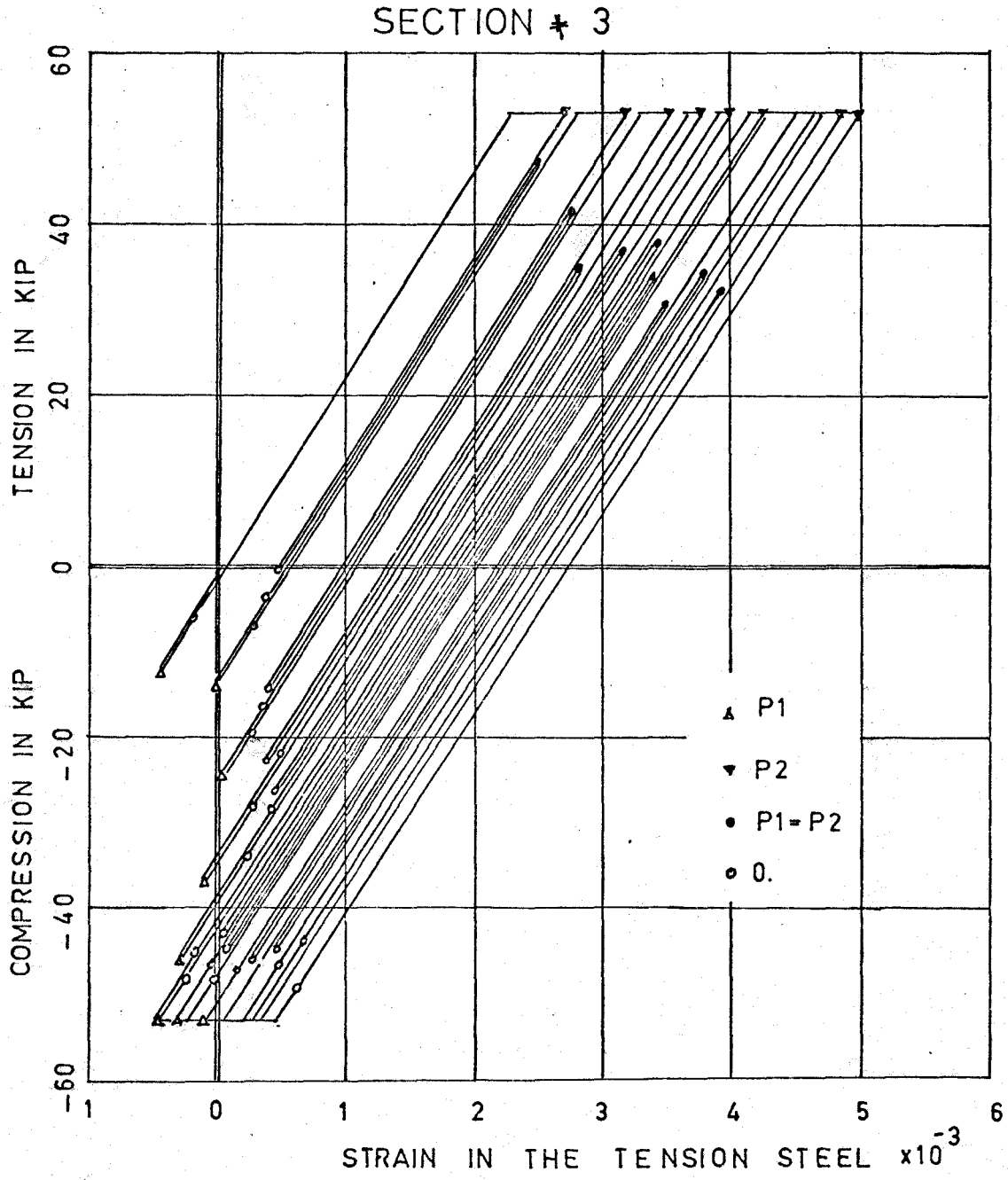

FIG. 4.36. STRESS VERSUS STRAIN IN TENSION STEEL TEST # 9

strain in the steel were simply drawn in the same order as the loads were applied.

The predicted strain data are drawn as dotted lines. The identification P_1 means again load applied in the left span, P_2 load in the right span. $P_1 = P_2$ means that both loads are applied at the same time and $P_1 = P_2 = 0$ indicates the situation for the residual strains at the end of a loading cycle.

4.6 PREDICTED SHAKE-DOWN LOAD AND THE ACTUAL TEST LOAD

According to the plastic theory the value of collapse load and shake-down load can be calculated by knowing the value of fully plastic moment for a given cross-section. This calculation (see Fig.4.36.a) gives the value of collapse load $P_C = 5.85 \frac{MP}{\ell}$ and value of shake-down load $P_S = 5.12 \frac{MP}{\ell}$.

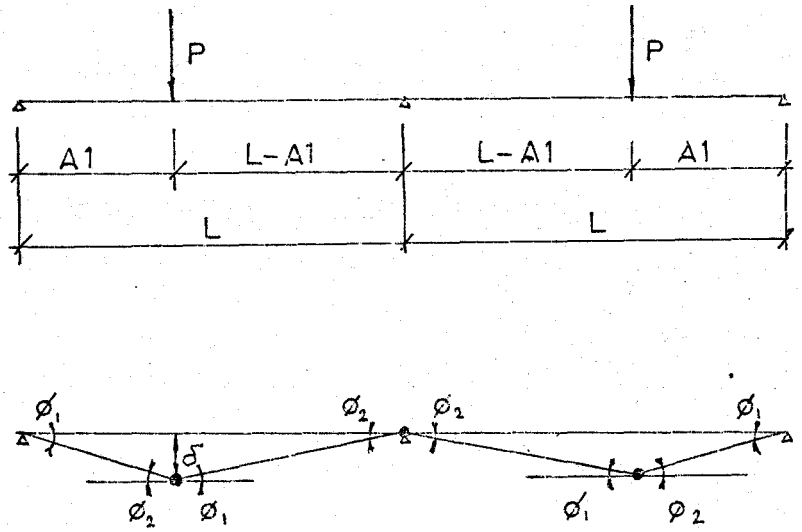

FIG. 4.36.a.

$$\phi_1 = \frac{f}{A1}$$

$$\phi_2 = \frac{f}{L-A1}$$

$$\phi_1 = \phi_2 \frac{(L-A1)}{A1}$$

$$MP(\phi_1 + \phi_2) + MP\,\phi_2 - P_C(\phi_2(L-A1))$$

$$P_C = MP \frac{(L+A1)}{A1(L\_A1)}$$

if A1 = 0.45L as in our case

$$P_C = 5.85 \frac{MP}{L}$$

Similar calculation for shake-down load:

TABLE 4.1

ELASTIC MOMENTS FOR A1-045L

CROSS-SECTION	1	2	3
P_1	+0.288PL	-0.0896PL	-0.0404PL
P_2	-0.0404PL	-0.0896PL	0.208PL
M_{max}	0.208PL	0	0.208PL
M_{min}	-0.0404PL	-0.1792PL	-0.0404PL

$$m_2(\phi_1 + \phi_2) - 2m_3\phi_2^2 + m_4(\phi_1 + \phi_2) = 0$$

$$\phi_2 = 0.818\phi_1$$

$$(MP - 0.208PL)\ 1.818\phi_1 - 2[-MP + 0.1792PL]\ 0.818\phi +$$
$$+ [MP - 0.208PL]\ 1.818PL = Q$$

$$P_S = P = 5.12\ \frac{MP}{L}$$

TABLE 4.2

COLLAPSE AND SHAKE-DOWN LOAD

				DIF. STEEL
F_C	3000	3400	3750	3100
MP	289	291	293	249
P_C	15.67	15.78	15.9	13.5
P_S	13.7	13.8	13.9	11.8

4.7 COMPARISON OF THE RESULTS

In the previous sections of this chapter the theoretical results and the test results were compared for each test and each critical cross-section separately. In this section, the test results and numerical analysis results are compared separately for each critical cross-section only and the data from all tests are drawn in one diagram.

The purpose is to show how the magnitude of the applied

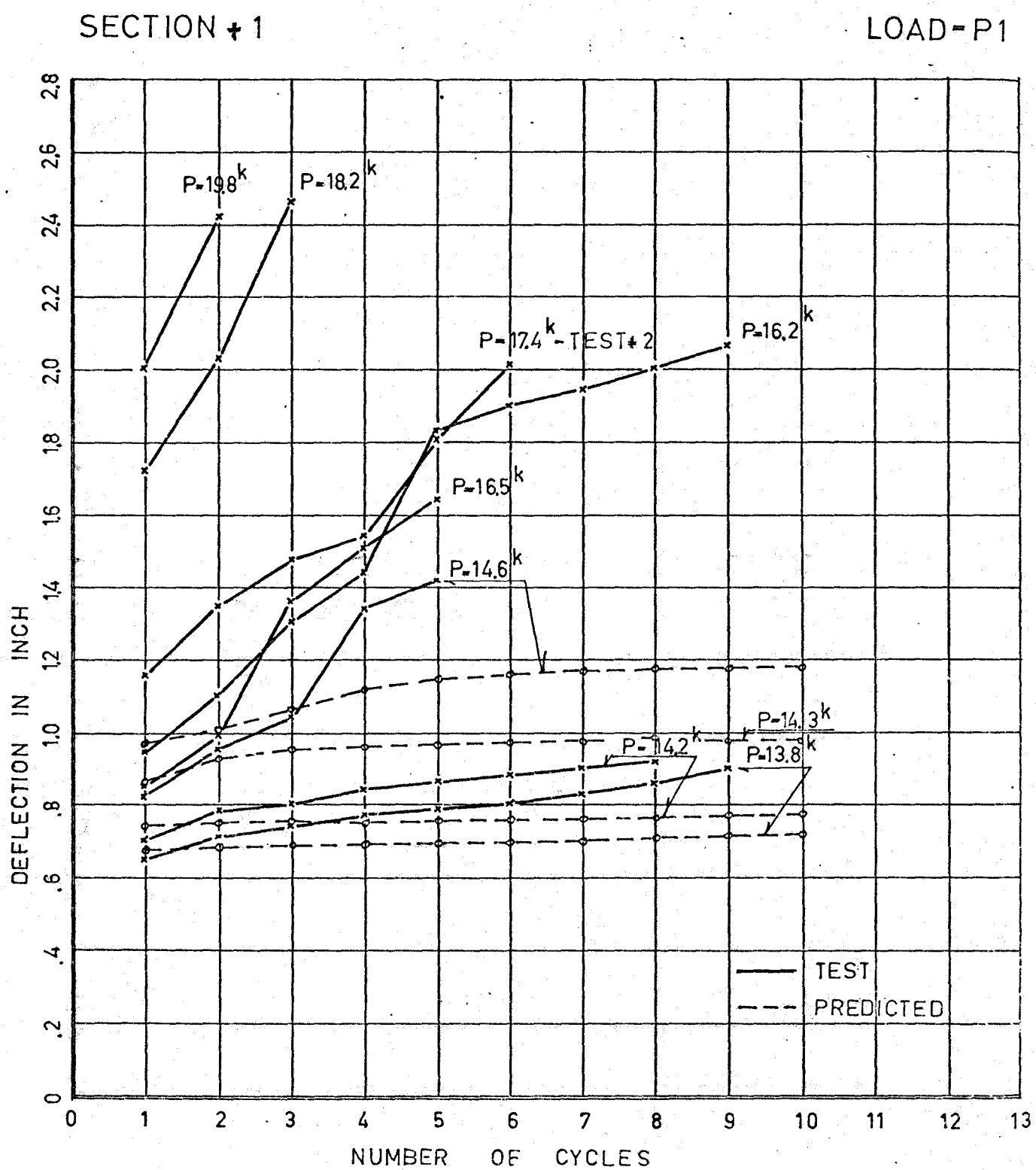

FIG. 4.37. DEFLECTION VERSUS LOAD AND CYCLES

SECTION # 3 LOAD - P2

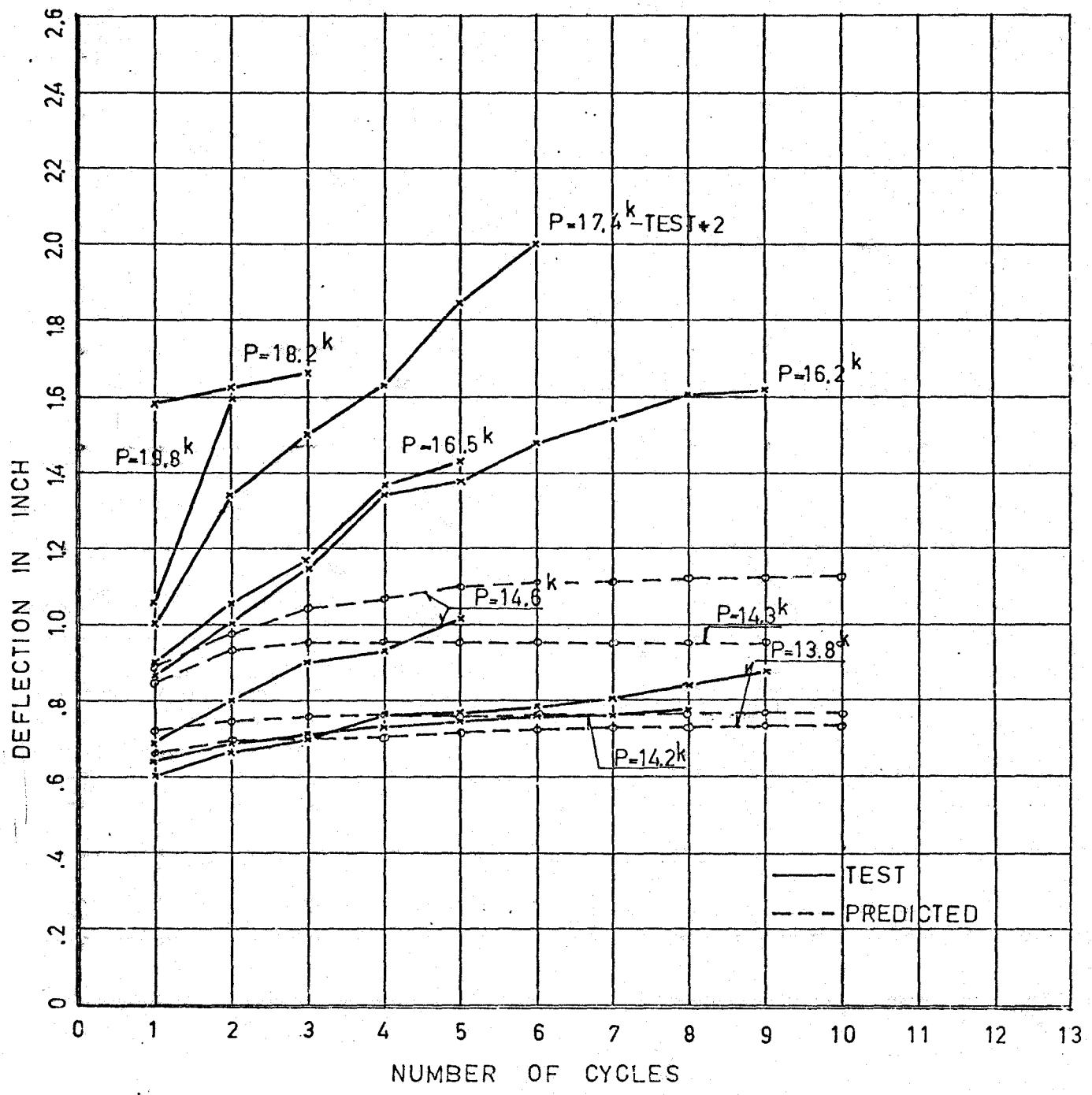

FIG. 4.38. DEFLECTION VERSUS LOAD AND CYCLES

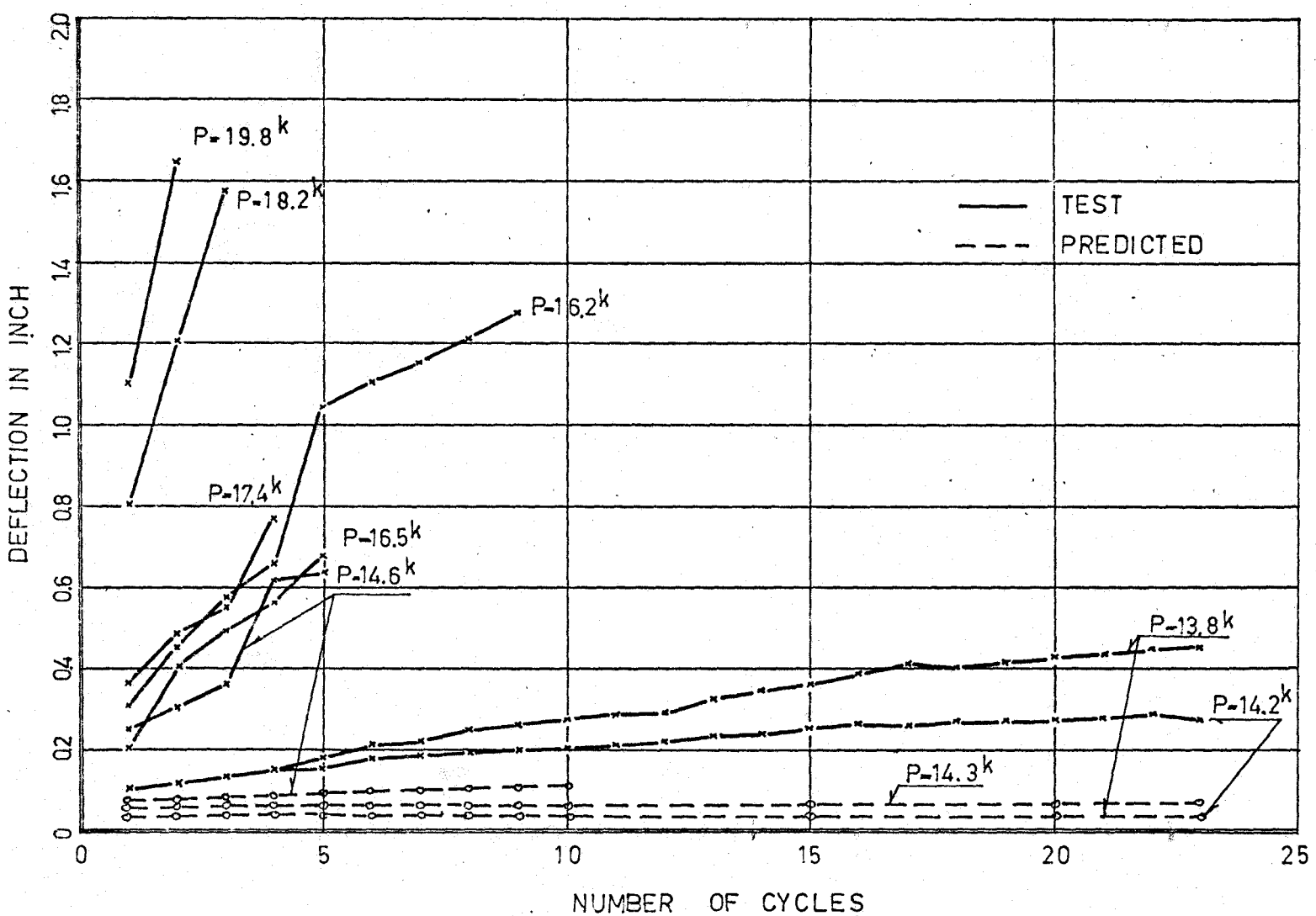

FIG. 4.39. RESIDUAL DEFLECTION VERSUS CYCLES

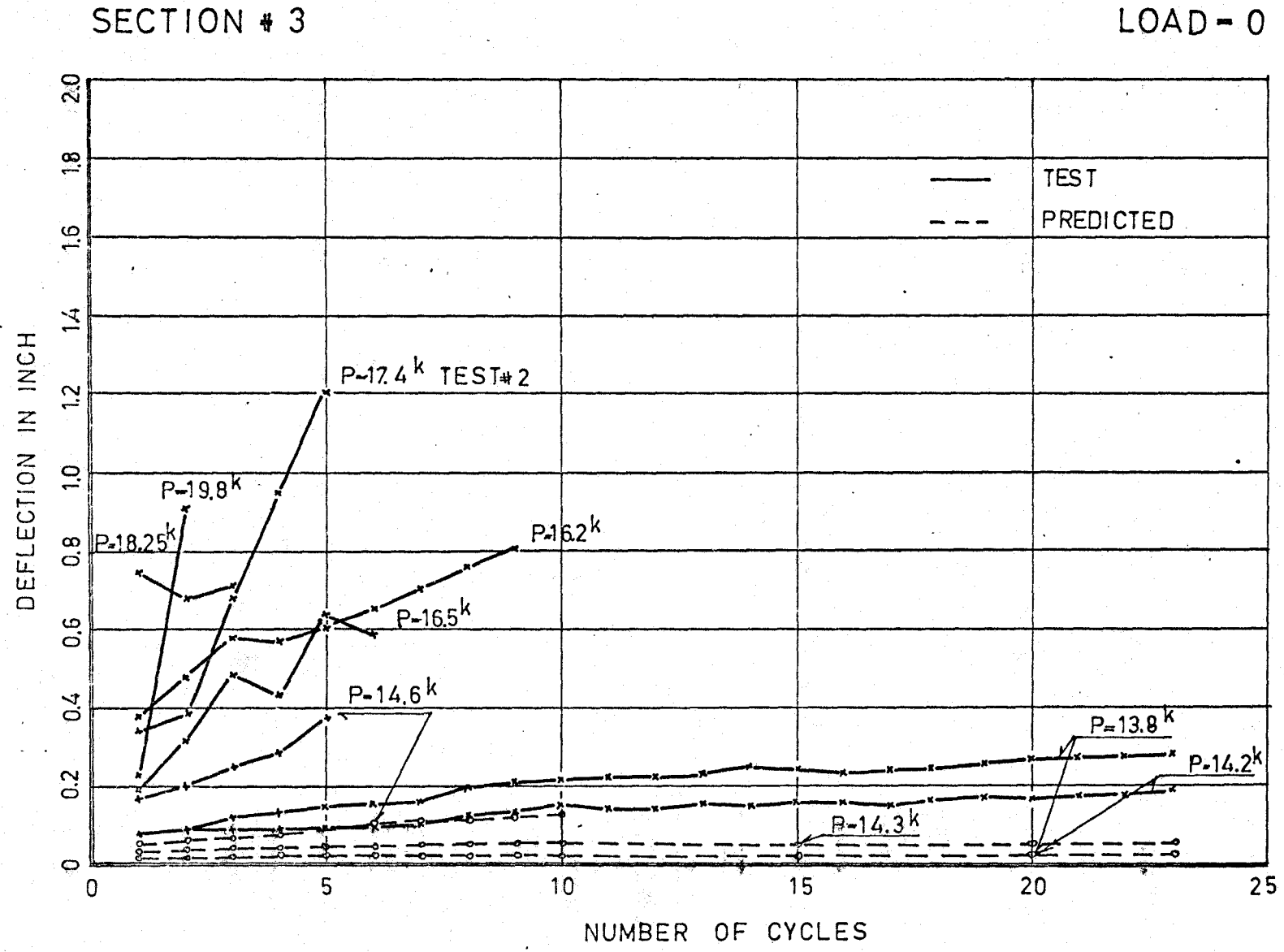

FIG. 4.40. RESIDUAL DEFLECTION VERSUS CYCLES

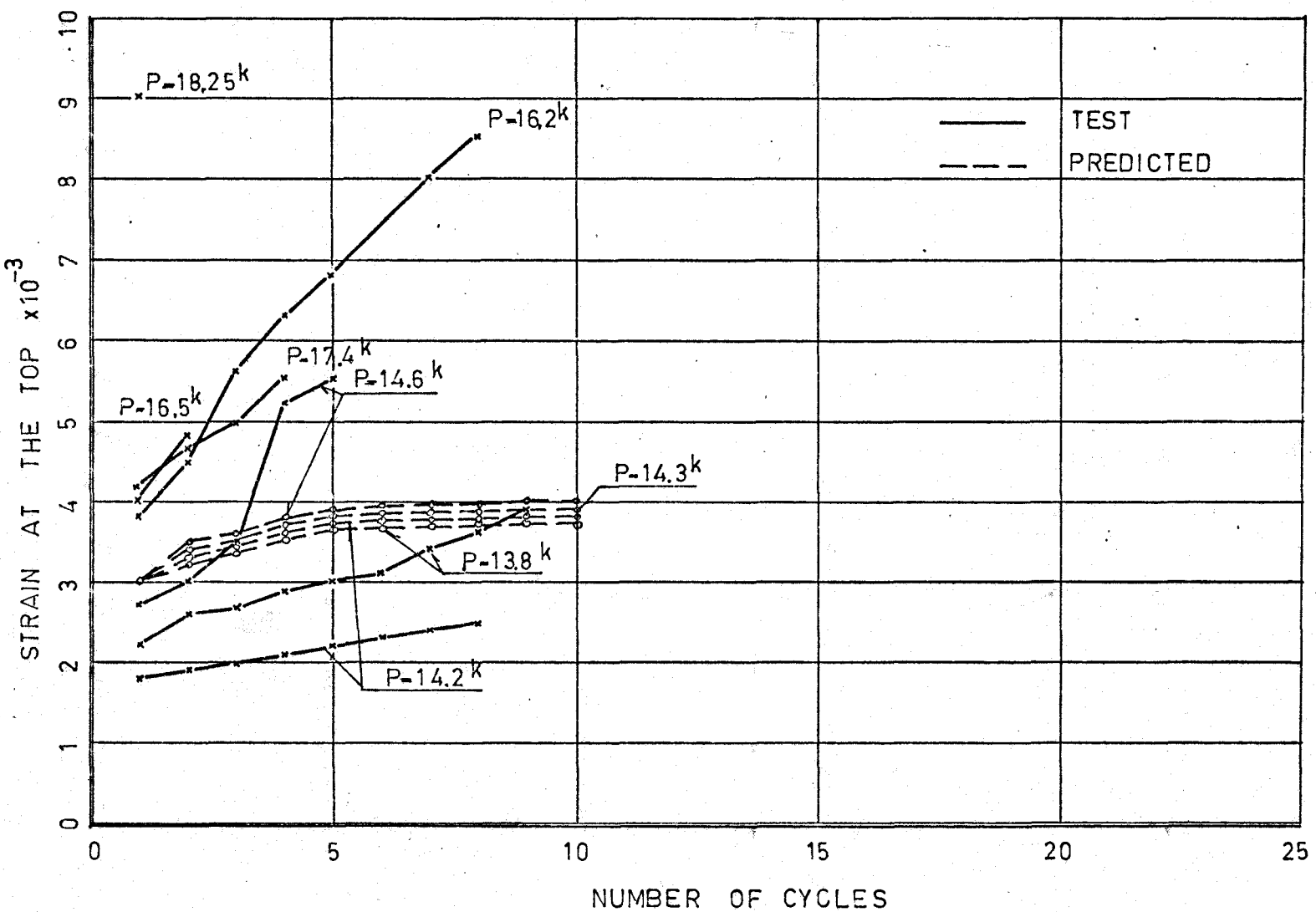

FIG. 4.41. STRAIN VERSUS LOAD AND CYCLES

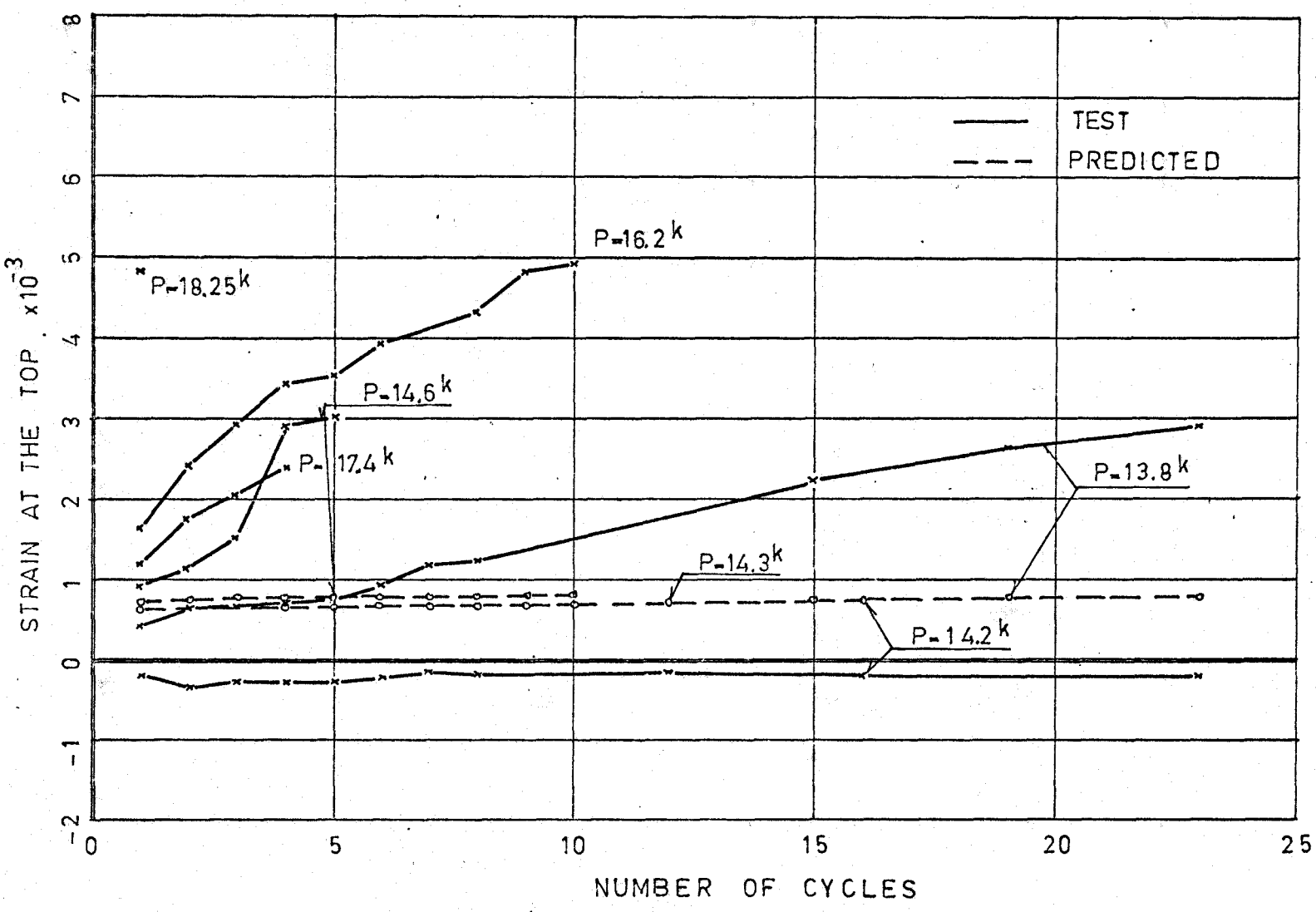

FIG.4.42. RESIDUAL STRAIN VERSUS CYCLES

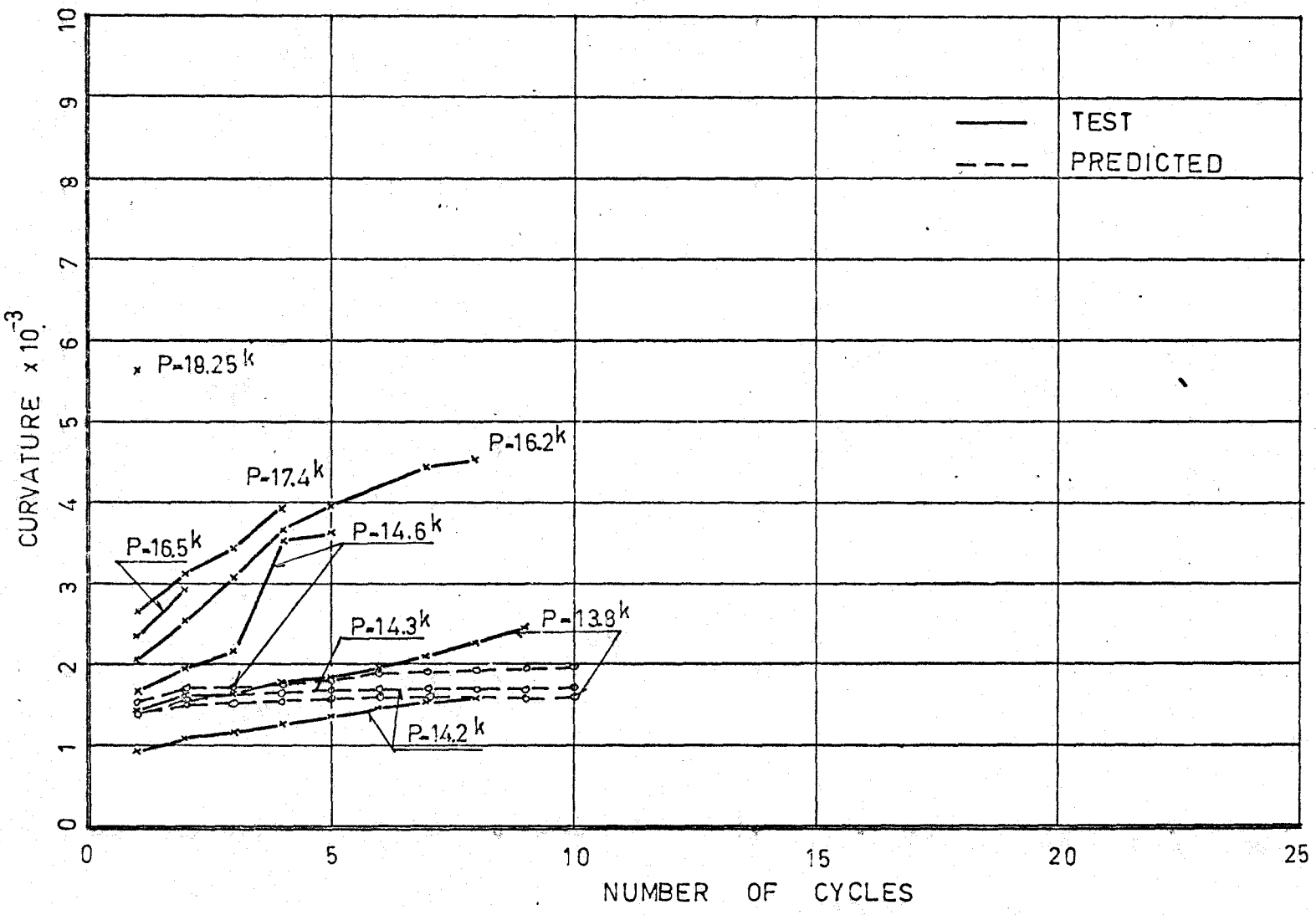

FIG.4.43. CURVATURE VERSUS LOAD AND CYCLES

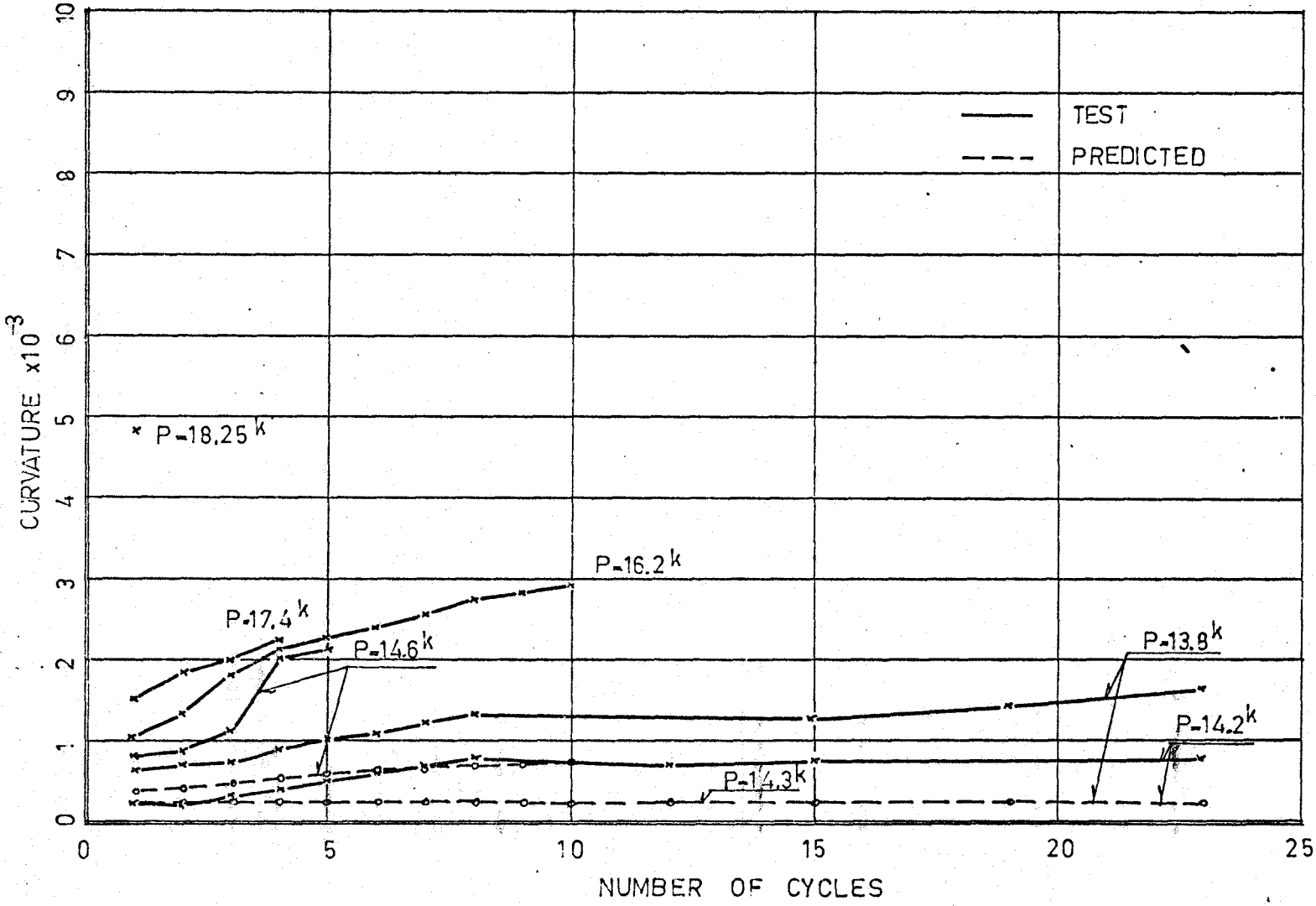

FIG. 4.44. RESIDUAL CURVATURE VERSUS CYCLES

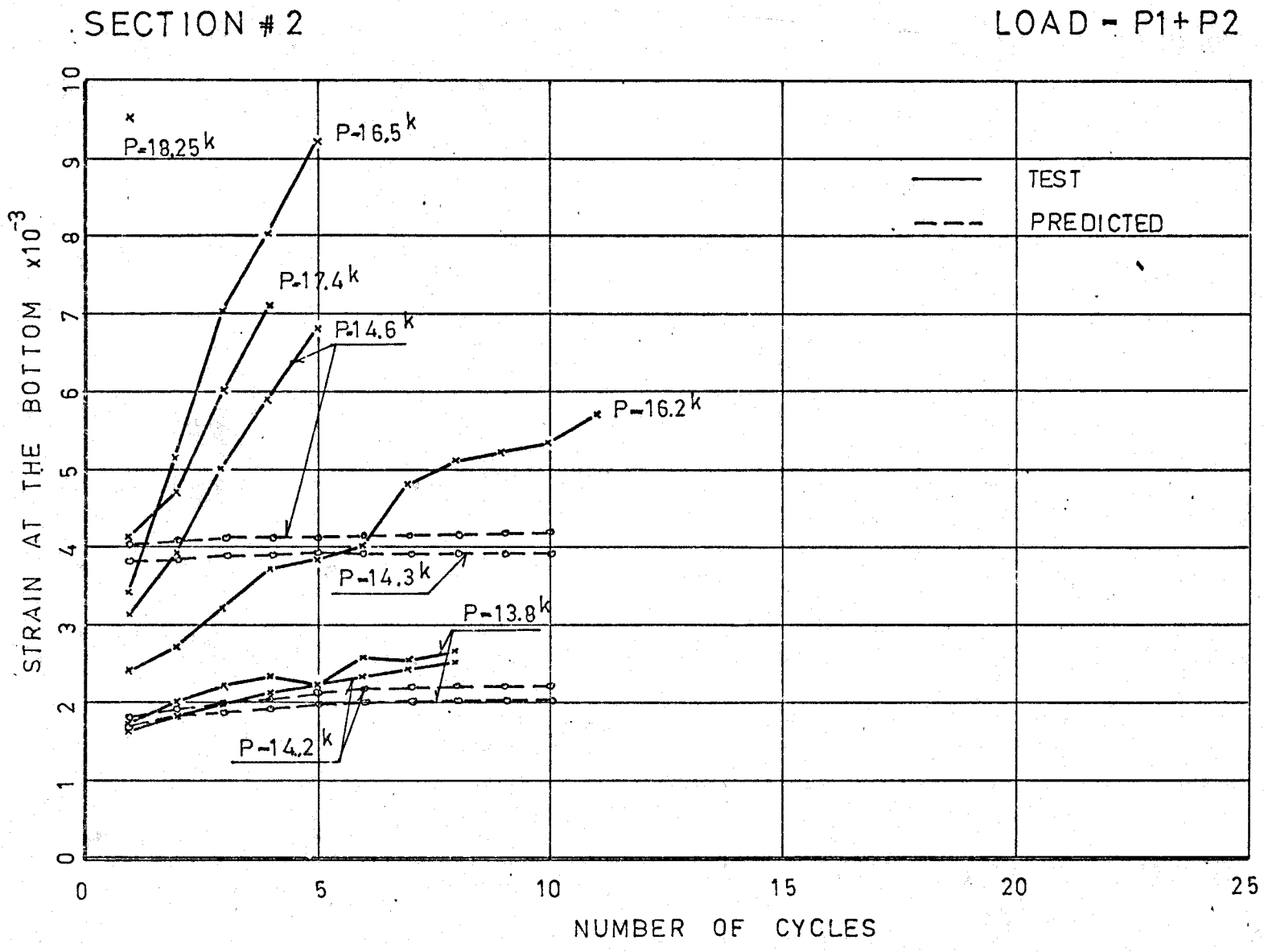

FIG. 4.45. STRAIN VERSUS LOAD AND CYCLES

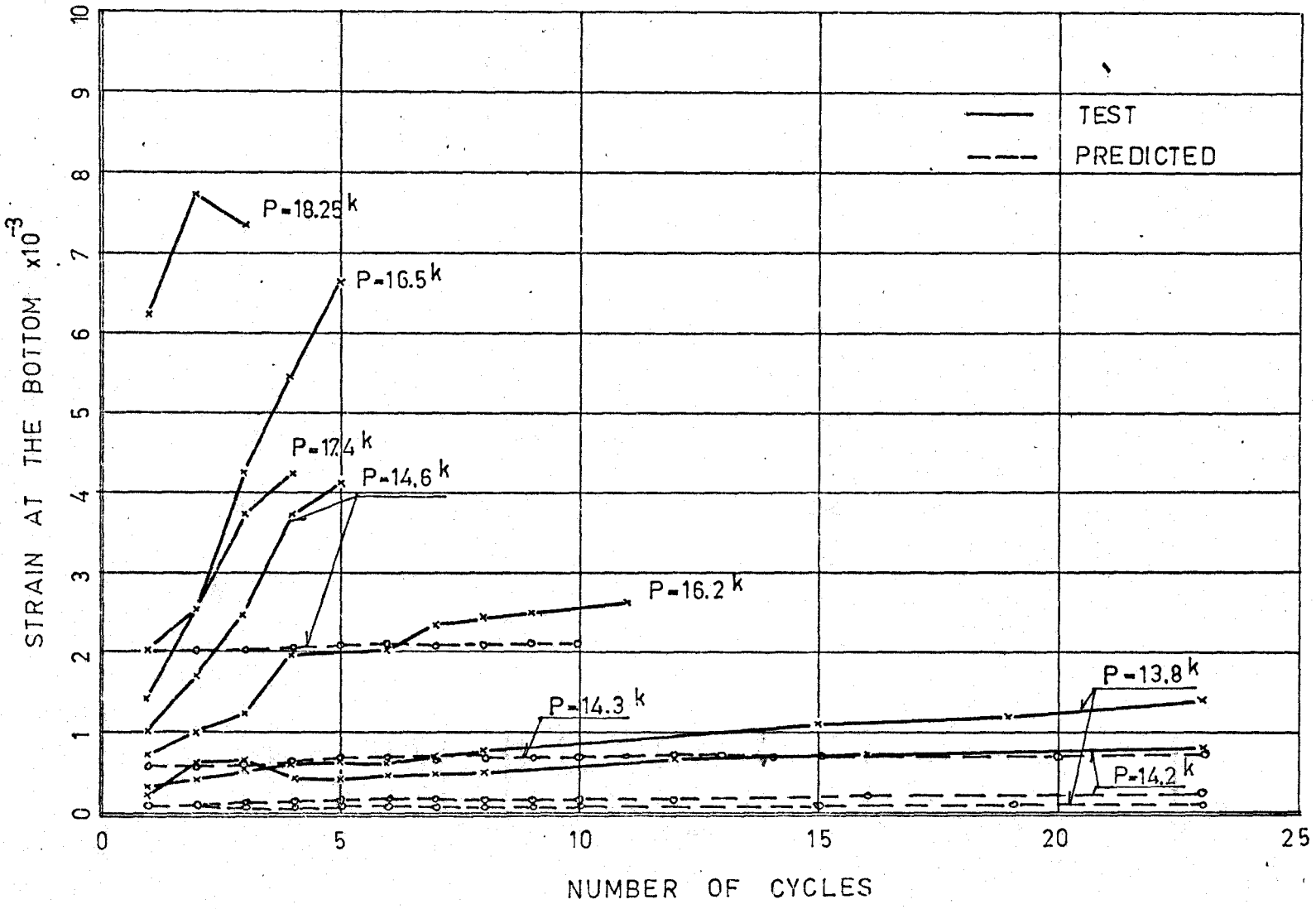

FIG. 4.46. RESIDUAL STRAIN VERSUS CYCLES

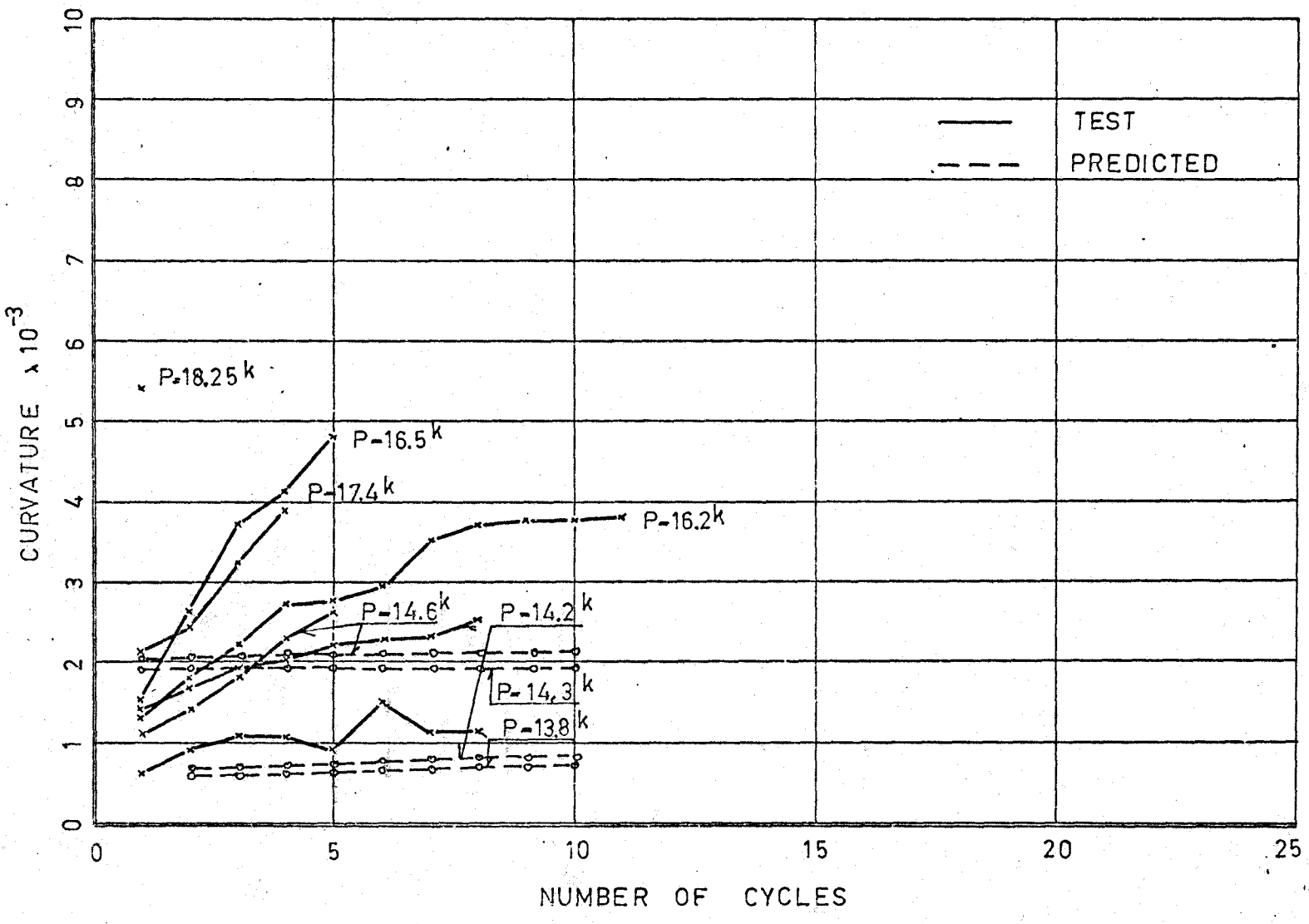

FIG.4.47. CURVATURE VERSUS LOAD AND CYCLES

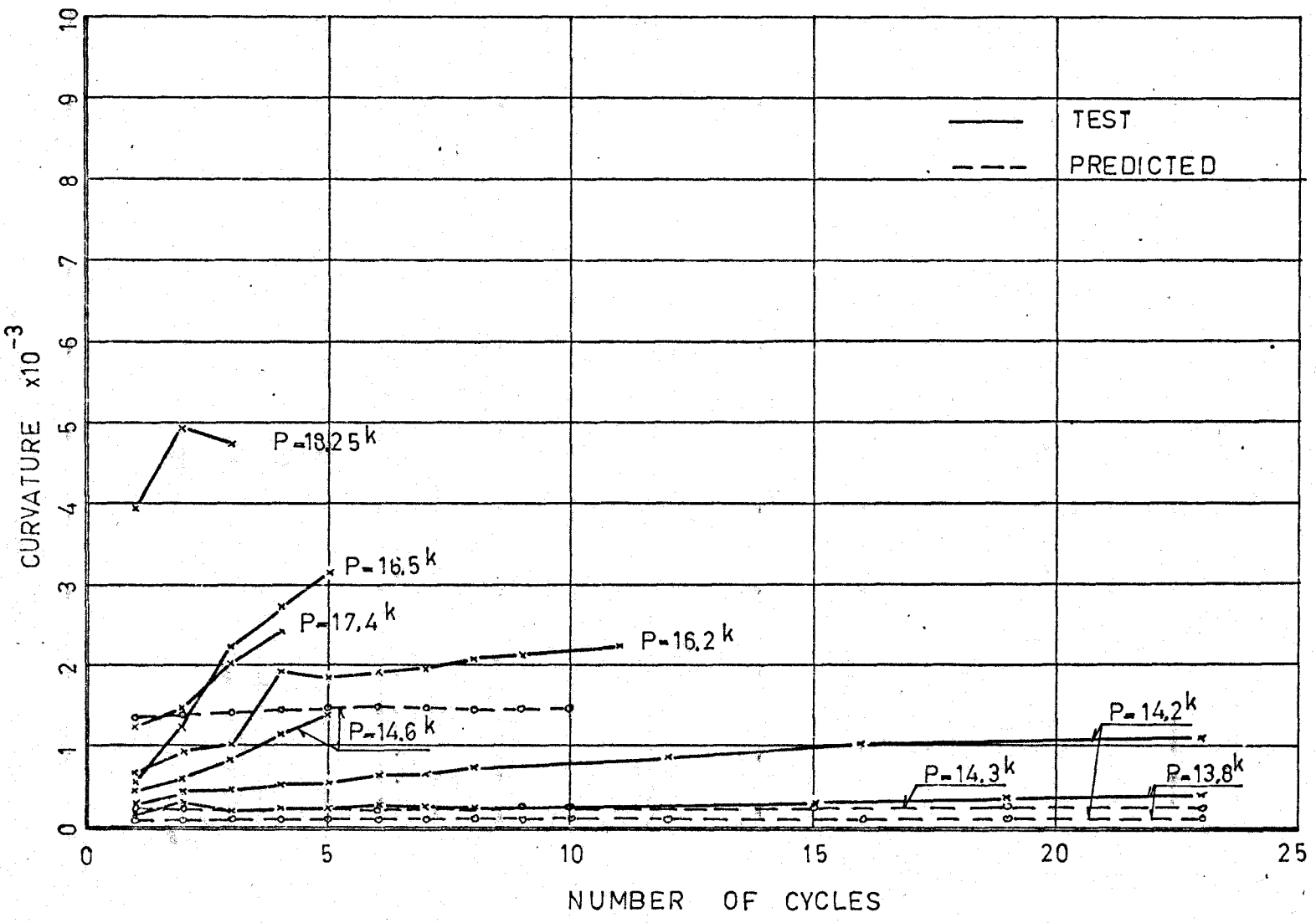

FIG.4.48. RESIDUAL CURVATURE VERSUS CYCLES

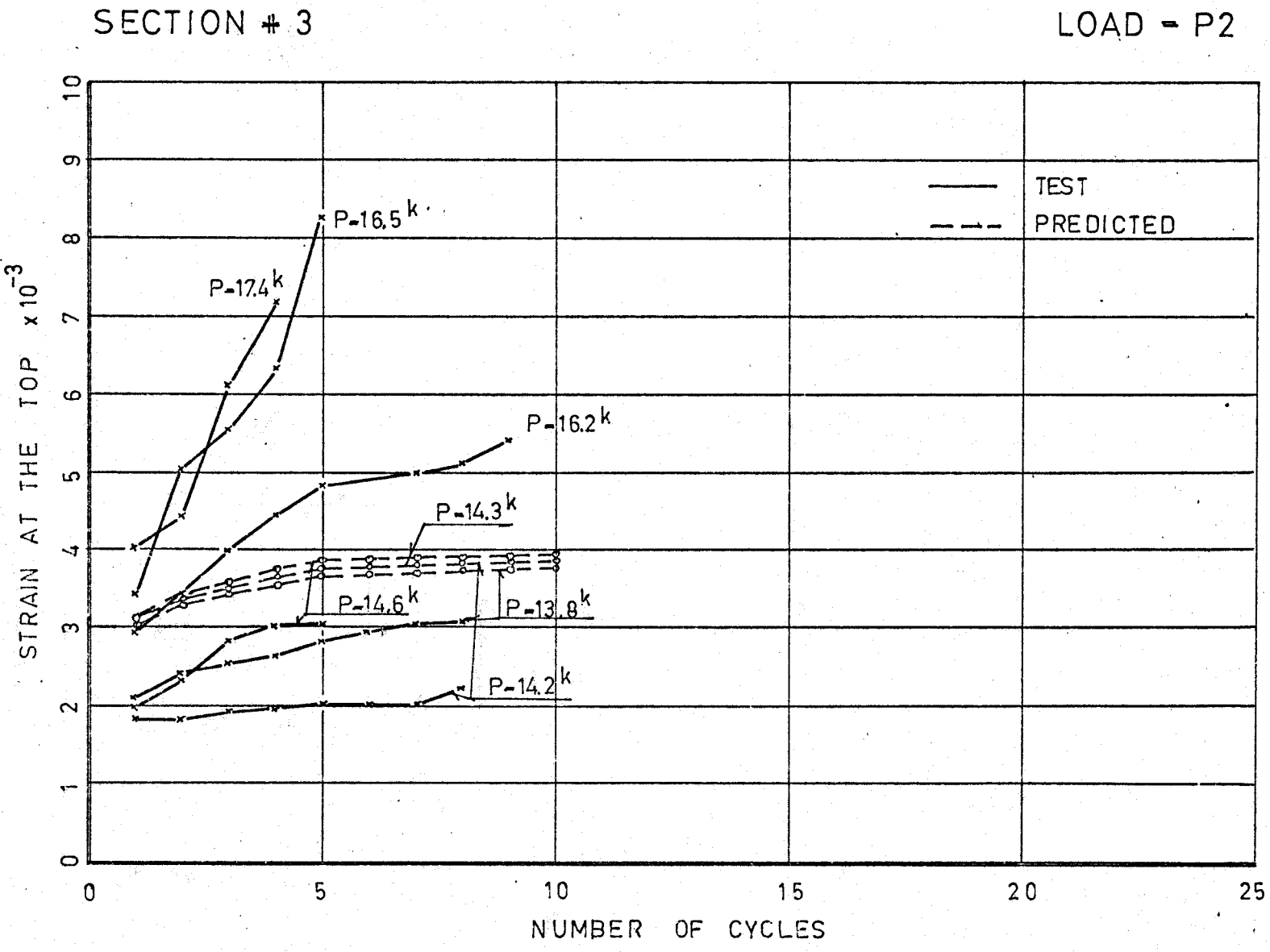

FIG. 4.49. STRAIN VERSUS LOAD AND CYCLES

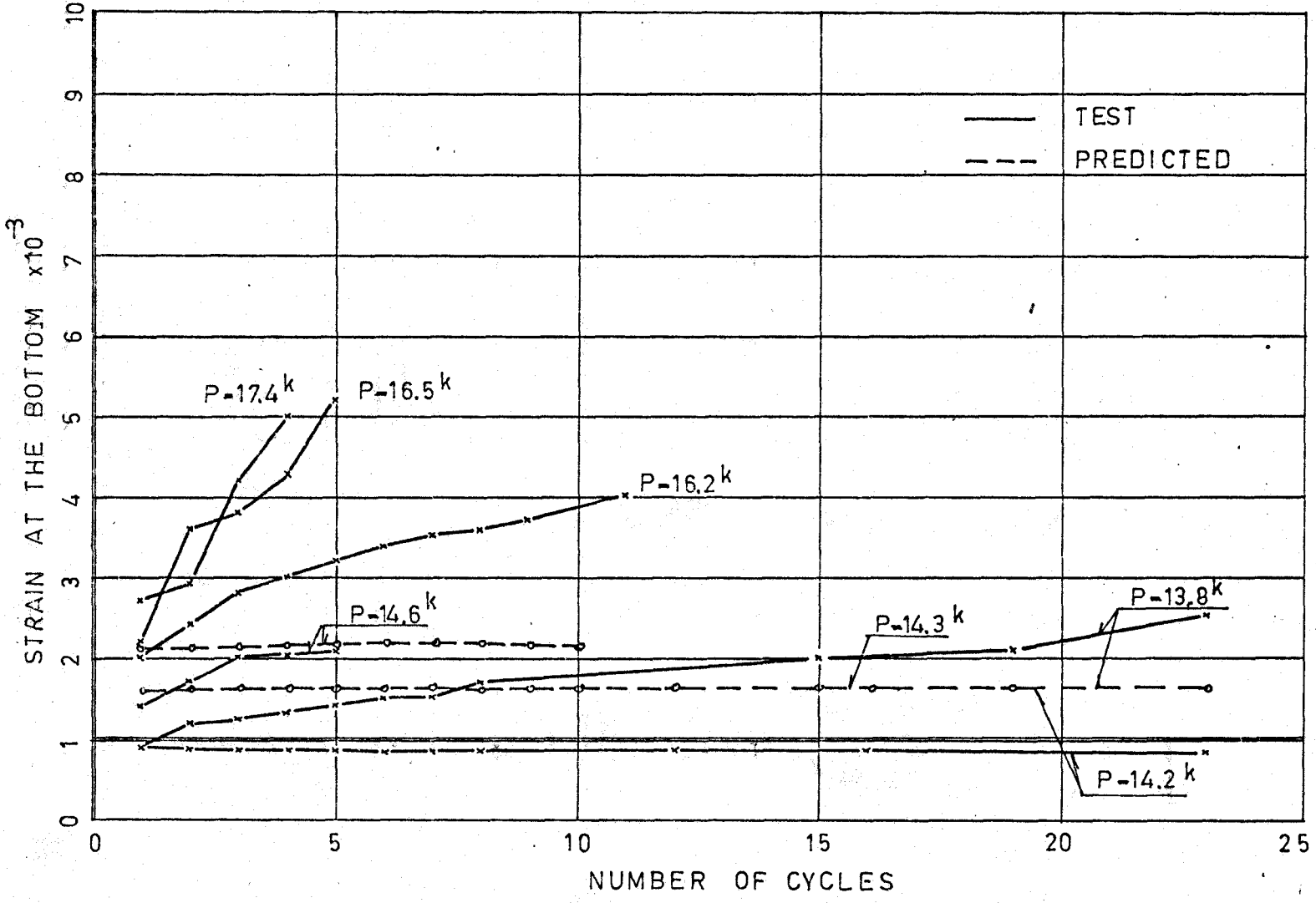

FIG. 4.50. RESIDUAL STRAIN VERSUS CYCLES

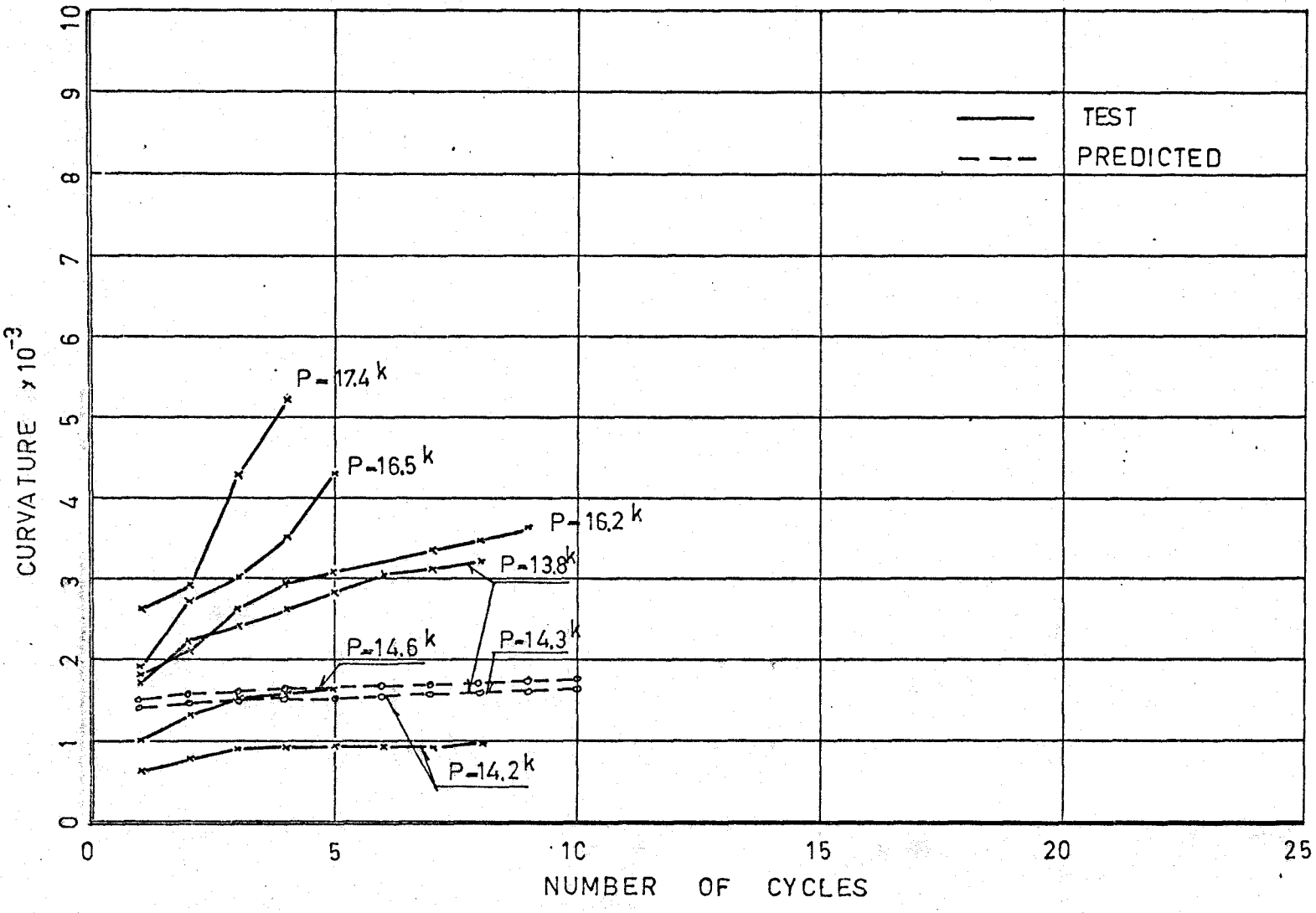

FIG. 4.51. CURVATURE VERSUS LOAD AND CYCLES

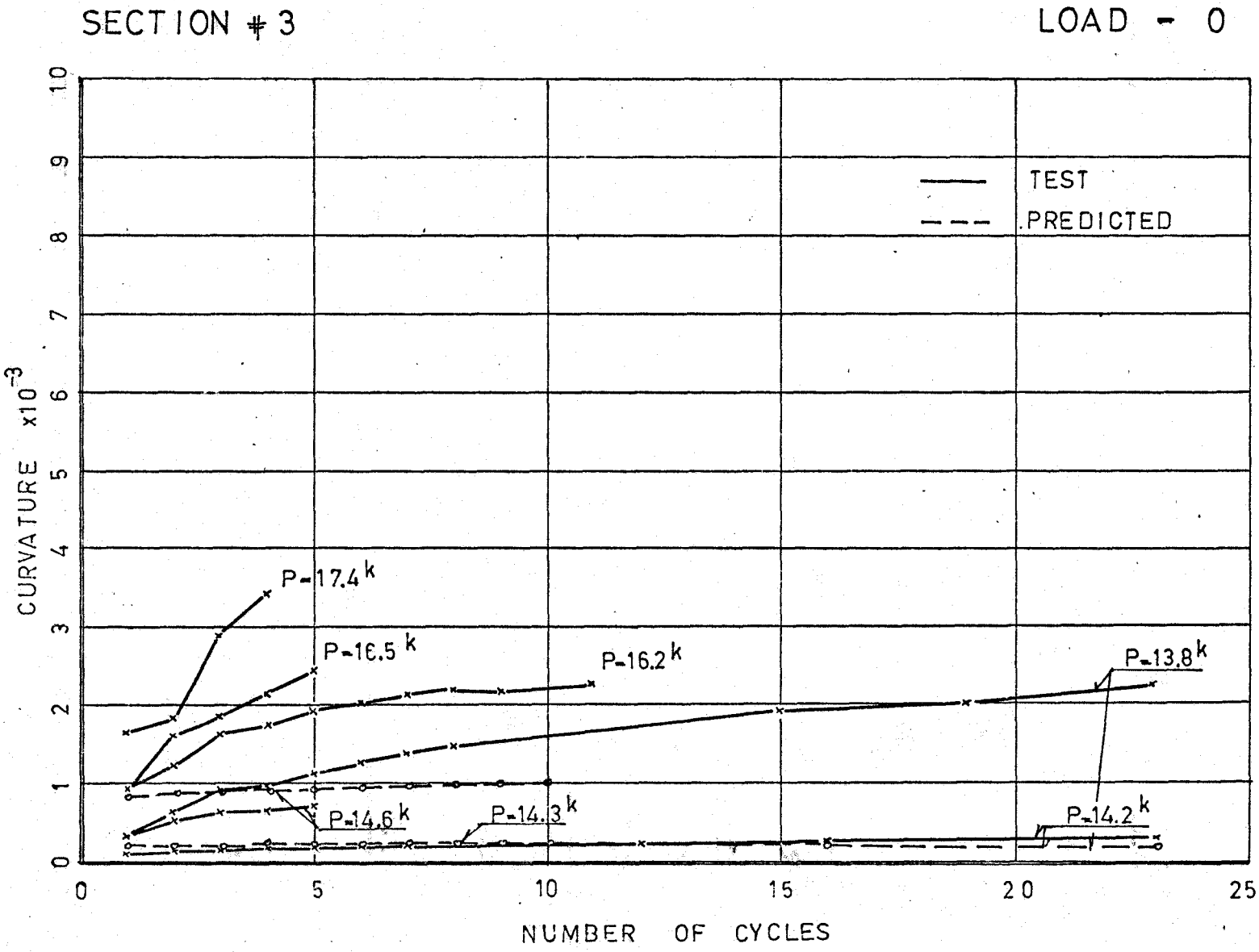

FIG. 4.52. RESIDUAL CURVATURE VERSUS CYCLES

load influences the strain history as well as the deflections in a particular cross-section.

First compared are the deflections measured under the applied loads. Included are only the largest deflections caused by applying one load only and the same span as in the investigated cross-section. Also shown are the residual deflections at the end of the loading cycle when no load is applied.

In the same order are drawn also the stains and curvatures in the compared cross-sections. Included are again only the maximum and the residual values. The reason why the results can be compared all together is that, except for the changing magnitude of the applied load, there was only one variable - concrete strength. As was shown by calculation (TABLE 4.2), the concrete strength variation doesn't have much influence on the value of the fully plastic moment for a given cross-section. Only the results from the test #2 should be drawn separately because the beam had a different amount and different properties of reinforcing steel. The results from this test were for practical reasons included with the rest of the results.

4.8 SUMMARY

The results of the tests and theoretical predictions presented in this chapter will be used to evaluate the numerical method of beam analysis which was described in

Chapter 3. In addition both sets of results provide information about proportional collapse, incremental collapse and shake-down.

Four aspects of the comparison between the theoretical prediction and the experimental results were mentioned in the course of explaining the methods used to display these results.

A more complete description and discussion of the relationship between the tests and the analysis is included in Chapter 6. The discussion of sources of errors is contained in Chapter 5. The possible magnitude of variations between tests and analysis are indicated.

CHAPTER 5

ERRORS IN THE NUMERICAL ANALYSIS OF BEAMS AND IN THE EXPERIMENTAL BEAM TESTS

5.1 INTRODUCTION

In this chapter references are made to sources of error and their possible influence on the interpretation of the theoretical and experimental results. An attempt is made toiindicate the possible magnitude of errors due to particular considerations. No methematical method in the probable error is accepted. However from personal observations and experience the magnitude of errors and the corresponding effects are estimated. The discrepancies in the test results were relatively small in magnitude. Also the numerical analysis was r asonably accurate. The existing inaccuracy in the analysis is a result of employing of simplified assumptions in stress-strain relationship of reinforcing steel.

5.2 ERRORS IN THE PREDICTION OF BEAM BEHAVIOUR DUE TO THE METHOD OF ANALYSIS

The beam analysis was accomplished by the use of a

simplified beam model as was described in Chapter 3. Some discrepancies resulted from the approximate nature of the model.

5.2.1 THE EFFECT OF THE BEAM MODEL

In the beam analysis, each investigated cross-section was divided into a number of strips. The force on each element was calculated using the strain at the centroid of the element. Similarly, for calculating moments, the force was assumed to act at the centroid of the element. This system would be correct if infinitely small elements could be employed. However to accommodate a reasonable computor solution time, relatively large elements were necessary. The variation in accuracy by changing the number of strips in the cross-section is shown in Fig. 5.1a.

The deflected shape of the beam was found by dividing the beam length into a number of segments and using the average curvatures from the cross-sections at the ends of each segment to calculate the displacement of one end of the segment with respect to the other end. The assumption of average curvature over a segment length is not exact, therefore the analysis is closer to being correct as beams are divided into more segments, which decreases the difference between the bending moments and the curvatures at the ends of each segment. The variation in accuracy depending on number of segments is shown in Fig. 5.1b. The datas for diagrams in Fig. 5.1 have been taken from Dr. R. Drysdale's thesis: "Creep in Reinforced Concrete Columns".

FIG. 5.1.a. THE ANALYSIS VARIATION CAUSED NUMBER OF STRIPS IN THE SECTION

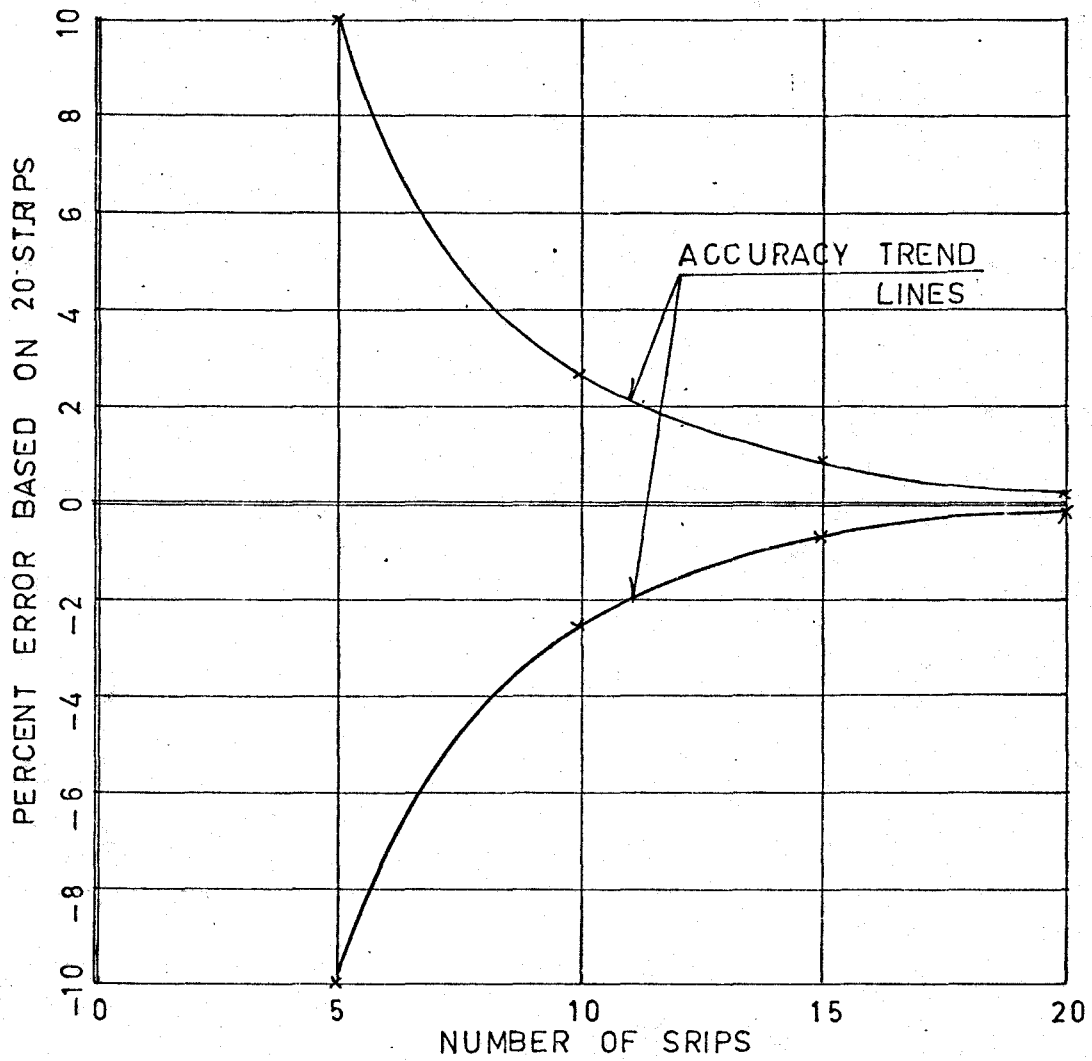

FIG. 5.1.b. THE ANALYSIS VARIATION CAUSED BY NUMBER OF SEGMENTS

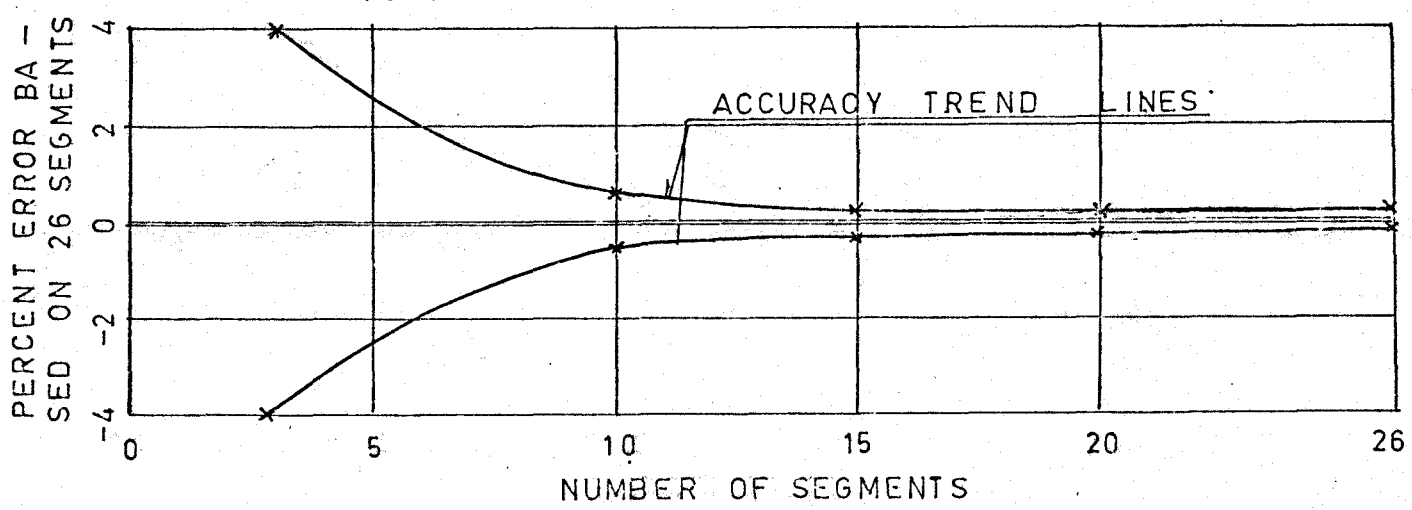

5.2.2 THE EFFECT OF THE LENGTH OF THE PLASTIC HINGE

The length of the plastic hinge was assumed constant throughout the test. This assumption was based on the theoretical moment-curvature diagram where the value of fully plastic moment stays constant by increasing curvature. The length of the plastic hinge has an influence on the average curvature in the plastic hinge, which is calculated as the hinge rotation over the hinge length. The value of MP as is shown in Chapter 6 does not stay constant when the curvature increases. The change in the MP is due to the strain hardening of reinforcing steel and the magnitude of increment of MP is proportional to the magnitude of increment of stress in the reinforcing steel.

5.2.3 THE EFFECT OF ERRORS CAUSED BY COMPUTER CONVERGENCE TOLERANCES

A different percent of tolerance limit was allowed in order to speed up computer convergence on to the required load and moments at each cross-section of the beam. This limit generally does not exceed 2%. Because of the system of convergence the calculated load was always very close to required value by the time the moment calculations were within the tolerance limit. Observations of computer print out of balanced moment compared to calculated bending moments showed that the individual tolerance errors tend to compensate for each other.

In addition to the tolerance error for convergence of calculated values of forces and bending moments there is another source of convergence error resulting from the tolerance allowed for convergence of the deflected shape. An accepted discrepancy of ±0.01 inches, which is equal in ±2 inch-kip change in the moment over the middle support, was used in the analysis. In the average the calculated value was less than the allowed tolerance.

5.3 ERRORS ASSOCIATED WITH THE USE OF IMPERFECT MATERIAL PROPERTIES AND ASSUMPTIONS

Many of the material properties used in the numerical analysis were derived experimentally and were therefore subject to experimental error. In addition some assumptions concerning material behaviour were made. The accuracy of some of these assumptions can not be checked without some additional studies which would be complete programs in themselves.

5.3.1 PROPERTIES OF REINFORCING STEEL

The stress-strain relationship for the reinforcing steel was found experimentally and indicated that there is strain hardening of the steel as shown in Fig. 2.3. Tests of 16 specimen (TABLE 2.4) indicated some deviation of the yield stress. There have been done only tests of specimens for each new shipment of reinforcing bars and not for every bar used in beam reinforcing. The deviation of 1 ksi from the average

yield stress 60.2 ksi will cause a calculated change of 1.7% in the value of MP.

The strain hardening of the steel was neglected as well as BAUSCHINGER'S effect. The strain hardening was neglected for practical reasons. When it would be included in the analysis it will cause an average 10% change in the fully plastic moment of the cross-section. Because the magnitude of MP was assumed constant and because it would be difficult to keep track in the changes of MP and plastic hinge length it was decided to neglect the strain hardening effect of the steel. The strain hardening has an influence on capacity of of the cross-section as well as on the behaviour of the beam.

The Bauschinger's effect which causes a non-linear stress-strain relationship for reloading the specimen in the opposite stress direction was not taken into account because it would be necessary to make a complex test series for each bar by discovering the true behaviour of the steel. Therefore it was assumed that the steel has its linear stress-strain relationship also in the reloading in the opposite direction. The Bauschingers effect does not have much influence on the capacity of the cross-section, but has an influence on the behaiour of the beam.

5.3.2 MATERIAL PROPERTIES OF THE CONCRETE

The derivation of the concrete stress-strain relationship is described in Chapter 2 and illustrated in Fig. 2.1. The strain results of the cylinder tests match up quite well with the mathematical curve. The greater of the concrete

stress-strain relationship obtained from the cylinder tests for each beam indicates that there are some differences between the actual and theoretical curve. However this shouldn't cause a problem because the equation for concrete stress-strain relationship used in the analysis was actually the expression for the average of the stress-strain curves and should cover the individual readings.

In the analysis no tensile stress was included in the behaviour of reactions, read from the load-cells, to the predicted reactions. The position of the loads and the length of the span was measured with a tape. A double measurement was done to make sure that the load was applied at the correct position. The expected error of 0.1 inch in positioning of the load would cause a change of 1.2% in bending moment.

5.4 ERRORS DUE TO VARIATIONS IN BEAM DIMENSIONS

The dimensions of the beam cross-section which were controlled by the forms were within 0.02 inches of the required size. The measured thicknesses to the trowelled surface were occasionally in error by as much as 0.2 inches. To minimize the effect of this variation, the beams were loaded so that the trowelled face was on the tension side on the main portion of the beam. The error in positioning of the reinforced bars in the cross-section was within 0.1 inches. The result of this discrepancy is in the range of 1.5% in the change of the capacity of the cross-section.

5.5 ERRORS RESULTING FROM THE LOAD CONTROL SYSTEM

The load cells used to measure the load on the beams and reactions under the supports were calibrated as was described in Section 2.4.2. The accuracy of the load sensing device for this 120 kip Baldwin Testing Machine was guaranteed to be within 0.5%. Any loading errors due to calibration of this testing machine were consistent.

A load-cell was discarded during calibration if the calibration curve was not repeated within 2% for several repetition of loading. However in the test #3 and #4 there was a failure of load-cells caused by the wrong calibration. The load-cells were re-calibrated after the test was finished and it was found that the actual applied load was higher than it was planned.

5.6 DEFLECTION AND STRAIN MEASUREMENT ERRORS

An examination of the methods of measuring deflections showed that any measurement could be made by as much as 0.003 inches due to human error. Then the deflection values could possibly vary a total of 0.06 inches because of opposite errors in the initial readings and measurement under the applied load. The Demec-strain indicator is read to the nearest division, which equals 10 micro-inches per inch. Repeated readings indicate that this instrument is reliable to one half of a division. Therefore the strain measurements were seldom wrong by more than 0.00001 inches per inch. However, incorrect

positions of the gauge points could result in some error.

5.7 SUMMARY OF ERRORS

Improvements in the beam model can be made to increase accuracy of the analysis but as was mentioned before it will cause an increase in computer time. There might be also more addition tests done to increase the accuracy of some of the employed assumptions.

CHAPTER 6

DISCUSSION AND RECOMMENDATIONS

6.1 INTRODUCTION

This chapter contains a discussion and comparison of the experimental and analytical results presented in Chapter 4. Sources of discrepancies between the test and predicted beam behaviour for the variable repeated loading are referred to and the trends of the correlations are pointed out. In conjunction with the discussion of the variations between the test and the predicted results, possible improvements in the method of analysis are suggested.

6.2 COMPARISON OF TEST DATA AND PREDICTED RESULTS

As was mentioned in Chapter 3, the numerical analysis was derived for predicting the behaviour of the beam for variable repeated loading. The adjusted computer program was run also for the proportional loading condition, but it stopped just prior to formation of the second plastic hinge. The magnitude of the load at which the program stopped in close and is assumed to be that of the predicted proportional collapse load, P_C. The predicted magnitude of the load P_C was 16 kips. When the applied load has a magnitude equal to or greater than that of P_C, the loading causes plastic collapse

of the beam according to the numerical analysis as well as the plastic theory. A number of tests with variable repeated loading have been done where the load magnitude was higher than the predicted P_C. These tests can not be compared directly with the numerical analysis, which is based on the idealized moment-curvature relationship.

6.2.1 PROPORTIONAL LOADING TESTS

Tests #1 and #10 were done in order to establish the value of Fully Plastic Moment MP and the proportional collapse load P_C. Some differences are evident between the predicted magnitudes of P_C and the actual collapse load. Also differences were observed between the theoretical plastic moment MP and the actual MP, which was calculated from the load-cells readings in test #10. Test #10 was most important because the cross-section of the beam used in this test had the same parameters as the cross-section used for 7 of the tests with variable repeated loading. The evaluation of the test is done in Section 4.4 and the moment-load, moment-curvature and deflection-load relationships are shown in Figures 4.3, 4.4 and 4.5. The theoretical value of MP (TABLE 4.2) is 249 inch-kips and 293 inch-kips respectively for tests #1 and #10 and the predicted value of collapse load P_C according to the plastic theory and the numerical analysis is correspondingly 13.5 kips and 16 kips.

Following the moment-load relationship for all three

critical cross-sections where the hinging action was expected, the first plastic hinge was created over the middle support at 12 kips load in test #1 and at the 16 kips load in test #10. To obtain a collapse mechanism one more plastic hinge was required under one of the applied loads. In test #1 the plastic hinges under the loads were formed simultaneously at the load of 15 kips. This is shown in Fig. 4.3. It is perhaps more clearly seen when comparing the load-deflection relationship illustrated in Fig. 4.4. The relationship is almost linear for both points under the applied loads until the loads reach the magnitude of 15 kips. Then the relative increase in deflection is much higher. However the beam did not collapse even if the magnitude of the load reached 20 kip. The first value of P_C, which can be called P_{C1} was established at 15 kips.

In test #10 the formation of the first plastic hinge took place again over the middle support at the load of 16 kips. The second plastic hinge formed at the critical cross-section #1 at the 15 kips load. This result could be due to an unaccurate strain reading from which the theoretical value of MP was calculated. As more realistic value seems to be that the plastic hinge was created at the load of 18 kips at critical section #3. When comparing the load-deflection relationship in Fig. 4.4, the relatively rapid increase in deflection starting at the load 18 kips tends to confirm this suggestion. As in the test #1, also in this test the beam did not collapse at the load 18 kips, which was established

to be the first collapse load P_{C1} and resisted even if the magnitude of the applied load was 20 kips. The highest magnitude of the load the beam was subjected to can be called the last applied collapse load P_{CL}.

TABLE 6.1

THEORETICAL AND ACTUAL P_C

TEST #	ACTUAL P_{C1}	ACTUAL P_{CL}	PLASTIC ANALYSIS P_{CT}	NUMERICAL ANALYSIS P_{CT}	P_{CT}/P_{C1}	P_{CT}/P_{CL}
1	15^K	20^K	13.5^K	13.5^K	90%	67.5%
10	18^K	20^K	15.9^K	16^K	89%	80%

The theoretical value of MP, calculated to be 293 inch-kips, when compared to the actual value of MP from test #10 (Fig. 4.5) does not match up very well. Also the theoretical moment-curvature relationship, which assumes a constant value of MP shows some discrepancies with the actual moment curvature relationship, where the value of MP steadily increases with increasing curvature.

The differences between the predictedP_C and the first collapse load P_{C1} and the last applied collapse load P_{CL} (TABLE 6.1) was caused by the fact that the actual capacity of the cross-section was higher than the predicted one when using the, ideal, stress-strain relationship for reinforcing steel.

6.2.2 INCREMENTAL COLLAPSE RESULTS

Eight beams were tested with variable repeated loading. The number of loading cycles applied to the test specimen and the magnitude of the load was varied from test to test. The results of the tests were drawn separately for the deflection-cycles relationships in Figures 4.6 to 4.12 and for the strain-cycles relationships in Figures 4.13 to 4.25. For illustration the stress-strain relationships for the tension steel in the critical cross-sections are also shown in Figures 4.26 to 4.36.

a) TEST #2

The magnitude of the load P applied to the beam was chosen as a result of a wrong estimate of a MP from the first proportional loading test. Both tests were done within a few days and therefore the analysis of the proportional loading was not complete. As a result the fully plastic moment for a cross-section with eight #4 bars as used in the first proportional loading test, was assumed more than 20% higher than was the actual capacity of the cross-section. According to the analysis of the first test the actual collapse load P_C and was 15^K and therefore each load applied to the test specimen with a magnitude equal to P_C or higher than P_C should cause a plastic collapse of the beam.

From the strain-cycles diagram and curvature-cycles diagram shown in Fig. 4.13, it can be seen that in the first loading cycle, when the single load P_1 in the left span

was applied, a plastic hinge was created in the critical cross-section #1 (strain $\approx 4 \times 10^{-3}$, curvature = 2.6×10^{-3}) but there was no plastic hinge at the critical section #2. The reading in strain reached 1.15×10^{-3} and curvature was 4×10^{-4}. Fig. 4.3 indicates that the curvature in the plastic hinge should be at least 1.25×10^{-3}. The collapse mechanism had not formed even in the second stage of the loading cycle when the load P_2 was applied in the right span. There was a plastic hinge in the cross-section #3 but again no plastic hinge at cross-section #2. Only when both loads P_1 and P_2 were applied simultaneously in both spans did a collapse mechanism form with plastic hinges in all three critical cross-sections. The explanation why the plastic collapse occurred only when both loads P_1 and P_2 were applied is probably in inaccurate estimate of theoretical moment-curvature diagram as well as inaccurate strain readings.

b) TEST #3 AND #4

In test #3 and in test #4 there was a failure of the load-cells which controlled the magnitude of the load. The load of 19.8 kips and 18.25 tips magnitude were higher than planned for these tests. In test #3 the deflections were so high that the demec gauge readings in the critical cross-sections were out of range. In test #4 some demec strain readings were obtained and they indicate as shown in Fig. 4.14 that the test specimens had formed a collapse mechanism in the first stage of the loading cycle. Crushing of the concrete

was observed in all critical cross-sections and therefore the test was stopped.

c) TEST #5

The magnitude of the load P = 16.5 kips was higher than the predicted collapse load and therefore the numerical analysis could not be done to be compared with the test results. The magnitude of the load lies between the actual collapse load P_C and the predicted shake-down load P_S. The behaviour of the beam under the applied loading cycles was expected to be as for an incremental collapse. The deflection-cycles relationship shown in Fig. 4.8 and the strain-cycles relationship and the curvature-cycles relationship shown in Fig. 4.15 seem to indicate that this is an incremental collapse. The deflections, strains and curvatures were quite rapidly increasing with each loading cycle. It was apparent that after a number of loading cycles the beam will collapse, therefore the experiment was stopped.

d) TEST #6

The bahaviour of this beam was very similar to test #5 even though the load P = 16.2 kips was slightly less than in the previous test. The discrepancies between the tests and the expected deflections, strains and curvatures can be explained by a number of practical errors and natural variability which have been described more detailed in Chapter 5. When it was apparent that the beam behaves as by an incremental collapse, the test was stopped.

e) TEST #7

Comparison of the test results with load magnitude of 14.6 kips and numerical analysis results in Fig. 4.10 and Fig. 4.19 indicated that the behaviour of the test specimen was very much like that expected for incremental collapse. The increments of deflection, strain and curvature were smaller than in previous tests but nonetheless steady increasing. At plastic hinge #1, the strain readings and curvatures from the test match up quite well with the predicted results in the first three loading cycles. Then there was a sudden jump in the test readings. Generally the same can be said about the plastic hinge #2, except that there was no sudden jump, but the test readings increased more rapidly then was predicted. The readings from plastic hinge #3 gave the best comparison with the predicted readings. There is also quite a difference between the test results for plastic hinges #1 and #3. All these factors indicate that the load P_1, applied in the left span of the beam had an increase in magnitude after three cycles were applied which had an influence on both plastic hinges #1 and #2 and increased their readings by 15%. This increase could be caused by an uncareful overloading of the load P_1 in one loading stage, which would cause more intensive cracking in both plastic hinges #1 and #2 and would have an influence on their stress-strain history.

f) TEST #8

According to the numerical analysis the magnitude of

the load P = 13.8 kips was not high enough to create through a number of loading cycles a sufficient number of plastic hinges for incremental collapse. In other words the load was below the actual shake-down limit.

The applied load was the same as the calculated shake-down load P_S according to the plastic theory (TABLE 4.2). Comparing the test results, the deflection readings at the plastic hinge #3 characteristic shape fairly close to that expected for shake-down. The deflections at plastic hinge #1 have conversely the character of an incremental collapse. The strain and curvature test results for critical section #1 define a flat curve throughout the first five loading cycles, than the increase is more rapid. The test results for the critical section #2 are quite close to the predicted results. According to the diagram in Fig. 4.2.1, the curvature reached a value of 1×10^{-3} in the third loading cycle and following this the diagram was more nearly constant. A fairly good agreement with the numeriaal analysis is also evident from the results for critical cross-section #3. Excluding the discrepancies for plastic hinge #1, the overall behaviour of the test specimen was very close to an expected shake-down result and seems to agree with the predicted shake-down load P_S calculated by the plastic theory. The numerical analysis has also predicted behaviour very close to the test results and similarly the loading cycles did not create a plastic hinge in critical section #2 and therefore the beam tends to behave

elasticaly after a number of cycles. In the test after 23 cycles of loading almost stable stage was achieved. In the analysis this stable configuration was reached at fewer cycles of load. The result of this test and analysis provided a lower bound for P_S.

g) TEST #9

The magnitude of the load P = 14.2 kips was chosen slightly higher than in test #8 because of an increased concrete strength. The behaviour of the beam in all aspects was very close to the expected behaviour for a shake-down situation. The applied load P was higher than the shake-down load P_S = 13.9 kips predicted by the plastic theory. The numerical analysis results match up very well with the test results. Again as in the previous test the predicted and the experimental results do not indicate the development of a plastic hinge in critical section #2 even after 23 loading cycles were applied and the beam tends to behave almost elastically after cyclic loading. Using the numerical analysis a condition for sufficient number of plastic hinges were developed for cyclic loading when the load was 14.3 kips. Therefore the shake-down load P_S according to the numerical analysis is between 14.2 kips and 14.3 kips. The difference between the predicted shake-down load from the plastic analysis and the numerical analysis is approximately 3%.

6.3 PREDICTED AND ACTUAL VALUE OF PLASTIC MOMENT MP

The value of MP was assumed constant throughout a number of load cycles. The values were set from 291 to 293 inch-kips depending on the concrete strength. For the tests following test #5 two additional load cells were installed under the supports in order to measure the magnitude of the reactions and therefore provide values of the actual MP. The results of these readings are summed up in TABLE 6.2 and in Fig. 6.1.

TABLE 6.2

ACTUAL MP IN INCH-KIPS

CYCLVS TEST	1	2	3	4	5	6	7	8	THEORETICAL MP
#5	309	331	335	340	347				293
#6	333	333	341	341	338				293
#7	309	316	321	309					293
#8	292	299	304	300	305	307	308		291
#9	307	319	319	320	326	325	319	320	293

TABLE 6.3

RATIO OF THEORETICAL AND ACTUAL MP

TEST	#5	#6	#7	#8	#9
THEORETICAL	293	293	293	291	293
HIGHEST ACTUAL	343	341	321	308	326
MP_T/MP_A	85.5%	86%	91.3%	95.2%	90%

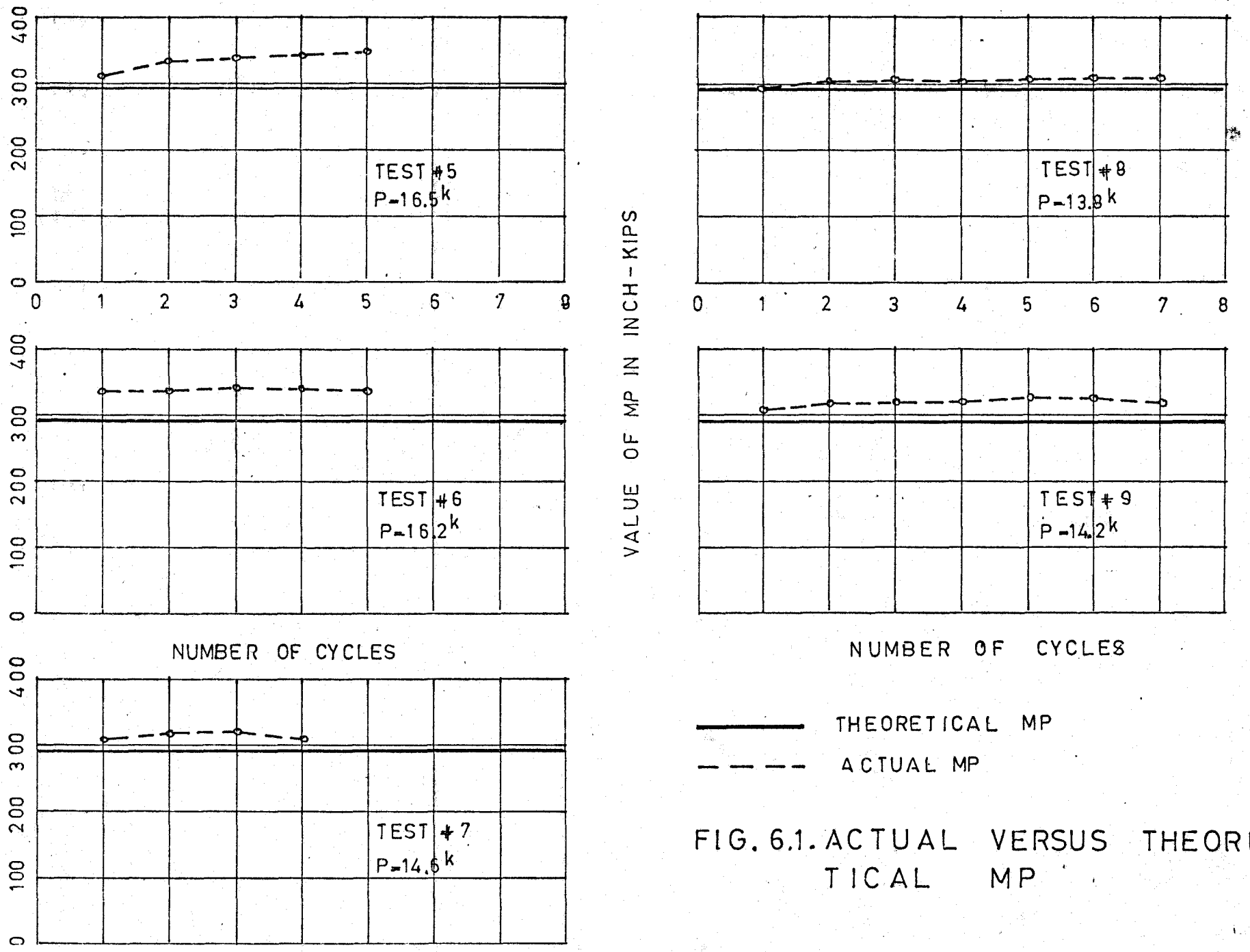

FIG. 6.1. ACTUAL VERSUS THEORETICAL MP

From the results the ratio of theoretical MP to actual MP(MP_T/MP_A) seems to decrease in each test with increased number of load applied cycles and also decreases with increasing magnitude of the applied load. These changes in magnitude of MP are probably caused by strain hardening of the reinforcing steel. The error between MP_T and MP_A from test to test is in range of 10% to 14.5% as indicated in TABLE 6.3.

6.4 SUMMARY OF THE RESULTS

Test #8 and #9 had behaved very close to the predicted behaviour for these shake-down cases. Therefore the value of the shake-down load according to the test results is taken as 14.2 kips. Table 6.4 shows the comparison of the test results with the predicted collapse load P_C and shake-down load P_S.

TABLE 6.4

ACTUAL AND PREDICTED P_C AND P_S

	TEST	NUMERICAL ANALYSIS	PLASTIC THEORY
P_C	18^K*	16^K	15.9^K
P_S	14.2^K	14.3^K	13.9^K
P_S/P_C	78.8%	89.3%	87.5%

* value of P_C as determined from the strain and deflection readings.

The discrepancies between the ratios of P_s/P_c for the tests and the predicted results are 8.7% and 10.5% for numerical analysis and plastic theory prediction respectively. The same difference is shown in Table 6.3 for the predicted and the actual values of MP. The difference between the actual and predicted behaviour is explained by the assumed idealized stress-strain relationship for steel and the constant value of MP. The prediction is quite accurate as far as lower strains are concerned thus the region around shake-down load. The discrepancies keep increasing by higher strains, when the load is close to the collapse load and the effect of strain hardening of steel is significant.

6.5 RECOMMENDED IMPROVEMENTS FOR THE METHOD OF ANALYSIS

As a result of the experience gained by developing the method of analysis presented in this thesis, a number of ways to improve it are suggested. These suggestions are either means for increasing accuracy or for decreasing the computer time required.

a) Moment-Curvature Relationship

Better analytical results would be obtained if the strain hardening of the reinforcing steel thus the changing value of MP was included in the analysis. An additional investigation to show how this would influence the plastic hinge length and therefore the hinge rotation should be done. When these aspects were included into the analysis the

accuracy would be significantly increased. As was mentioned previously, inclusion of these aspects should increase the predicted collapse value by approximately the magnitude of the apparent discrepancies found for the present analysis.

b) Material Properties

CONCRETE - more attention should be given to the stress-strain relationship for concrete when subjected to cyclic loading. The theoretical values of this relationship obtained from expressions derived by SINHA[3] generally match up well with the test results obtained from cylinder tests. Observed magnitude of the discrepancies could be decreased, when larger number of cylinders would be tested with cyclic loading and the coefficients used in the theoretical expressions will be derived directly from these cylinder tests.

STEEL - as was mentioned before, the strain hardening of the reinforcing steel, when included in the analysis, will significantly decrease the magnitude of discrepancies between the test results and the analytical results.

c) TIME DEPENDENT PROPERTIES

The number of iterating cycles and therefore significant computer time would be saved by better initial estimate of distribution of residual moments. The shape of the residual moment diagram is known. The initial estimate of the magnitude of residual moment over the middle support could be more accurately calculated by multiplying the value of bending moment over the middle support from previous loading stages by a constant coefficient.

CHAPTER 7

SUMMARY AND CONCLUSION

7.1 SUMMARY OF THE INVESTIGATION

The main purpose of the investigation reported in this thesis was to provide additional information to aid in understanding continuous beam behaviour. The specific area of interest was the behaviour of continuous reinforced concrete beams subjected to variable repeated loading.

A beam testing program was designed to provide a thorough investigation of a particular beam with a limited number of variables. These tests furnished a reliable source of information which was necessary for an accurate appraisal of the proposed method of analysis. The method of analysis was based on an approximate beam model which involved dividing the beam into a number of smaller segments. For the analysis, information about the physical properties of the concrete and the steel was needed. Additional tests were performed to determine the required properties.

7.2 CONCLUSION

The test results showed that the general behaviour of the reinforced concrete beams is very close to the expected behaviour for incremental collapse and for shakedown as pre-

dicted for steel structures. The results of themselves provide the values of shakedown load P_s and proportional collapse load P_c.

The numerical analysis results verified the accuracy of the analytical method when comparing the results with the test results for the shakedown loads. Greater discrepancies were observed when the magnitude of the loads was closer to the proportional collapse load. These differences were mainly due to the employing of simplified assumptions for the stress-strain relationship of the reinforcing steel. The neglection of the strain hardening effect of the steel, which influenced the capacity of the cross-section and the overall behaviour of the beam, resulted in underestimated values of the fully plastic moment MP. Strain hardening of the steel also is responsible for some differences from the predicted deflections. The Bauschinger's effect due to reversed of plastic straining in the steel was neglected in the analysis. This effect actually softens the behaviour of the beam and results in larger deflections than predicted by the numerical analysis. This partially also explains the differences between actual and predicted deflections. Prior to reaching the region of strain hardening and prior to repeated loading in the plastic range, the predicted behaviour was relatively accurate.

The simple plastic theory showed good agreement with the test value of shakedown load as well as with the value

of shakedown load predicted by numerical analysis. The difference between the plastic theory and numerical analysis predictions and the test collapse load was due to underestimation of the value of the fully plastic moment, MP. Also the numerical analysis predictions were less accurate when the magnitudes of the loads were closer to the value of collapse load. In other words accuracy decreased when the strain hardening effect of the steel was greater than that which occurred at lower loads.

The numerical analysis is slightly more accurate in prediction of shakedown than the simple plastic theory and has the advantage of predicting the deflections and strains. In addition, the analysis can be used when axial force exist on the members. This is a more common situation in real structures.

The following conclusions are made:

1. When Limit Design proceedings are employed in design method it has been shown that variable repeated loading may be an important consideration.
2. For reinforced concrete members which are very much under-reinforced and are not subjected to axial forces the plastic method provides satisfactory prediction of shake down and proportional collapse loads. However for higher percentage of reinforcement there is no restriction on the rotation which can limit the capacity of the structure by causing failure prior to formation of a collapse mechanism.

3. The numerical analysis is reasonably accurate in prediction of strains and deflections when the loads are in the magnitude close to the value of shakedown load. The analysis can limit rotation and therefore indicate material failure. The analysis with the present assumptions for steel behaviour provides lower bound for proportional collapse and under estimates the deflections for repeated loading. Therefore for more accurate prediction of incremental collapse and proportional collapse the strain hardening and Bauschinger's effect for steel should be included in the analysis.
4. Experimental verification of this method of analysis for members with reinforcement ratio closer to the critical reinforcement ratio will be required.

APPENDIX

FORTRAN PROGRAM: - THE ANALYSIS OF CONTINUOUS REINFORCED CONCRETE BEAMS SUBJECTED TO VARIABLE REPEATED LOADING

NOMENCLATURE:

The meanings of the variables named in the program are listed below. Those that do not appear here are defined by the context in which they are used. Several dimensions are included as constants but can easily be changed.

A - Length of the span in inches

AA,BB,CC,DD,ALFA,AA1,BB1,E1,F,G,

OH,OJ,OK,OL - coefficients in the stress-strain equations for concrete

A1,A2,A3,A4,A5 - distance between the critical cross-sections in inches

AC - width of the cross section

AL - length of the segment

AM - bending moment

AR, AX - area of one strip in the cross-section

AS - area of reinforcing steel

CURV - curvature in the cross-section

DEF - deviation of one end of the segment due to the average curvature over the segment

APPENDIX CONT'D

DEFE - the angle of deviation of the segment

DEFL - the whole deviation of the end of the segment

DEFO - deflection at the end of the segment

DL - distance between the top of the strip in the cross-section and the top of the cross-section

D1 - compression force in concrete

D2 - force in top reinforcing steel

D3 - force in bottom reinforcing steel

D22 - force in the top reinforcing steel in previous loading stage

D33 - force in the bottom

EC - modulus of elasticity for concrete

EPA, EPTT - strain in the strip of the cross-section

EPT, EPSTT - strain at the top of the cross-section

EPB, EPSBB - strain at the bottom of the cross-section

EPS1 - changed strain at the top of the cross-section due to the iteration process

EPST1 - strain in the strip of the cross-section from previous loading stage

EPX0,EPS0,EPS01 - value of strain in the strip of the cross-section when the stress is equal to zero

FEMAB

FEMBA

FEMBC

FEMCB - fixed end moments, used in moment distribution method

APPENDIX CONT'D

GRG - average curvature over the plastic hinge length

H - height of the cross-section

HS - distance between the centroid of reinforcing steel and top or bottom of the cross-section

OMAB, OMSC, OMCB - bending moments at the supports as a result of moment distribution method

OM1, OM2, OM3 - bending moments at the critical cross-sections

OMP - value of fully plastic moment

OMY - value of plastic moment when the tension reinforcing steel is in yield

P_1, P_2 - magnitude of applied load in the left and right span

RADR, RBDL, RBDR, RCDL - reactions due to continuity of the beam

RASR, RBSL, RBSR, RCSL - reactions calculated as on simple beam

SIGMA1 - value of concrete stress for a strip of the cross-section from previous loading stage

SS, SST - the strain in top reinforcing steel

SB, SSB - the strain in bottom reinforcing steel

STX, STRC - stress in the concrete for a strip of the cross-section

SSTO, SSBO - value of strain in reinforcing steel when stress is equal to zero

SST1, SSB1 - strain in reinforcing steel from previous loading stage

APPENDIX CONT'D

TANI, TANE - rotation of the plastic hinge from right and left side of the hinge

W, WA - centroid of the cross-section from the top of the section

WCC - centroid of compression concrete force

WX - changed centroid of the cross-section due to iteration process

Y1, Y2, Y3, Y4, Y5, Y6 - distances between the left hand support of the beam and beginning and end of each plastic hinge.

XX1 - deflection under the plastic hinge

```
      NUMERICAL ANALYSIS COMPUTOR PROGRAM
C
      DIMENSION EPT(26),EPB(26),WA(26)
      COMMON /D/ P1(138),P2(138),AM(26,138),CURV(27),
     1           R1(138),R2(138),R3(138)
      COMMON /C/ AL(26),RAD(26),DEFO(26)
C        COMPRESSION IS TAKEN AS POSITIVE,TENSION
C        AS NEGATIVE
      READ(5,31)AC,AS,H,HS
      READ(5,30)A1,A2,A3,A4,A
      OMP=250.
      OMY=230.
      P=14.6
      RRS1=P*A2/A
      RRS2=P*(A1+A4)/A
      BM1=(OMP-RRS1*A1)*A/A1
      BM2=-OMP
      BM3=A*(OMP+P*(A+A3-A1)-RRS1*(A+A3)-RRS2*A3)/(A-A3)
C        THE DISTANCE BETWEEN THE LEFT SUPPORT
C        AND THE BEGINNING OR THE END OF EACH
C        EXPECTED PLASTIC HINGE
      Y1=OMY*A/(BM1+RRS1*A)
      Y2=A*(OMY-A1*P)/(BM1+A*RRS1-P*A)
      Y3=(A*(OMY+P*A1))/(OMP+A*P-A*RRS1)
      Y4=(2.*OMP-OMY-P*A1+A*RRS2)/(OMP/A+RRS1-P+RRS2)
      Y5=(OMY+A*RRS2-2.*BM3-P*A1)/(-BM3/A-P+RRS1+RRS2)
      Y6=(OMY-2.*BM3-P*A1+A*RRS2-P*(A+A3))/(-BM3/A+RRS1-P+RRS2-P)
C        DEVIDING THE BEAM INTO 26 SEGMENTS
      READ(5,32)(AL(I),I=1,26)
      SAL=0.
```

```
      DO 33 I=1,26
      AL(6)=A1-Y1
      AL(7)=Y2-A1
      AL(13)=A-Y3
      AL(14)=Y4-A
      AL(20)=(A+A3)-Y5
      AL(21)=Y6-(A+A3)
      IF(I.EQ.5) AL(I)=Y1-SAL
      IF(I.EQ.12) AL(I)=Y3-SAL
      IF(I.EQ.19) AL(I)=Y5-SAL
      IF(I.EQ.8) AL(I)=AL(I)-AL(7)+0.2
      IF(I.EQ.15) AL(I)=AL(I)-AL(14)+0.2
      IF(I.EQ.22) AL(I)=AL(I)-AL(21)+0.1
      SAL=SAL+AL(I)
   33 CONTINUE
C        N-NUMBER OF LOADING STAGES
      N=11
      DO 12 J=2,N
      NN=1
      READ(5,40)P1(J),P2(J)
      WRITE(6,200)P1(J),P2(J)
      P11=P1(J)
      P22=P2(J)
      OU2=0.0
      GRC=0.0
      CURV(0)=0.0
      DEFR=5.0
```

```
      R1(J)=0.0
      R2(J)=0.0
      R3(J)=0.0
      R1(1)=0.0
      R2(1)=0.0
      R3(1)=0.0
      K=J-1
C          FIXED END BENDING MOMENTS
      FEMAB=-(P11*A1*A2*A2)/(A*A)
      FEMBA=(P11*A1*A1*A2)/(A*A)
      FEMBC=-(P22*A3*A3*A4)/(A*A)
      FEMCB=(P22*A3*A4*A4)/(A*A)
      OMAB=FEMAB
      OMBA=FEMBA
      OMBC=FEMBC
      OMCB=FEMCB
C          MOMENT - DISTRIBUTION METHOD
   10 OMAB1=OMAB-OMAB
      OMBA=OMBA-0.5*OMAB
      OMAB=OMAB1
      OMB=OMBA+OMBC
      OMBA=OMBA-0.5*OMB
      OMBC=OMBC-0.5*OMB
      OMCB=OMCB-0.25*OMB
      OMCB1=OMCB-OMCB
      OMBC=OMBC-0.5*OMCB
      OMCB=OMCB1
      OMB=OMBA+OMBC
```

```
      OMBC=OMBC-0.5*OMB
      OMBA=OMBA-0.5*OMB
      OMAB=OMAB1-0.25*OMB
      OMB=OMBA+OMBC
      IF(ABS(OMAB).GT.1.) GO TO 10
      IF(OMCB.NE.0.) GO TO 10
      OMA=OMAB
      OMB=OMBC
      OMC=OMCB
C        REACTIONS DUE TO THE BENDING MOMENT  OVER
C        THE MIDDLE SUPPORT
      RADR=(OMB-OMA)/A
      RBDL=(OMA-OMB)/A
      RBDR=(OMC-OMB)/A
      RCDL=(OMB-OMC)/A
C        REACTIONS AS ON SIMPLE BEAM DUE TO THE
C        APPLIED LOAD
      RASR=P11*A2/A
      RBSL=P11*A1/A
      RBSR=P22*A4/A
      RCSL=P22*A3/A
      OMD1=OMB*A1/A
      OMS1=RASR*A1
C        BENDING MOMENTS IN THE POSITION OF
C        EXPECTED PLASTIC HINGES
      OA1=OMD1+OMS1
      OA2=OMB
      OMD3=OMB*A4/A
```

```
      OMS3=RCSL*A4
      OA3=OMD3+OMS3
      IF(J.EQ.2) GO TO 81
C        ADDING THE BENDING MOMENTS FROM PREVIOUS
C        LOADIND STAGE
      OM1=OA1+AM(6,K)
      OM2=OA2+AM(13,K)
      OM3=OA3+AM(20,K)
      GO TO 82
   81 OM1=OA1
      OM2=OA2
      OM3=OA3
   82 X1=0.
      X2=0.
      X3=0.
      X4=0.
      X5=0.
      X6=0.
      A5=A+A3
      GO TO 22
C        CHANGE IN THE B. MOMENT OVER THE MIDDLE
C        SUPPORT WHEN THE DEFLESTED SHAPE OF THE BEAM
C        DOES NOT GO THROUGH THE MIDDLE SUPPORT
   34 DG=DEFO(13)
      IF(ABS(DG).GE.DEFR) DG=DG/2.
      OU2=OM2-DG*OM2*0.8
      IF(ABS(DG).GE.7.E-01) OU2=OM2-DG*OM2*0.5
```

```
      IF(AM(13,K).LE.(-OMP)) OU2=OM2-DG*OM2*0.25
      IF(OM2.LT.(-200.)) OU2=OM2+DG*OM2*5.E-01
      DEFR=DEFO(13)
      OK=AM(13,K)+OU2
      IF(OK.LT.0.AND.OK.GT.(-3.)) OU2=OU2-3.
      IF(OK.GT.0.AND.OK.LT.3.) OU2=OU2+3.
      OM2=OU2
      GRC=1.0
   22 CONTINUE
C        CALCULATION OF B. MOMENT IN EACH SEGMENT
C        OF THE BEAM
      RAG=OA2/A+R1(K)
      RBG=-2.*RAG
      SAL=0.0
      OK=5.
      DO 11 I=1,26
      L=I-1
      SAL=SAL+AL(I)
      RAS1=RASR
      RBS1=RBSL+RBSR
      RAS=RAS1*SAL
      RBS=RBS1*(SAL-A)
      P1S=P11*(SAL-A1)
      P2S=P22*(SAL-A-A3)
      IF(OM1.GE.OMP.AND.OM2.LE.(-OMP)) GO TO 500
C        WHEN ONE OF THE B. MOMENTS EXCEED THE VALUE
C        OF MP,MOMENT DIAGRAM IS KNOWN
      IF(OM1.GE.OMP) GO TO 24
```

```
      IF(OM2.LE.(-OMP)) GO TO 26
      IF(OM3.GE.OMP) GO TO 27
      IF(OM2.EQ.OU2) GO TO 25
      OM1=OA1
      OM2=OA2
      OM3=OA3
      GO TO 29
   24 OM2=BM1
      X1=Y1
      X2=Y2
      GO TO 25
   26 OM2=-OMP
      X3=Y3
      X4=Y4
      GO TO 25
   27 OM2=BM3
      X5=Y5
      X6=Y6
   25 CONTINUE
      RAG=OM2/A
      RBG=-2.*RAG
   29 RAD1=RAG*SAL
      RBD1=RBG*(SAL-A)
      IF(SAL.GT.A5) GO TO 18
      IF(SAL.GT.A) GO TO 17
      IF(SAL.GT.A1) GO TO 16
      AM(I,J)=RAD1+RAS
      GO TO 15
```

```
   16 AM(I,J)=RAD1+RAS-P1S
      GO TO 15
   17 AM(I,J)=RAD1+RBD1+RAS-P1S+RBS
      GO TO 15
   18 AM(I,J)=RAD1+RBD1+RAS-P1S+RBS-P2S
   15 CONTINUE
      IF(P11.LT.0.OR.P22.LT.0.) GO TO 400
      GO TO 401
C        BY UNLOADING THE B. MOMENTS FROM PREVIOUS
C        LOADING STAGEARE ADDED
  400 AM(I,J)=AM(I,J)+AM(I,K)
      IF(I.EQ.13) OK=AM(I,J)
      IF(ABS(OK).LT.3.) GO TO 402
      GO TO 401
  402 IF(OK.LT.0.) OA2=OM2-3.
      IF(OK.GT.0.) OA2=OM2+3.
      GO TO 22
  401 OM=AM(I,J)
      IF(ABS(OM)-0.10) 51,51,53
C        SUBROUTINE FOR BALANCING THE CROSS-SECTION
   53 CALL CURVAM (AC,AS,H,HS,I,J,P11,P22,OM,0.,GRC,CRUV,EPSTT,
     1              EPSBB,W)
      CURV(I)=CRUV
      EPT(I)=EPSTT
      EPB(I)=EPSBB
      WA(I)=W
      GO TO 65
   51 CURV(I)=0.0
```

```
C        RADIUS OF THE SEGMENT
   65 RAD(I)=2./(CURV(I)+CURV(I-1))
   11 CONTINUE
      IF(OM1.GE.OMP) GO TO 13
      IF(OM2.LE.(-OMP)) GO TO 83
      IF(OM3.GE.OMP) GO TO 84
C        DEFLECTED SHAPE OF THE BEAM WHEN NON
C        OF THE B. MOMENTS ARE EQ. MP
      CALL PRDO(A)
      NN=NN+1
      IF(NN.GE.5) GO TO 85
      IF(ABS(DEFO(13))-0.01) 85,85,34
C        DEFLECTED SHAPE OF THE BEAM WHEN OM1.EQ.MP
   13 CALL PRDA(A,X1,X2,GRG,DEFR)
      GO TO 85
C        DEFLECTED SHAPE OF THE BEAM WHEN OM2.EQ.MP
   83 CALL PRDB(A,X3,X4,GRG,GEFR)
      GO TO 85
C        DEFLECTED SHAPE OF THE BEAM WHEN OM3.EQ.MP
   84 CALL PRDC(A,X5,X6,GRG,DEFR)
   85 SAL=0.0
      WRITE(6,201)
      DO 47 I=1,26
C        CORRECTION DUE TO THE ROTATION OF PLASTIC HINGE
      SAL=SAL+AL(I)
      IF(SAL.GT.(X1+0.2).AND.SAL.LT.(X2-0.2)) GO TO 48
      IF(SAL.GT.(X3+0.2).AND.SAL.LT.(X4-0.2)) GO TO 48
      IF(SAL.GT.(X5+0.2).AND.SAL.LT.(X6-0.2)) GO TO 48
```

```
      GO TO 47
   48 DEFO(I)=DEFR
      CALL CURVAM(AC,AS,H,HS,I,J,P11,P22,OMP,GRG,GRC,CRUV,EPSTT,
     1            EPSBB,W)
      CURV(I)=CRUV
      EPT(I)=EPSTT
      EPB(I)=EPSBB
      WA(I)=W
   47 WRITE(6,71) I,SAL,AM(I,J),WA(I),EPT(I),EPB(I),CURV(I),DEFO(I)
      IF(P11.LT.0.OR.P22.LT.0.) GO TO 100
      GO TO 12
C        REACTIONS DUE TO THE RESIDUAL MOMENTS
  100 R1(J)=AM(13,J)/A
      R3(J)=R1(J)
      R2(J)=-(R1(J)+R3(J))
   12 CONTINUE
   30 FORMAT(5F10.4)
   31 FORMAT(4F10.4)
   32 FORMAT(1F10.3)
   40 FORMAT(2F10.4)
   70 FORMAT(1F8.3)
   71 FORMAT(1I5,5X,1F10.3,5X,1F10.3,5X,1F10.3,5X,3E15.6,5X,1F10.3/)
   72 FORMAT(2E15.6)
  200 FORMAT(10X,3HP1=,1F10.3,10X,3HP2=,1F10.3//)
  201 FORMAT(3X,4HZONE,10X,1HL,12X,2HOM,13X,1HW,15X,3HEPT,12X,3HEPB,
     1       12X,4HCURV,15X,4HDEFL//)
  500 STOP
      END
```

```
      SUBROUTINE CURVAM (AC,AS,H,HS,I,J,P1,P2,OM,GRG,GRC,CURV,EPSTT,
     1                   EPSBB,W)
      DIMENSION EPS(26,3,21),EPSO(26,3,21),STRC(26,3,21),SS(26,150),
     1          SB(26,150),WR(26,150),AR(21),BRK(21)
      COMMON AA,BB,CC,DD,ALFA,AA1,BB1,E1,F,G
C        SUBROUTINE DOES THE BALANCING OF CROSS-SECTION
C        CHOOSEN VALUES OF STRAIN AT THE TOP
      EPST=4.E-04
      W=2.6
      K=J-1
      JJ=3
      KK=JJ-1
      LL=KK-1
      M=1
      IF(J.GT.2) GO TO 52
      GO TO 54
C        AFTER THE FIRST LOADING STAGE THE STRAIN
C        DISTRIBUTION IN FIRST ITERATIVE CYCLE IS
C        THE SAME AS IN THE PREVIOUS L. STAGE
   52 EPST=EPS(I,KK,1)
      W=WR(I,K)
      IF(GRC.NE.0.) W=WR(I,J)
C        COEFFICIENTS INTO THE STRESS-STRAIN EQUATIONS
   54 AA=-1.725
      BB=-2.39
      CC=-6.199
      DD=16.951
      ALFA=0.111
      AA1=AA+ALFA*DD
```

```
      BB1=BB+2.*ALFA*CC
      E1=2.*ALFA
      F=ALFA*BB+(ALFA**2)*CC
      G=ALFA*ALFA
      SXX=0.0
      SA=0.0
   20 CONTINUE
      N=1
  220 CONTINUE
      IF(J.GT.2) GO TO 23
      EPT1=0.0
      SAREA=0.0
      SBRK=0.0
C        INPUT-STRAIN AT THE TOP,CENTROID
C        OUTPUT-STRAIN AT THE BOTTOM AND IN THE STEEL
      CALL STRAIN (EPST,W,H,HS,EPSTT,EPSBB,SST,SSB)
      DO 11 L=1,21
      DL=L*H/20.-H/20.
C        STRESSES IN THE CROSS-SECTION BY HTE FIRST LOADING
      CALL ARAL(L,H,DL,W,EPSTT,STX,EPA,AX,BRX)
      STRC(I,JJ,L)=STX
      EPS(I,JJ,L)=EPA*1.E-03
      AR(L)=AX
      BRK(L)=BRX
      SAREA=SAREA+AR(L)
      SBRK=SBRK+BRK(L)
   11 CONTINUE
      IF(EPT1.NE.0.) GO TO 25
```

```
      SST1=0.
      SSB1=0.
      GO TO 25
   23 SST1=SS(I,K)
      SSB1=SB(I,K)
C        STRAIN DISTRIBUTION THROUGHOUT CROSS-SECTION
      CALL STRAIN (EPST,W,H,HS,EPSTT,EPSBB,SST,SSB)
      IF(P1.GT.0.OR.P2.GT.0.) GO TO 24
      SAREA=0.0
      SBRK=0.0
      DO 53 L=1,21
      DL=L*H/20.-H/20.
      SIGMA1=STRC(I,LL,L)
      EPS1=EPS(I,LL,L)*1.E+03
      IF(J.LE.4) GO TO 39
      EPX0=EPS0(I,KK,L)
C        STRESSES IN THE C.S. BY UNLOADING
   39 CALL BARAL(L,H,DL,W,EPSTT,EPS1,SIGMA1,STX,EPTT,AX,BRX,EPX0,J)
      STRC(I,JJ,L)=STX
      EPS(I,JJ,L)=EPTT*1.E-03
      EPS0(I,JJ,L)=EPX0
      AR(L)=AX
      BRK(L)=BRX
      SAREA=SAREA+AR(L)
      SBRK=SBRK+BRK(L)
   53 CONTINUE
      GO TO 25
```

```
   24 SAREA=0.0
      SBRK=0.0
      DO 26 L=1,21
      DL=L*H/20.-H/20.
      SIGMA1=STRC(I,KK,L)
      EPS1=EPS(I,KK,L)*1.E+03
      EPSO1=EPSO(I,KK,L)
C        STRESSES IN THE C.S. BY RELOADING
      CALL CARAL(L,H,DL,W,EPSTT,EPS1,SIGMA1,EPSO1,STX,EPTT,AX,BRX)
      STRC(I,JJ,L)=STX
      EPS(I,JJ,L)=EPTT*1.E-03
      AR(L)=AX
      BRK(L)=BRX
      SAREA=SAREA+AR(L)
      SBRK=SBRK+BRK(L)
   26 CONTINUE
   25 IF(EPSTT.LT.0.) GO TO 125
      SSTEEL=AS*STRC(I,JJ,4)
      SAREA=SAREA-SSTEEL
      SBRK=SBRK-SSTEEL*(H-HS)
      GO TO 127
  125 SSTEEL=AS*STRC(I,JJ,18)
      SAREA=SAREA-SSTEEL
      SBRK=SBRK-SSTEEL*HS
  127 IF(SAREA.EQ.0.) GO TO 128
C        CENTROID OF THE AREA OF COMPR. CONCR.
      WCC=SBRK/SAREA-(H-W)
```

```
C         FORCE IN CONCRETE
      D1=-AC*SAREA*1.E+03
      GO TO 129
  128 WCC=0.0
      D1=0.0
C         FORCE IN THE TEN AND IN THE COMPR. STEEL
  129 CALL STRSC(I,J,AS,SST,SST1,D2)
      CALL STRSS(I,J,AS,SSB,SSB1,D3)
C         BALANCING C.S. DUE TO FIRST CONDITION
C         SUM OF THE FORCES EQ. ZERO
      S=D1+D2+D3
      IF(ABS(S).GE.ABS(SA)) S=S/10.
      IF(ABS(S).LT.100.) GO TO 21
      N=N+1
      IF(N.GE.25) GO TO 21
      IF(EPSBB.GT.0.) S=-S
      IF(W.LT.0.OR.W.GT.H) S=-S
      SA=S
      WX=W+S*8.E-05
      IF(ABS(SST).GE.2.2E-03) WX=W+S*2.E-05
      IF(ABS(SSB).GE.2.2E-03) WX=W+S*2.E-05
      IF(WX.GT.0.AND.WX.LT.2.E-01) WX=2.E-01
      IF(WX.LT.0.AND.WX.GT.(-3.E-01)) WX=-3.E-01
      IF(W.LT.0.AND.WX.GT.0.) GO TO 88
      IF(W.GT.0.AND.WX.LT.0.) GO TO 89
      W=WX
      GO TO 220
   88 W=1.0
```

```
      IF(EPST.LT.0.) EPST=-EPST
      IF(EPST.LT.2.E-04) EPST=2.E-04
      GO TO 220
   89 W=-1.0
      IF(EPST.GT.0.) EPST=-EPST
      IF(EPST.GT.(-5.E-05)) EPST=-5.E-05
      GO TO 220
   21 IF(GRG.NE.0.) GO TO 18
      IF(W.LT.0.) GO TO 34
      IF(W.GT.H) GO TO 34
C        INTERNAL MOMENT IN C.S.
      OM1=(-D1*WCC-D2*(W-HS)+D3*(H-W-HS))*1.E-03
      GO TO 35
   34 OM1=((D3-D2)*(H-2.*HS)/2.)*1.E-03
      IF(GRG.NE.0.) GO TO 18
C        BALANCING C.S. DUE TO THE SECOND CONDITION
C        SUM OF THE MOMENTS EQ. ZERO
   35 SX=OM1-OM
      M=M+1
      IF(M.GE.30) GO TO 18
      IF(ABS(SX).LT.0.5) GO TO 18
      IF(ABS(SX).GE.ABS(SXX)) SX=SX/10.
      EPST1=EPST-SX*3.E-05
      IF(ABS(SST).GE.2.2E-03) EPST1=EPST-SX*1.E-05
      IF(ABS(SSB).GE.2.2E-03) EPST1=EPST-SX*1.E-05
      SXX=SX
      IF(EPST.GT.0.AND.EPST1.LT.0.) GO TO 68
      IF(EPST.LT.0.AND.EPST1.GT.0.) GO TO 67
```

```
      EPST=EPST1
      GO TO 20
   68 WX=5.6
      IF(OM1.LT.0.AND.OM.LT.0.) WX=-1.0
      IF(EPST1.GT.(-5.E-05)) EPST1=-5.E-05
      W=WX
      EPST=EPST1
      GO TO 20
   67 IF(OM1.GT.0.AND.OM.GT.0.) GO TO 69
      W=2.4
      EPST=EPST1
      GO TO 20
   69 W=2.*W
      EPST=EPST1
      GO TO 20
   18 CONTINUE
      CURV=(EPSTT-EPSBB)/H
      IF(GRG.NE.0.) GO TO 51
      GO TO 50
C        BALANCING C.S. WHEN THERE IS A PLASTIC
C        HINGE ROTATION
   51 GRGA=CURV-GRG
      M=M+1
      IF(M.GE.15) GO TO 50
      IF(ABS(GRGA).LT.1.E-04) GO TO 50
      EPST1=EPST-GRGA
      IF(EPST.LT.0.AND.EPST1.GT.0.) W=2.4
      EPST=EPST1
```

```
      GO TO 20
   50 SS(I,J)=SST
      SB(I,J)=SSB
      WR(I,J)=W
      DO 111 L=1,21
      DL=L*H/20.-H/20.
      EPS(I,KK,L)=EPS(I,JJ,L)
      EPSO(I,KK,L)=EPSO(I,JJ,L)
      STRC(I,KK,L)=STRC(I,JJ,L)
      IF(P1.LT.0.OR.P2.LT.0.) GO TO 111
      EPS(I,LL,L)=EPS(I,KK,L)
      STRC(I,LL,L)=STRC(I,KK,L)
  111 CONTINUE
      RETURN
      END
```

CD TOT 0210

```
      SUBROUTINE ARAL(L,H,DL,W,EPSTT,STR,EPA,AR,BRK)
      DIMENSION STRC(21)
      COMMON AA,BB,CC,DD,ALFA,AA1,BB1,E1,F,G
C
C        SUBROUTINE CALCULATES STRESS CORRESPONDING
C        TO THE STRAIN IN EACH STRIP OF C.S.
      EPA=EPSTT*(W-DL)*1.E+03/W
      IF(EPA.LT.0.) GO TO 10
      EPSE=EPA/(1.-ALFA*EPA)
      EPSE2=EPSE*EPSE
      Q1=1.+E1*EPSE+G*EPSE2
      Q2=CC+BB1*EPSE+F*EPSE2
      Q3=DD*EPSE+AA1*EPSE2
C        STRESS
      STRC(L)=(-Q2-SQRT(Q2**2-4.*Q1*Q3))/(2.*Q1)
      IF(L.EQ.1) GO TO 30
      AR=H*(STRC(L)+STRC(L-1))/40.
      PRC=H-DL+H/40.
      BRK=AR*PRC
      GO TO 20
C        NO TENSION IN CONCRETE ASSUMED
   10 STRC(L)=0.0
   30 AR=0.0
      BRK=0.0
   20 STR=STRC(L)
      RETURN
      END
```

```
      SUBROUTINE BARAL(L,H,DL,W,EPSTT,EPS1,SIGMA1,STR,EPTT,
     1                 AR,BRK,EPS0,J)
      DIMENSION STRC(21)
      COMMON AA,BB,CC,DD,ALFA,AA1,BB1,E1,F,G
C
C        S. CALCULATES STRESSES CORRESPONDING TO THE
C        STRAINS IN EACH STRIP OF C.S. BY UNLOADING
      OH=0.09
      OJ=0.52
      EC=-DD/CC
C        STRAIN
      EPTT=EPSTT*(W-DL)*1.E+03/W
      IF(EPS1.LT.9.E-01) GO TO 15
      B=(SIGMA1+OH)/(2.*OJ)
      X=EPS1+B-SQRT((EPS1+B)*(EPS1+B)-EPS1*EPS1)
      Q1=OJ/X
      Q2=-2.*OJ
      Q3=OJ*X-OH
C        STRAIN WHEN COMPR.STRESS EQ. ZERO
      EPS0=(-Q2+SQRT(Q2*Q2-4.*Q1*Q3))/(2.*Q1)
      IF(EPTT.LT.0.) GO TO 10
      IF(EPS0.GT.EPTT) GO TO 12
C        STRESS
      STRC(L)=(OJ*(EPTT-X)*(EPTT-X))/X-OH
      IF(L.EQ.1) GO TO 11
      GO TO 14
   12 IF(EPS0.EQ.0.) GO TO 16
C        TENSION IN CONCRETE ASSUMED UP TO 2.E-04
      IF((EPS0-EPTT).GT.2.E-01) GO TO 10
```

```
      STRC(L)=-EC*(EPSO-EPTT)
      IF(L.EQ.1) GO TO 11
      GO TO 14
   15 IF(J.GE.4) GO TO 12
   16 STRC(L)=EC*EPTT
      EPSO=0.0
      IF(L.EQ.1) GO TO 11
   14 AR=H*(STRC(L)+STRC(L-1))/40.
      PRC=H-DL+H/40.
      BRK=AR*PRC
      IF(STRC(L).LT.0.) STRC(L)=0.0
      GO TO 20
   10 STRC(L)=0.0
   11 AR=0.0
      BRK=0.0
   20 STR=STRC(L)
      RETURN
      END
```

CD TOT 0047

```
      SUBROUTINE CARAL(L,H,DL,W,EPSTT,EPS1,SIGMA1,EPS01,STR,EPTT,AR,BRK)
      DIMENSION STRC(21)
      COMMON AA,BB,CC,DD,ALFA,AA1,BB1,E1,F,G
C
C          S. CALCULATES STRESSES BY RELOADING
      OK=2.52
      OL=1.03
      EC=-DD/CC
      EPTT=EPSTT*(W-DL)*1.E+03/W
      IF(EPTT.LT.0.) GO TO 10
      IF(EPS1.LT.EPS01) EPS1=EPS01
      IF(EPS01.EQ.EPS1) SIGMA1=0.0
      IF(EPTT.LT.EPS01) GO TO 15
      Y=(SIGMA1+OK)/(EPS1+OL)
      STRC(L)=Y*(EPTT+OL)-OK
      EPSE=EPTT/(1.-ALFA*EPTT)
      EPSE2=EPSE*EPSE
      Q1=1.+E1*EPSE+G*EPSE2
      Q2=CC+BB1*EPSE+F*EPSE2
      Q3=DD*EPSE+AA1*EPSE2
      SIGA=(-Q2-SQRT(Q2*Q2-4.*Q1*Q3))/(2.*Q1)
      IF(STRC(L).GT.SIGA) STRC(L)=SIGA
      IF(EPS01.EQ.0.) STRC(L)=SIGA
      IF(L.EQ.1) GO TO 11
      GO TO 14
   15 IF((EPS01-EPTT).GT.2.E-01) GO TO 10
      STRC(L)=-EC*(EPS01-EPTT)
      IF(L.EQ.1) GO TO 11
   14 AR=H*(STRC(L)+STRC(L-1))/40.
```

```
      PRC=H-DL+H/40.
      BRK=AR*PRC
      IF(STRC(L).LT.0.) STRC(L)=0.0
      GO TO 20
   10 STRC(L)=0.0
   11 AR=0.0
      BRK=0.0
   20 STR=STRC(L)
      RETURN
      END
```

CD TOT 0039

```
      SUBROUTINE PRDO(A)
      DIMENSION DEF(26),DEFE(26),DEFL(26)
      COMMON /C/ AL(26),RAD(26),DEFO(26)
C        DEFLECTED SHAPE OF THE BEAM WHEN NON OF B.M.
C        IS EQ. MP
      SAL=0.
      SDEF=0.
      SDEFE=0.0
      DO 10 I=1,26
      K=I-1
C        DEVIATION DUE TO THE CURVATURE OVER THE SEGMENT
      DEF(I)=AL(I)*AL(I)/(2.*RAD(I))
C        FULL ANGLE OF DEVIATION
      DEFE(I)=AL(I)/RAD(I)
      IF(K-1) 80,80,60
C        SUM OF THE ANGLES FROM PREVIOUS SEGMENTS
   60 SDEFE=SDEFE+DEFE(K)
C        FULL DEVIATION OF THE CURVE
   80 SDEF=SDEF+AL(I)*SDEFE+DEF(I)
      DEFL(I)=SDEF
   10 CONTINUE
      DO 20 I=1,26
      SAL=SAL+AL(I)
C        DEFLECTION AFTER THE CURVE WAS ROTATED TO
C        RIGHT SUPPORT
      DEFO(I)=DEFL(26)*SAL/(2.*A)-DEFL(I)
   20 CONTINUE
      RETURN
      END
```

```
      SUBROUTINE PRDA (A,X1,X2,GRG,DEFR)
      DIMENSION DEF(26),DEFE(26),DEFL(26)
      COMMON /C/ AL(26),RAD(26),DEFO(26)
C        DEFLECTED SHAPE OF THE BEAM WHEN OM1.EQ.MP
      SDEF=0.
      SDEFE=0.0
      SAL=2.*A
      DEFO(26)=0.
C        STARTING FROM THE RIGHT HAND SUPPORT
      I=25
   14 L=I+1
      K=I-1
C        THE DISTANCE BETWEEN LEFT SUPPORT AND SEGMENT
      SAL=SAL-AL(L)
      IF(I.EQ.7) GO TO 31
      GO TO 33
   31 AK1=AL(L)
      SAL=X2
   33 IF(SAL.EQ.X2) GO TO 51
      DEF(I)=AL(L)*AL(L)/(2.*RAD(L))
      DEFE(I)=AL(L)/RAD(L)
      GO TO 52
   51 DEF(I)=AK1*AK1/(2.*RAD(L))
      DEFE(I)=AK1/RAD(L)
      SDEFE=SDEFE+DEFE(L)
      SDEF=SDEF+AK1*SDEFE+DEF(I)
      GO TO 100
   52 IF(L-26) 120,121,121
  120 SDEFE=SDEFE+DEFE(L)
```

```
  121 SDEF=SDEF+AL(L)*SDEFE+DEF(I)
  100 DEFL(I)=SDEF
      IF(SAL.EQ.X2) GO TO 28
      I=I-1
      GO TO 14
   28 N=I
C         ROTATION OF PLASTIC HINGE ON RIGHT SIDE
      TAN1=AK1/RAD(L)
      SDEFA=DEFL(13)
      I=25
      SAL=2.*A
   19 L=I+1
      K=I-1
      IF(I.EQ.N) GO TO 15
      SAL=SAL-AL(L)
      GO TO 16
   15 SAL=SAL-AK1
C         DEFLECTIONS AFTER THE CURVE WAS ROTATED
C         THROUGH THE MIDDLE SUPPORT
   16 DEFO(I)=SDEFA*(2.*A-SAL)/A-DEFL(I)
      IF(I.EQ.N) GO TO 29
      I=I-1
      GO TO 19
C         DEFLECTION IN THE PLASTIC HINGE
   29 XX1=DEFO(N)
      SAL=0.
      SDEF=0.
      SDEFE=0.0
```

```
      I=1
   43 K=I-1
      L=I+1
      SAL=SAL+AL(I)
      IF(I.EQ.5) GO TO 35
      GO TO 36
   35 AK2=AL(I)
      SAL=X1
   36 IF(SAL.EQ.X1) GO TO 53
      DEF(I)=AL(I)*AL(I)/(2.*RAD(I))
      DEFE(I)=AL(I)/RAD(I)
      IF(K-1) 70,70,60
   60 SDEFE=SDEFE+DEFE(K)
      GO TO 70
   53 DEF(I)=AK2*AK2/(2.*RAD(I))
      DEFE(I)=AK2/RAD(I)
      SDEFE=SDEFE+DEFE(K)
      SDEF=SDEF+AK2*SDEFE+DEF(I)
      GO TO 110
   70 SDEF=SDEF+AL(I)*SDEFE+DEF(I)
  110 DEFL(I)=SDEF
      IF(SAL.EQ.X1) GO TO 38
      I=I+1
      GO TO 43
   38 M=I
C        ROTATION OF PLASTIC HINGE FROM THE LEFT
      TAN2=AK2/RAD(I)
      SAL=0.
```

```
C         AVERAGE CURVATURE OVER PLASTIC HINGE
      GRG=(TAN1+TAN2)/(X2-X1)
      I=1
   39 IF(I.EQ.M) GO TO 20
      SAL=SAL+AL(I)
      GO TO 21
   20 SAL=SAL+AK2
C         DEFLECTIONS FROM LEFT SIDE OF PL. HINGE
C         AFTER THE CURVE WAS ROTATED TO THE KNOWN VALUE
C         OF DEFLECTION IN PL. HINGE
   21 DEFO(I)=DEFL(I)+(XX1-DEFL(M))*SAL/X1
      IF(I.EQ.M) GO TO 46
      I=I+1
      GO TO 39
   46 DEFR=DEFO(M)
      WRITE(6,210) X1,X2,AK1,AK2,TAN1,TAN2,GRG
  210 FORMAT(7E15.6)
      RETURN
      END
```

CD TOT 0104

```
      SUBROUTINE PRDB (A,X3,X4,GRG,DEFR)
      DIMENSION DEF(26),DEFE(26),DEFL(26)
      COMMON /C/ AL(26),RAD(26),DEFO(26)
C        DEFLECTED SHAPE OF THE BEAM WHEN OM2.EQ.MP
      SDEF=0.
      SAL=0.0
      SDEFE=0.0
      DEFO(26)=0.
C        STARTING FROM LEFT HAND SUPPORT
      I=1
   14 L=I+1
      K=I-1
      SAL=SAL+AL(I)
      IF(I.EQ.12) GO TO 31
      GO TO 33
   31 AK1=AL(I)
      SAL=X3
   33 IF(SAL.EQ.X3) GO TO 51
      DEF(I)=AL(I)*AL(I)/(2.*RAD(I))
      DEFE(I)=AL(I)/RAD(I)
      IF(K-1) 70,70,60
   60 SDEFE=SDEFE+DEFE(K)
      GO TO 70
   51 DEF(I)=AK1*AK1/(2.*RAD(I))
      DEFE(I)=AK1/RAD(I)
      SDEFE=SDEFE+DEFE(K)
      SDEF=SDEF+AK1*SDEFE+DEF(I)
      GO TO 100
   70 SDEF=SDEF+AL(I)*SDEFE+DEF(I)
```

```
100 DEFL(I)=SDEF
    IF(SAL.EQ.X3) GO TO 28
    I=I+1
    GO TO 14
 28 N=I
    TAN1=AK1/RAD(I)
    SDEFA=DEFL(12)
    I=1
    SAL=0.0
 19 L=I+1
    K=I-1
    IF(I.EQ.N) GO TO 15
    SAL=SAL+AL(I)
    GO TO 16
 15 SAL=SAL+AK1
 16 DEFO(I)=SDEFA*SAL/X3-DEFL(I)
    IF(I.EQ.N) GO TO 29
    I=I+1
    GO TO 19
 29 XX1=DEFO(N)
    SAL=2.*A
    SDEF=0.0
    SDEFE=0.0
    I=25
 43 K=I-1
    L=I+1
    SAL=SAL-AL(L)
    IF(I.EQ.14) GO TO 35
```

```
      GO TO 36
   35 AK2=AL(L)
      SAL=X4
   36 IF(SAL.EQ.X4) GO TO 53
      DEF(I)=AL(L)*AL(L)/(2.*RAD(L))
      DEFE(I)=AL(L)/RAD(L)
      GO TO 52
   53 DEF(I)=AK2*AK2/(2.*RAD(L))
      SDEFE=SDEFE+DEFE(L)
      SDEF=SDEF+AK2*SDEFE+DEF(I)
      GO TO 110
   52 IF(L-26) 120,121,121
  120 SDEFE=SDEFE+DEFE(L)
  121 SDEF=SDEF+AL(L)*SDEFE+DEF(I)
  110 DEFL(I)=SDEF
      IF(SAL.EQ.X4) GO TO 38
      I=I-1
      GO TO 43
   38 M=I
      TAN2=AK2/RAD(L)
      GRG=(TAN1+TAN2)/(X4-X3)
      SAL=2.*A
      I=25
   39 IF(I.EQ.M) GO TO 20
      L=I+1
      SAL=SAL-AL(L)
      GO TO 21
   20 SAL=SAL-AK2
```

```
 21 DEFO(I)=DEFL(M)*(2.*A-SAL)/(2.*A-X4)-DEFL(I)
    IF(I.EQ.M) GO TO 46
    I=I-1
    GO TO 39
 46 DEFR=DEFO(M)
    DEFO(12)=0.0
    WRITE(6,210) X3,X4,AK1,AK2,TAN1,TAN2,GRG
210 FORMAT(7E15.6)
    RETURN
    END
```

CD TOT 0095

```
      SUBROUTINE PRDC (A,X5,X6,GRG,DEFR)
      DIMENSION DEF(26),DEFE(26),DEFL(26)
      COMMON /C/ AL(26),RAD(26),DEFO(26)
C          DEFLECTED SHAPE OF THE BEAM WHEN OM3.EQ.MP
      SDEF=0.
      SDEFE=0.0
      SAL=0.0
      DEFO(26)=0.
      I=1
   14 L=I+1
      K=I-1
      SAL=SAL+AL(I)
      IF(I.EQ.19) GO TO 31
      GO TO 33
   31 AK1=AL(I)
      SAL=X5
   33 IF(SAL.EQ.X5) GO TO 51
      DEF(I)=AL(I)*AL(I)/(2.*RAD(I))
      DEFE(I)=AL(I)/RAD(I)
      IF(K-1) 70,70,60
   60 SDEFE=SDEFE+DEFE(K)
      GO TO 70
   51 DEF(I)=AK1*AK1/(2.*RAD(I))
      DEFE(I)=AK1/RAD(I)
      SDEFE=SDEFE+DEFE(K)
      SDEF=SDEF+AK1*SDEFE+DEF(I)
      GO TO 100
   70 SDEF=SDEF+AL(I)*SDEFE+DEF(I)
  100 DEFL(I)=SDEF
```

```
      IF(SAL.EQ.X5) GO TO 28
      I=I+1
      GO TO 14
   28 N=I
      TAN1=AK1/RAD(I)
      SDEFA=DEFL(13)
      I=1
      SAL=0.0
   19 L=I+1
      K=I-1
      IF(I.EQ.N) GO TO 15
      SAL=SAL+AL(I)
      GO TO 16
   15 SAL=SAL+AK1
   16 DEFO(I)=SDEFA*SAL/A-DEFL(I)
      IF(I.EQ.N) GO TO 29
      I=I+1
      GO TO 19
   29 XX1=DEFO(N)
      SAL=2.*A
      SDEF=0.0
      SDEFE=0.0
      I=25
   43 K=I-1
      L=I+1
      SAL=SAL-AL(L)
      IF(I.EQ.21) GO TO 35
      GO TO 36
```

```
 35 AK2=AL(L)
    SAL=X6
 36 IF(SAL.EQ.X6) GO TO 53
    DEF(I)=AL(L)*AL(L)/(2.*RAD(L))
    DEFE(I)=AL(L)/RAD(L)
    GO TO 52
 53 DEF(I)=AK2*AK2/(2.*RAD(L))
    DEFE(I)=AK2/RAD(L)
    SDEFE=SDEFE+DEFE(L)
    SDEF=SDEF+AK2*SDEFE+DEF(I)
    GO TO 110
 52 IF(L-26) 120,121,121
120 SDEFE=SDEFE+DEFE(L)
121 SDEF=SDEF+AL(L)*SDEFE+DEF(I)
110 DEFL(I)=SDEF
    IF(SAL.EQ.X6) GO TO 38
    I=I-1
    GO TO 43
 38 M=I
    TAN2=AK2/RAD(L)
    GRG=(TAN1+TAN2)/(X6-X5)
    SAL=2.*A
    WRITE(6,210) X5,X6,AK1,AK2,TAN1,TAN2,GRG
210 FORMAT(7E15.6)
    I=25
 39 IF(I.EQ.M) GO TO 20
    L=I+1
    SAL=SAL-AL(L)
```

```
      GO TO 21
   20 SAL=SAL-AK2
   21 DEFO(I)=(XX1-DEFL(M))*(2.*A-SAL)/(2.*A-X6)+DEFL(I)
      IF(I.EQ.M) GO TO 46
      I=I-1
      GO TO 39
   46 DEFR=DEFO(M)
      RETURN
      END
```

CD TOT 0094

```
      SUBROUTINE STRAIN (EPST,W,H,HS,EPSTT,EPSBB,SST,SSB)
C          STRAIN DISTRIBUTION THROUGHOUT C. S.
      WW=ABS(W)
      IF(EPST.LT.0.) GO TO 11
   12 EPSTT=EPST
      IF(W.LT.0.) GO TO 10
      IF(W.GT.H) GO TO 30
      EPSBB=-EPSTT*(H-W)/W
C          STRAIN IN THE TOP AND IN THE BOTTOM STEEL
      SST=EPSTT*(W-HS)/W
      SSB=-EPSTT*(H-W-HS)/W
      GO TO 20
   10 EPSBB=EPSTT*(WW+H)/WW
      SST=EPSTT*(WW+HS)/WW
      SSB=EPSTT*(WW+H-HS)/WW
      GO TO 20
   30 EPSBB=EPSTT*(W-H)/W
      SST=EPSTT*(W-HS)/W
      SSB=EPSTT*(W-H+HS)/W
      GO TO 20
   11 IF(W.LT.0.) GO TO 12
      IF(W.GT.H) GO TO 12
      EPSTT=EPST
      EPSBB=-EPST*(H-W)/W
      SST=-EPSBB*(W-HS)/(H-W)
      SSB=EPSBB*(H-W-HS)/(H-W)
   20 RETURN
      END
```

```
      SUBROUTINE STRSC(I,J,AS,SST,SST1,D2)
      COMMON /A/ DT(26,138)
C        STRESS-STRAIN HISTORY OF THE TOP STEEL
      K=J-1
      E1=25.4E+06
      IF(J.GT.2) GO TO 40
   30 IF(ABS(SST).GT.0.0022) GO TO 10
C        FORCE IN THE STEEL IN FIRST LOADING STAGE
      DT(I,J)=-E1*AS*SST
      GO TO 50
   10 DT(I,J)=AS*0.0022*E1
      IF(SST.LT.0.) DT(I,J)=-DT(I,J)
   50 D2=DT(I,J)
      RETURN
C        FORCE IN THE STEEL FROM PREVIOUS LOADING STAGE
   40 D22=DT(I,K)
      SST0=SST1+D22/(E1*AS)
      SST10=ABS(SST-SST0)
      IF(SST10.GT.0.0022) GO TO 90
      DT(I,J)=AS*E1*(SST0-SST)
      GO TO 70
   90 DT(I,J)=AS*E1*0.0022
      IF(SST.GT.SST0) DT(I,J)=-DT(I,J)
   70 D2=DT(I,J)
      RETURN
      END
```

CD TOT 0026

```
      SUBROUTINE STRSS(I,J,AS,SSB,SSB1,D3)
      COMMON /B/ DT(26,138)
C          STRESS-STRAIN HISTORY OF THE BOTTOM STEEL
      K=J-1
      E1=25.4E+06
      IF(J.GT.2) GO TO 40
   30 IF(ABS(SSB).GT.0.0022) GO TO 10
      DT(I,J)=-E1*AS*SSB
      GO TO 50
   10 DT(I,J)=AS*0.0022*E1
      IF(SSB.GT.0.) DT(I,J)=-DT(I,J)
   50 D3=DT(I,J)
      RETURN
   40 D33=DT(I,K)
      SSB0=SSB1+D33/(E1*AS)
      SSB10=ABS(SSB-SSB0)
      IF(SSB10.GT.0.0022) GO TO 90
      DT(I,J)=AS*E1*(SSB0-SSB)
      GO TO 70
   90 DT(I,J)=AS*E1*0.0022
      IF(SSB.GT.SSB0) DT(I,J)=-DT(I,J)
   70 D3=DT(I,J)
      RETURN
      END
```

CD TOT 0024

BIBLIOGRAPHY

1) Hognestad, E., Hansen, N.W., and McHenry, D., "Concrete Stress Distribution in Ultimate Strength Design", ACI Journal, Proceedings V.52, No.4, December 1955, pp. 455-480.

2) Kriz, L.B., and Lee, S.L., "Ultimate Strength of Over-Reinforced Beams", Proceedings, ASCE, V.86, EM3, June 1960, p. 95.

3) Sinha, B.P., Kurt H. Gerstle, and Leonard G. Tulin, "Stress-Strain Relation for Concrete Under Cyclic Loading", Proceedings V.61, ACI, February 1964, pp. 195-211.

4) Massonnet, C.E. and Save, M.A., "Plastic Analysis and Design".

5) Neal, B.G., "The Plastic Methods of Structural Analysis, Great Britain, 1956.

6) Love, A.E.H., "A Treatise on the Mathematical Theory of Elasticity, Cambridge, 1892.

7) Ewing, J.A., "The Strength of Materials, Cambridge, 1899.

8) Greenberg, H.J. and Prager, W., "On Limit Design of Beams and Frames", ASCE, 1952.

9) Prager, W., "Introduction to Plasticity", Addison Wesley, 1959.

10) Beedle, L.S., "Plastic Design of Steel Frames", 1958.

11) Baker, A.L.L., "The Ultimate Load Theory Applied to The Design of Reinforced Concrete Frames", London, 1956.

BIBLIOGRAPHY CONT'D

12) Mattock, A.H., "Rotation Capacity of Hinging Regions In Reinforced Concrete Beams", Flexural Mechanics of Reinforced Concrete, 1964.

13) Cohn, M.Z., "Optimum Limit Design for Reinforced Concrete Continuous Beams", Institute of Civil Engineers, Vol. 30, 1965.

14) Gerstle, K.H. and Tulin, L.G., "Behaviour of Reinforced Concrete Beams Subjected to Cyclical Bending Loads", Revista IMCYC, 1967.

NOMENCLATURE AND DEFINITION

ε_s - elastic strain in reinforcing steel

ε_y - plastic strain in reinforcing steel

f'_c - concrete strength

f_s - elastic stress in reinforcing steel

f_y - yield stress in reinforcing steel

K_p - curvature of the cross-section when the internal moment reaches value of fully plastic moment MP

K_y - curvature of the cross-section when the internal moment reaches value of MY

MP - fully plastic moment - internal moment of the cross-section when tensile reinforcement is in yield and the stress in top compression fibres in concrete is equal to f'_c.

MY - value of an internal moment of the cross-section when the tensile reinforcement reaches yield point

m - residual moment

M_{min}, - minimum elastic moments

M_{max} - maximum elastic moments

P - magnitude of the load

P_c - collapse load

P_s - shakedown load

δ - deflection

ϕ - rotation

ε - strain

σ - stress